UNIVERSIDADE FEDERAL DE SANTA CATARINA
CENTRO TECNOLÓGICO
PROGRAMA DE PÓS-GRADUAÇÃO EM ENGENHARIA AMBIENTAL

Tomas Carlotto

Development of a 2D-3D coupled Catchment-Lake model for multi-core and GPU architectures

Florianópolis
2022

Tomas Carlotto

Development of a 2D-3D coupled Catchment-Lake model for multi-core and GPU architectures

Tese submetida ao Programa de Pós-Graduação em Engenharia Ambiental da Universidade Federal de Santa Catarina para obtenção do título de Doutor em Engenharia Ambiental.
Orientador: Prof. Pedro Luiz Borges Chaffe, Dr.

Florianópolis
2022

Ficha de identificação da obra elaborada pelo autor,
através do Programa de Geração Automática da Biblioteca Universitária da UFSC.

Carlotto, Tomas
Development of a 2D-3D coupled Catchment-Lake model for multi-core and GPU architectures / Tomas Carlotto ; orientador, Pedro Luiz Borges Chaffe, 2022.
111 p.

Tese (doutorado) - Universidade Federal de Santa Catarina, Centro Tecnológico, Programa de Pós-Graduação em Engenharia Ambiental, Florianópolis, 2022.

Inclui referências.

1. Engenharia Ambiental. 2. Modelo hidrológico. 3. Modelo hidrodinâmico. 4. Computação de alto desempenho. 5. Ecossistema lacustre. I. Luiz Borges Chaffe, Pedro. II. Universidade Federal de Santa Catarina. Programa de Pós Graduação em Engenharia Ambiental. III. Título.

Tomas Carlotto

Development of a 2D-3D coupled Catchment-Lake model for multi-core and GPU architectures

O presente trabalho em nível de doutorado foi avaliado e aprovado por banca examinadora composta pelos seguintes membros:

Prof. Edson Cezar Wendland, Dr.
Universidade de São Paulo

Prof. Jose Mario Vicensi Grzybowski, Dr.
Universidade Federal da Fronteira Sul

Prof. Roberto Valmir da Silva, Dr.
Universidade Federal da Fronteira Sul

Prof. Leonardo Hoinaski, Dr.
Universidade Federal de Santa Catarina

Certificamos que esta é a **versão original e final** do trabalho de conclusão que foi julgado adequado para obtenção do título de Doutor em Engenharia Ambiental.

Documento assinado digitalmente
LEONARDO HOINASKI
Data: 13/04/2022 08:49:07-0300
CPF: 007.028.269-28
Verifique as assinaturas em https://v.ufsc.br

Prof. Leonardo Hoinaski, Dr.
Coordenação do Programa de Pós-Graduação

Documento assinado digitalmente
Pedro Luiz Borges Chaffe
Data: 12/04/2022 20:46:09-0300
CPF: 005.170.430-76
Verifique as assinaturas em https://v.ufsc.br

Prof. Pedro Luiz Borges Chaffe, Dr.
Orientador

Florianópolis, 2022.

AGRADECIMENTOS

Ao Professor Pedro Luiz Borges Chaffe, pelas orientações e pelo tempo expressivo dedicado as revisões e análises críticas que promoveram a constante melhoria deste trabalho.

Ao Professor Leonardo Hoinaski e ao Laboratório de Controle da Qualidade do Ar (LCQAr) por proporcionarem o acesso ao *cluster* usado para as simulações computacionais.

A minha família, em especial, meus avós Hélio Luiz Carlotto e Isaura Dóris Klin Carlotto pelo incentivo, apoio e sabedoria compartilhada.

A minha namorada Denise Machado pelo apoio, compreensão e carinho nesta etapa tão importante.

Aos meus colegas do Laboratório de Hidrologia (LabHidro), pela colaboração e disponibilidade para conversas construtivas e inspiradoras.

Ao CNPq pela bolsa de estudos.

A busca pelo conhecimento é algo gratificante na mesma medida de vosso esforço em fazer o seu melhor trabalho com os recursos que lhe estiverem disponíveis!

RESUMO

As interações entre os fluxos de água da bacia hidrográfica e a hidrodinâmica dos lagos podem ser estudadas com modelos hidrológicos e hidrodinâmicos acoplados. Porém o acoplamento de modelos geralmente resulta no aumento da complexidade, tanto conceitual quanto computacional e a aplicação desses modelos exige uma estrutura robusta de modelagem, conhecimentos avançados de programação, maior quantidade de dados, configurações extensas e na maioria dos casos, tempo computacional significativo. O progresso das tecnologias de computação e das técnicas de modelagem indicam que a computação de alto desempenho em clusters e dispositivos massivamente paralelos como as Unidades de Processamento Gráfico (GPU) podem ajudar a amenizar o problema do tempo computacional. Por outro lado, métodos de automatização podem reduzir a complexidade na aplicação dos modelos acoplados, quando estabelecem a troca contínua (*seamless*) de dados entre os modelos hidrológico e hidrodinâmico. Esta tese tem como principal objetivo realizar o acoplamento entre um modelo bidimensional de fluxo de águas superficiais baseado nas equações de águas rasas (SW2D) e o modelo hidrodinâmico EFDC-MPI (versão paralelizada do Environmental Fluid Dynamic Code). Para isso, duas etapas principais foram realizadas: (i) desenvolvimento do modelo bidimensional de águas rasas acelerado por GPGPU; (ii) acoplamento do modelo resultante SW2D-GPU com o modelo EFDC-MPI e automatização da criação dos arquivos de configuração e de entrada de dados e parâmetros. O modelo SW2D-GPU simula os fluxos de água na bacia hidrográfica considerando o processo de evaporação, captação de água e de forma simplificada também considera as perdas por interceptação e infiltração. O modelo EFDC-MPI pode simular fluxos uni, bi e tridimensionais e é capaz de simular o processo de umedecimento e secagem em lagos podendo lidar com eventos transitórios e intermitentes de entradas de água vindas de rios ou encostas da bacia hidrográfica. O acoplamento destes dois modelos resultou no modelo SW2D-EFDC de alto desempenho computacional para realizar simulações da hidrodinâmica de ecossistemas lacustres. O modelo SW2D-EFDC pode ser usado em desktops, clusters com múltiplos processadores e GPUs. Desta forma, permite simulações hidrológicas e hidrodinâmicas em grandes áreas e com alta resolução espacial; simula a hidrodinâmica em ecossistemas lacustres com pouca disponibilidade de dados medidos e simula as interações entre lago e bacia hidrográfica. O modelo SW2D-EFDC foi testado em simulações da hidrodinâmica da lagoa do Peri considerando as influências das entradas de água vindas da bacia hidrográfica em diferentes cenários de vento e transporte de traçador virtual. Os testes do modelo acoplado reforçam que ele é uma ferramenta promissora para estudar os processos hidrológicos e hidrodinâmicos em corpos d'água como lagos, lagoas e reservatórios, bem como, as interações com a bacia hidrográfica.

Palavras-Chave: modelo hidrológico; modelo hidrodinâmico; EFDC; computação de alto desempenho; ecossistema lacustre.

RESUMO EXPANDIDO

INTRODUÇÃO

Compreender as interações entre a hidrodinâmica dos lagos e os processos hidrológicos que ocorrem na bacia é fundamental para a gestão dos ecossistemas lacustres, visando o desenvolvimento sustentável e a qualidade de vida (LI *et al.*, 2016; MONTANARI *et al.*, 2013). Essas interações podem ser estudadas com modelos hidrológicos e hidrodinâmicos acoplados capazes de usar tecnologias modernas de computação de alto desempenho em *clusters* e em dispositivos massivamente paralelos, como Unidades de Processamento Gráfico (GPU).

Modelos computacionais são ferramentas essenciais para entender a hidrologia da bacia e investigar a eficácia de ações corretivas para melhorar a qualidade da água e avaliar os efeitos de mudanças nos regimes hidrológicos sobre a disponibilidade hídrica em lagos e reservatórios (BENNINGTON *et al.*, 2010; COUTURE *et al.*, 2014; RODRIGUES *et al.*, 2021). O desenvolvimento tecnológico e o consequente aumento da capacidade dos computadores de realizar grandes quantidades de cálculos também passaram a exigir o desenvolvimento de modelos matemáticos e computacionais compatíveis, capazes de utilizar tais tecnologias (O'DONNCHA *et al.*, 2019). Este é um aspecto fundamental a ser considerado nos próximos anos, em que o desenvolvimento científico e tecnológico na área de recursos hídricos estará intimamente relacionado à criação de ferramentas computacionais focadas em gerar conhecimento sobre processos hidrológicos e relações ecossistêmicas em bacias hidrográficas em um cenário de mudanças climáticas e de preocupações com a segurança hídrica e energética (GETIRANA; LIBONATI; CATALDI, 2021).

Nesta tese, foi realizado o acoplamento entre um modelo bidimensional de escoamento superficial baseado em equações de águas rasas (SW2D-GPU) e o modelo hidrodinâmico tridimensional EFDC-MPI de alto desempenho computacional. O desenvolvimento deste trabalho foi feito em duas etapas: (i) implementação e paralelização do modelo bidimensional de águas rasas em linguagem CUDA C/C++ para computação de alto desempenho em GPU, e (ii) acoplamento do modelo SW2D-GPU com o modelo hidrodinâmico EFDC-MPI para proporcionar a modelagem hidrodinâmica 3D do lago considerando os fluxos difusos de água vindos da bacia hidrográfica, transporte de solutos e influências do vento.

O modelo computacional resultante do acoplamento foi denominado SW2D-EFDC e tem as seguintes potencialidades: (i) permite simulações hidrológicas e hidrodinâmicas em grandes áreas e com alta resolução espacial; (ii) simula a hidrodinâmica em ecossistemas lacustres com pouca disponibilidade de dados medidos; (iii) simula as interações dos fluxos entre bacias hidrográficas e lagos; (iv) é ideal para simulações utilizando GPU e *clusters* com milhares de processadores (CPUs) e também pode ser utilizado em computadores comuns de escritório; e (v) é um modelo de código aberto disponibilizado em um repositório GitHub (<https://github.com/LabHidro/SW2D-EFDC>). O modelo SW2D-EFDC foi testado na bacia da lagoa do Peri, principal fonte de água doce da ilha de Florianópolis/SC, considerando as influências das entradas de água vindas da bacia hidrográfica em diferentes cenários de vento e transporte de traçador virtual.

OBJETIVO

Desenvolver um modelo acoplado 2D-3D Bacia-Lago em arquiteturas *multi-core* e GPU para modelagem hidrológica-hidrodinâmica acoplada de ecossistemas lacustres.

METODOLOGIA

Desenvolvimento do modelo 2D de águas rasas acelerado por GPU (SW2D-GPU)

O modelo SW2D-GPU foi desenvolvido com base em uma versão sequencial do modelo bidimensional (2D) de águas rasas previamente implementado em Fortran (LEE, 2013; NOH *et al.*, 2016). Realizei a paralelização e reescrevi completamente o código numérico do modelo na linguagem de programação CUDA C/C++. Também propuz e implementei uma formulação para estimar a evaporação potencial em função da temperatura e da radiação solar. Além disso, foi incluída a opção de adicionar um número ilimitado de séries temporais de vazão em diferentes locais da rede de drenagem. A versão paralela do modelo manteve a mesma ordem de tarefas da implementação sequencial original para fornecer uma comparação de desempenho entre as duas versões.

As principais etapas do código em CUDA C/C++ são mostrados na Figura 4. As partes do código com maior demanda computacional são executadas na GPU com processamento paralelo e as demais partes são executadas na CPU com processamento sequencial. A versão sequencial do modelo tem a mesma sequência de operações, mas todas as etapas são processadas na CPU. Tanto o modelo SW2D-GPU paralelizado quanto a versão sequencial são implementados com precisão dupla.

O diagrama na Figura 4 ilustra a estrutura do modelo e a sequência de operações para aproximar a solução das equações de águas rasas usando o método Leapfrog em um esquema de diferenças finitas. Primeiro, os dados de entrada são lidos e armazenados na memória da CPU e, em seguida, os dados usados no processamento paralelo nos kernels implementados em CUDA C/C++ são copiados para a memória da GPU. Em seguida, a solução das equações de águas rasas é realizada de forma iterativa na qual os cálculos distribuídos no espaço são executados em paralelo na GPU, mas a evolução temporal ocorre sequencialmente na CPU, de modo que os cálculos de u, v e h são realizados para todas as posições do domínio computacional de forma alternada de acordo com o método Leapfrog.

Para exemplificar a aplicabilidade e testar o desempenho do modelo SW2D-GPU em comparação com a versão sequêncial, foram utilizados dois estudos de caso: (i) simulação de inundação em área urbana em que a área de estudo foi o *campus* da Universidade Federal de Santa Catarina; e (ii) simulação integrada dos fluxos de água entre bacia hidrográfica e lago para estimar a variação dos níveis da água em função de variáveis meteorológicas e captação de água para consumo humano, tendo com área de estudo a bacia da Lagoa do Peri. A análise de desempenho foi baseada em: (i) comparação entre o tempo total que cada versão do modelo (paralelo e sequencial) leva para completar as simulações de teste; e (ii) comparação dos tempos de computação das funções processadas na GPU em relação aos tempos das funções equivalentes do modelo sequencial executado na CPU.

Acoplamento dos modelos SW2D-GPU e EFDC-MPI

O modelo SW2D-EFDC foi desenvolvido para aproveitar o poder de processamento paralelo de GPUs e de *cluster* com várias CPUs. A estrutura do modelo é ilustrada na Figura 16. O módulo de acoplamento foi implementado no modelo SW2D-GPU, e contém as funções para mapear as fronteiras entre bacia e lago e para automatizar os processos de criação da malha do domínio computacional e das entradas necessárias para as simulações acopladas (Figura 16).

O esquema de acoplamento usado aqui contém funções que automatizam o processo de criação de entradas do modelo EFDC-MPI durante a execução do modelo SW2D-GPU. As entradas que não dependem da solução das equações de águas rasas ou da identificação da fronteira bacia-lago (tais como: os arquivos que definem a malha, a decomposição do domínio computacional e as condições iniciais de temperatura, salinidade e concentrações de corantes (traçador)) são criadas na inicialização do modelo SW2D-GPU. As séries temporais de salinidade, temperatura

e concentração de corante que são condições de contorno aplicadas apenas nas fronteiras entre a bacia e o lago, e as séries temporais de fluxo que dependem da solução das equações de águas rasas são criadas no final da execução do modelo SW2D-GPU.

O modelo SW2D-EFDC acopla os fluxos de água entre a bacia hidrográfica e o lago (Figura 18a) e também estabelece uma ligação com as trocas de calor (Figura 18b) e os processos de transporte no lago. O modelo SW2D-EFDC simula a hidrodinâmica 2D-3D do sistema lacustre e fornece uma visão detalhada dos perfis verticais de velocidade, temperatura e composição química da água (no momento, apenas traçador virtual (dye)) no lago (Figura 18c). No domínio do lago é utilizado uma discretização vertical *Sigma Stretch* no qual a resolução vertical é distribuída de acordo com o número de camadas e a altura da água acima do fundo do lago em cada posição do domímio. O cálculo para determinar a resolução vertical de cada camada é realizado internamente pelo modelo EFDC-MPI com base no número de camadas definidas previamente.

Para o acoplamento dos modelos SW2D-GPU e EFDC-MPI, a resolução vertical de cada célula do lago é dividida igualmente entre as camadas. Da mesma forma, os fluxos de água que entram no lago são divididos pelo número de camadas e distribuídos uniformemente em cada camada de células nas fronteiras entre a bacia e o lago. (Figura 18e). O modelo SW2D-EFDC foi aplicado na simulação da hidrodinâmica da Lagoa do Peri considerando as entradas de água provenientes da bacia hidrográfica. As simulações foram realizadas para dois cenários: (i) sem vento; e (ii) incluindo o vento (somente na área do lago). Para ajudar a visualizar as entradas de água e a hidrodinâmica no lago, o transporte de um traçador virtual (dye) foi incluído na simulação. Durante as simulações, foram registradas as variações do nível da água no lago. Primeiro, apenas o modelo SW2D-GPU foi usado para verificar se os parâmetros utilizados forneceriam uma boa representação das variações do nível da água no lago em 2D. Em seguida, foi aplicado o modelo acoplado SW2D-EFDC e novamente foram registrados os nível da água simulados. Dessa forma, foi possível comparar os dois modelos e verificar o principio da conservação das massas e também que as entradas de água no lago usando o modelo SW2D-EFDC são compatíveis com as do SW2D-GPU.

RESULTADOS

O modelo SW2D-GPU demonstrou alto desempenho computacional, com simulações até 34 vezes mais rápidas do que as realizadas com a versão sequencial do modelo quando aplicado em um domínio computacional com até 7 milhões de células (Figura 13). Além de ter uma melhora significativa no desempenho, o modelo agora também conseguiu representar o processo de evaporação potencial em corpos d'água. O modelo obteve bons resultados na simulação de inundação na área do campus da Universidade Federal de Santa Catarina (UFSC) considerando entradas de água de diferentes sub-bacias, conseguindo estimar a distribuição espaço-temporal da inundação e o nível da água em diferentes locais da rede de drenagem (Figura 9). Também simulou satisfatóriamente os fluxos de águas na bacia da Lagoa do Peri onde conseguiu representar as interações entre os fluxos de água da bacia hidrográfica com o lago, obtendo como principais resultados, a distribuição espaço-temporal dos fluxos na bacia hidrográfica e a variação dos níveis da água no lago, considerando a interferência humana por meio da captação de água (Figura 12).

O nível do lago foi bem representado tanto pelo modelo SW2D-GPU quanto pela versão acoplada SW2D-EFDC (Figura 21). O acoplamento entre os dois modelos foi bem estabelecido de modo que não houve perdas significativas de água na interface entre a bacia hidrográfica e o lago. Verificou-se uma pequena diferença nos níveis simulados após 80 h (Figura 21), em que os níveis simulados pelo modelo acoplado SW2D-EFDC são ligeiramente superiores. Após verificar que o acoplamento foi bem sucedido no que diz respeito à representação da variação dos níveis da água, foi possível explorar outros aspectos da hidrodinâmica do lago e visualizar onde ocorrem as principais entradas de água e como a concentração de corante (traçador) se propaga no interior do lago. A Figura 22 apresenta os resultados das simulações dos fluxos de água na bacia e a hidrodinâmica do lago em cenários com e sem vento em que, além das velocidades da

água, também foi simulado o transporte de traçador virtual. Esta simulação mostra os locais onde ocorrem as principais entradas de água no lago e também revela a importância de se considerar as entradas difusas de água, principalmente em condições em que a dinâmica das águas é fortemente influenciada pelo vento.

CONSIDERAÇÕES FINAIS

O acoplamento do modelo SW2D-GPU com o modelo hidrodinâmico EFDC-MPI proporcionou a modelagem hidrodinâmica 3D da Lagoa do Peri considerando as entradas difusas de água vindas da bacia hidrográfica, transporte de traçador virtual e as influências do vento. Esse acoplamento resultou no modelo SW2D-EFDC que utiliza processamento paralelo em arquiteturas *multi-core* e GPU. Assim, minimiza o problema do longo tempo computacional, que é um dos principais obstáculos para a aplicação de modelos acoplados em simulações do mundo real. Outro problema inerente à complexidade dos modelos é a preparação das entradas para iniciar a simulação, principalmente na parte do modelo hidrodinâmico 3D. No modelo SW2D-EFDC, os processos de criação das entradas e configuração do modelo hidrodinâmico 3D foram automatizados para garantir a continuidade da solução e a troca de dados entre o modelo SW2D-GPU e o modelo EFDC-MPI sem a necessidade de intervenção humana. Assim o acoplamento dos modelos permitiu dar um passo importante para estudar a influência dos fluxos da bacia hidrográfica na hidrodinâmica de lagos, de forma automatizada e com recursos computacionais de alto desempenho. Porém uma série de limitações ainda permanecem e oferencem oportunidades para estudos futuros.

Um dos desafios para a modelagem hidrológica-hidrodinâmica acoplada é a representação bidirecional dos fluxos (bacia $\rightarrow$ lago; lago $\rightarrow$bacia). No modelo SW2D-EFDC os fluxos ocorrem apenas da bacia para o lago, essa foi uma forma simples adotada para testar como o modelo EFDC-MPI se comportaria diante de um acoplamento envolvendo toda a fronteira entre bacia hidrográfica e lago. Os resultados dos testes mostraram bom desempenho computacinal e não houve perda de estabilidade numérica, indicando que um esquema de acoplamento mais complexo envolvendo a representação bidirecional dos fluxos é viável e recomendada para estudos futuros. Esta melhoria, além de habilitar os fluxos de retorno do lago para os rios da bacia hidrográfica, também proporcionará abordar problemas em que a área do lago varia significativamente.

As potencialidades do modelo hidrodinâmico EFDC-MPI podem ser melhor exploradas e testadas a medida que houver maior disponibilidade de dados. Para isso a formulação do esquema de acoplamento e de criação das condições iniciais pode ser melhorado para proporcionar abordagens mais detalhadas da distribuição espaço-temporal das concentrações de solutos, salinidade e temperaturas da água. Além disso, na continuidade do desenvolvimento do modelo SW2D-EFDC a consideração do módulo de qualidade da água (que já está implementado no modelo EFDC-MPI), é um procedimento recomendado para viabilizar estudos avançados da hidrodinâmica do lago considerando reações fisico-quimicas e biológicas.

O desenvolvimento de uma abordagem integrada considerando as águas subsuperficiais também é uma oportunidade para pesquisas futuras no desenvolvimento do modelo SW2D-EFDC. Visto que o modelo EFDC tem condições de fronteira compatíveis para interagir com os fluxos de águas subterrâneas o que facilita a tarefa de acoplamento com um modelo integrado de fluxo de águas superficiais e subsuperficiais. Neste ponto, o modelo SW2D-EFDC pode ser integrado com um modelo de fluxo subsuperficial ou novas combinações de modelos também podem ser testadas.

Palavras-Chave: modelo hidrológico; modelo hidrodinâmico; EFDC; computação de alto desempenho; ecossistema lacustre.

ABSTRACT

The interactions between the water flows of the catchment and the lake hydrodynamics can be studied with coupled hydrological and hydrodynamic models. However, coupled models are usually more complex, both conceptually and computationally. The application of these models requires a robust modeling framework, advanced programming skills, greater amount of data, extensive configurations, and in most cases, significant computational time. The progress of computing technologies and modeling techniques indicates that high-performance computing in clusters and massively parallel devices such as Graphics Processing Units (GPU) can help amend the problem of computational time. On the other hand, automation methods can reduce the complexity in the application of coupled models, when they establish the seamless exchange of data between hydrological and hydrodynamic models. In this dissertation, the coupling between a surface water model based on two-dimensional shallow water equations (SW2D-GPU) and the EFDC-MPI hydrodynamic model (parallelized version of the Environmental Fluid Dynamic Code) was performed. For this, two main steps were performed: (i) development of the two-dimensional shallow water model accelerated by GPGPU; (ii) coupling the SW2D-GPU model with the EFDC-MPI model and automating the creation of configuration files and input of data and parameters. The SW2D-GPU model simulates the water flows in the catchment considering the process of evaporation, water abstraction and, in a simplified way, it also considers the losses by interception and infiltration. The EFDC-MPI model can simulate one, two and three-dimensional flows and is capable of simulating the wetting and drying process in lakes, being able to deal with transient and intermittent events of water coming from rivers or catchment hillslopes. The coupling of these two models resulted in the SW2D-EFDC model with high computational performance for simulating the hydrodynamics of lake ecosystems. The SW2D-EFDC model can be used on desktops, multi-core clusters and GPUs. It allows hydrological and hydrodynamic simulations in large areas and with high spatial resolution; simulates hydrodynamics in lake ecosystems with little availability of gauge data and simulates catchment-lake interactions. The SW2D-EFDC model was tested in simulations of the hydrodynamics of the Peri lake, considering the influences of water inflows from the catchment in different scenarios of wind and tracer transport. The tests of the coupled model reinforce that it is a promising tool to study the hydrological and hydrodynamic processes in water bodies such as lakes, lagoons and reservoirs, as well as the interactions with the catchment.

Keywords: hydrological model; hydrodynamic model; EFDC; high performance computing; lake ecosystem.

LIST OF FIGURES

LIST OF TABLES

LIST OF SYMBOLS

x - x direction
y - y direction
z - z direction
i - Spatial variation index in the x direction [-]
j - Spatial variation index in the y direction [-]
t - Time
$\triangle t$ - Time step
$\triangle x$ - Spatial resolution in the x direction [m]
$\triangle y$ - Spatial resolution in the y direction [m]
h - Water depth [m]
g - Acceleration of gravity [ms^{-2}]
$H = h + z$, where z is the topographic elevation [m]
u - Velocities in the x direction [ms^{-1}]
v - Velocities in the y direction [ms^{-1}]
w - Velocities in the z direction [ms^{-1}]
r_{e} - Effective rainfall [mm]
r - Rainfall [mm]
INF - Percentage of rainfall infiltration loss [%]
INT - Percentage of rainfall interception loss [%]
LWL - Lake water loses [%]
q_{ex}- Source and sink term [$\mathrm{m}^3\mathrm{s}^{-1}$]
E - Potential evaporation [mm]
f_1 - Friction term in the x direction
f_2 - Friction term in the y direction
n - Manning's roughness coefficient
h_{min} - Minimum water depth to activate potential evaporation [m]
t_{k} - Monitoring time interval of the data [s]
ρ_{w} - Density of the water [kgm^{-3}]
l_{v} - Latent heat of vaporization [Jkg^{-1}]
α - Albedo
R_{g} - Global solar radiation [Wm^{-2}]
R_{s} - Net radiation [Wm^{-2}]
$T(t)$ - Air temperature [°C]
η - Water level [m]
z_{b} - Bottom bed or topography elevation [m]
p - Pressure [$m^2 s^{-2}$]
f - Coriolis parameter

A_{V}- Vertical diffusivity [$\mathrm{m^2 s^{-1}}$]
Q_{u} and Q_{y} - Affluent–effluent movement terms [$\mathrm{kg.m^{-3}}$]
m_{x} and m_{y} - Square roots of the diagonal components [m]
Q_{yn}- Flows that enter the lake from the northern boundary
Q_{ys}- Flows entering the lake from the southern boundary
Q_{xe}- Flows entering the lake from the eastern boundary
Q_{xw}- Flows entering the lake from the western boundary

LIST OF ABBREVIATIONS

2D - Two-dimensional
3D - Three-dimensional
HPC - High performance computing
GPGPU - General Purpose Graphics Processing Units
CUDA - Compute Unified Device Architecture
MPI - Message Passing Interface
GPU - Graphic Processing Unit
CPU - Central Processing Unit
DEM - Digital Elevation Model
EFDC-MPI - Parallelized version of the Environmental Fluid Dynamic Code
SW2D-GPU - Two-dimensional shallow water model accelerated by GPGPU

CONTENTS

1 INTRODUCTION

Lakes and reservoirs play an important ecological and environmental role and also support valuable economic activities for the human population, such as water collection, energy generation, irrigation, fishing and leisure (LI *et al.*, 2016; MESSAGER *et al.*, 2016). However, these ecosystems are sensitive to climate change and human activities that occur in the catchment in which they are located (COUTURE *et al.*, 2014). Therefore, understanding the interactions between the hydrodynamics of lakes and the hydrological processes that occur in the catchment is fundamental for the management of these resources, aiming at sustainable development and quality of life (LI *et al.*, 2016; MONTANARI *et al.*, 2013). These interactions can be studied with coupled hydrological and hydrodynamic models capable of using modern high-performance computing technologies in clusters and in massively parallel devices such as Graphics Processing Units (GPU).

Computer models are essential tools for understanding the catchment hydrology and for investigating the effectiveness of corrective actions aimed at improving water quality and for evaluating the effects of changes in hydrological regimes on water availability in lakes and reservoirs (BENNINGTON *et al.*, 2010; COUTURE *et al.*, 2014; RODRIGUES *et al.*, 2021). Technological development and the consequent increase in the capacity of computers to perform large amounts of calculations also began to require the development of compatible mathematical and computational models capable of using such technologies (O'DONNCHA *et al.*, 2019). This is a fundamental aspect to be considered in the next years, in which scientific and technological development in the area of water resources will be closely related to the creation of computational tools focused on generating knowledge about hydrological processes and ecosystem relationships in catchments in a scenario of climate change and concerns about the country's water and energy security (GETIRANA; LIBONATI; CATALDI, 2021).

In this dissertation, the coupling between a two-dimensional model of surface water flow based on shallow water equations (SW2D) and the three-dimensional hydrodynamic model EFDC of high computational performance was carried out in a framework capable of using from desktops to clusters with multiple processors, massively parallel devices such as GPUs (Graphics Processing Unit) and supercomputers (CARLOTTO; SILVA; GRZYBOWSKI, 2019; CARLOTTO *et al.*, 2021; CARLOTTO; SILVA; GRZYBOWSKI, 2018). The resulting computational model is called SW2D-EFDC and has the following potentialities: (i) it enables hydrological and hydrodynamic simulations in large areas and with high spatial resolution; (ii) it simulates hydrodynamics in lake ecosystems with little availability of gauged data; (iii) it simulates catchment and lake interactions; (iv) it is ideal for simulations using GPUs and clusters with thousands of processors (CPUs) and can also be used in common office computers; and (v) it is an open source model made available on a GitHub repository. These potentialities allow exploring important problems that have motivated several researches around the world, dedicated to answering the following

questions:

- How do changes in hydrological regimes influence lake hydrodynamics? (KUMMU *et al.*, 2014; MAURICIO *et al.*, 2018)
- What are the relationships between water levels in the lake and water flows from the catchment? (LI *et al.*, 2014; MUNAR *et al.*, 2019)

The SW2D-EFDC model was tested in the Peri lake catchment, the main source of freshwater on the island of Florianópolis/SC. The SW2D-EFDC model can be applied in several catchments to help understand the hydrological and hydrodynamic processes in water bodies such as lakes, lagoons and reservoirs, considering the interactions with the catchment and the effects of human actions.

Why couple high computational performance hydrological and hydrodynamic models?

Hydrological processes within catchments are highly variable in space and time and influence the hydrodynamics of water bodies such as lakes and reservoirs (ZHANG *et al.*, 2019). Therefore, approaches that disregard the heterogeneity of catchments limit the understanding of important aspects such as: impacts of land use, vegetation, and climatic variables on the quality and quantity of water in these water bodies (MAURICIO *et al.*, 2018). To insert the hydrological components of the catchment into the hydrodynamics of the lake, most studies use data from flows gauged in the main rivers of the catchment (BOCANIOV *et al.*, 2016; KUMMU *et al.*, 2014; LEON *et al.*, 2011; UMGIESSER *et al.*, 2016). However, in many catchments this procedure is seriously restricted by the limited availability of monitored data and human and financial resources to carry out field monitoring (DARGAHI; SETEGN, 2011; LOPES *et al.*, 2018). In addition, this approach generally disregards diffuse water and nutrient inputs that may occur through slope and groundwater transport, for example. A solution to this limitation is obtained through methods based on coupling hydrological models and hydrodynamic models (ALARCON *et al.*, 2014; HWANG *et al.*, 2021; SHIN *et al.*, 2019; ZHANG *et al.*, 2017). The central idea of these methods is to model the hydrology of the catchment using a hydrological model that estimates water levels and flows in places where there is no monitoring, then the results are inserted into the hydrodynamic model as boundary conditions (MAURICIO *et al.*, 2018).

Several works use the coupling of hydrological and hydrodynamic models in studies that consider the effects of catchment hydrology on lake hydrodynamics, for example: Huang *et al.* (2016) coupled the two-dimensional (2D) hydrological model (Xinanjiang model) and the EFDC (Environmental Fluid Dynamics Code) hydrodynamic model, in which the Xinanjiang model was used to simulate the flows of six main rivers that were

later inserted into the EFDC hydrodynamic model in the form of boundary conditions, so they were able to investigate the impacts of a water transfer project on the hydrodynamics of Lake ChaoHu in China; Zhang *et al.* (2017) coupled the SWAT (Soil and Water Assessment Tool) model and the Delft3D hydrodynamic model to simulate the interactions between water flows in ungauged areas between Lake Poyang and its catchment in China; and Hwang *et al.* (2021) used the coupling of the SWAT model with the EFDC model to evaluate the improvement of the water quality of the Ganwol estuarine reservoir considering an agricultural system and diffuse source pollution in a catchment located in South Korea.

Although the coupling of models provides more detailed studies of hydrology and hydrodynamics in lake ecosystems, it also has some limitations related to the simulation time, as it solves the equations of the two models and exchanges data between them with conventional programming methods that perform sequential calculations, it is usually a time-consuming process (LOPES *et al.*, 2018). This problem can be minimized by using hydrological and hydrodynamic models prepared to use high performance computing and parallel processing methods in multiprocessor clusters, supercomputers, or in massively parallel devices such as General Purpose Graphics Processing Units (GPGPU) (CARLOTTO; SILVA; GRZYBOWSKI, 2018; CARLOTTO; SILVA; GRZYBOWSKI, 2019; CARLOTTO *et al.*, 2021).

Why use the EFDC hydrodynamic model?

The EFDC (Environmental Fluid Dynamics Code) model is one of the most used and technically defensible hydrodynamic models for hydrodynamic simulation (LAI; WANG; LI, 2016). It is open source and can simulate one, two and three-dimensional flows, sediment transport, thermal and biological processes in rivers, lakes, reservoirs and estuaries (HWANG *et al.*, 2021). The EFDC model has been applied to hundreds of water bodies, including rivers, lakes, reservoirs, wetlands, estuaries and coastal regions, being a key tool for studies ranging from environmental and water quality assessment to support and verification of regulatory requirements and water resources management (AHN *et al.*, 2021b; HUI *et al.*, 2021; SONG *et al.*, 2021; ZHENG *et al.*, 2021).

The EFDC model is capable of simulating the wetting and drying process in lakes and can deal with transient and intermittent events of water, nutrients and sediments coming from rivers or hillslopes (HAMRICK, 1992; HWANG *et al.*, 2021). It can also model the mixing process, changes in salinity and concentrations of sediment, contaminants and estimate variables related to eutrophication of water bodies (HAMRICK, 1992). In addition, it has a Lagrangian particle tracking model that provides the study of travel time and the trajectory of particulate materials transported by the water flow (HAMRICK, 1996). Recently, parallelized versions of the EFDC model were developed by O'Donncha, Ragnoli e Suits (2014) and Ahn *et al.* (2021a) to provide fast and efficient simulations

in high-performance computing structures such as clusters with multiple processors and massively parallel devices.

The improvements made to the EFDC model and the constant interest of the scientific community in using it in complex real-world applications to understand biological processes such as algal blooms and physical-chemical and water quality processes underscore the model's effectiveness and reliability for future applications and collaborations that aim to integrate with other models to address even broader problems occurring at a catchment scale (AHN *et al.*, 2021a; CARLOTTO; CHAFFE, 2021; HUI *et al.*, 2021; SONG *et al.*, 2021; ZHENG *et al.*, 2021).

Why use the two-dimensional shallow water model (SW2D-GPU)?

The SW2D-GPU model is a model developed for parallel processing in GPU in order to provide fast and efficient simulations of surface water flows in catchments (CARLOTTO *et al.*, 2021). The SW2D-GPU model was implemented in CUDA C/C++ language and compared with a traditional version of the shallow water 2D model implemented for sequential CPU processing with Fortran language. The GPU-accelerated version was up to 34 times faster than the sequential version in tests with computational grids with active cells ranging between 55000 and 7 million (CARLOTTO *et al.*, 2021). This model proved to be efficient in simulating surface water flows in catchments containing shallow lakes, through tests in the Peri lake catchment. It was also successfully applied in the simulation of urban floods in the area of the Federal University of Santa Catarina (UFSC) and in the rupture of an evapoinfiltration pond located on the banks of Lagoa da Conceição, all these study areas are located on the island of Florianópolis in southern Brazil (CARLOTTO *et al.*, 2021). In addition, sequential versions with CPU processing using theoretical bases similar to those of the SW2D model have already been applied in simulations of surface water flows in urban areas and with complex topographies, showing good results (LEE *et al.*, 2014; LEE *et al.*, 2016).

The development of the SW2D-GPU model is part of this dissertation, so the knowledge acquired (model structure, computational implementation and numerical methods) offers research opportunities to broaden the range of applications of this model for simulations including lake hydrodynamics and aspects related to water quality and transport of contaminants. The applications of the SW2D-GPU model mentioned above are presented in detail in Chapter 3.

Why the Peri lake catchment as a study area?

During the development of the coupled SW2D-EFDC model, several tests were necessary. In order to provide agility in the development process, it is important that the tests are carried out in an catchment of small scale in which the hydrological, meteorological

and hydrodynamic processes that will be part of the scope of application of the resulting model occur and that this catchment is being studied and monitored. This is the case of the Peri lake catchment (CARLOTTO *et al.*, 2021; CHAFFE *et al.*, 2021; PEREZ *et al.*, 2020; SANTOS *et al.*, 2021). The characteristics of this catchment meet the following requirements for the model tests:

- It is a catchment with an area of approximately 20 km^2, ideal for testing the model;
- It has a lake with a surface area of approximately 5 km^2. Therefore, it is a favorable environment for carrying out hydrodynamic simulations and evaluating the interactions between the lake and the water inflows coming from the catchment;
- It is a shallow lake and sensitive to periods of drought. This sensitivity will allow testing the model in the face of hydroclimatic changes, followed by verification of the impacts on the lake's water quality;
- It has rivers, small streams and hillslope flows, which are being studied and monitored. Therefore, hydrological processes can be studied, modeled and verified with data;
- The catchment is covered by Atlantic Forest in three stages - initial, intermediate and advanced, and coastal vegetation restinga. This makes it possible to analyze the effects of different types of vegetation on the catchment hydrology and, consequently, on the hydrodynamics of the lake;
- Part of the catchment is used by local residents for family farming with small plantations and cattle raising. This provides the evaluation of models regarding the representativeness of the effects of land use and occupation on the quantity and quality of water in the lake;
- It is a coastal catchment in which the modeling of interactions between freshwater lake and sea salt water (modeling of the saline wedge and the effects on salinity of lake waters) is also an option to be investigated by modeling;
- It has a weather station with automatic monitoring of data on rainfall, temperature, air humidity, solar radiation and wind speed.

In addition to meeting the above requirements, the Peri lake catchment has an important economic, ecological and social role for the island of Florianópolis/SC, maintaining a great diversity of species of the local fauna. The lake is the largest source of fresh water in Florianópolis, used to supply water to more than 40000 homes in the south and east of the island. The Peri lake catchment with an area of 20 km^2 and predominant Atlantic forest vegetation forms a suitable experimental field to elucidate important questions that will help to understand the interactions between lake, catchment and atmosphere,

as well as their ecosystem functions. Therefore, the use of the Peri lake catchment for testing and application of the SW2D-EFDC model can represent important gains both at a theoretical-scientific level and in an applied study to generate fundamental knowledge to support management plans for this lake ecosystem.

This dissertation is structured in 5 chapters. Chapter 1 presents the introduction, the main justifications and objectives of the dissertation. Chapter 2 presents a brief review of the literature on "hydrological and hydrodynamic modeling in lake ecosystems" highlighting the main studies of coupled modeling identified in 90 studies published in the period from 2010 to 2021. Chapter 3 presents the development of the parallel version of the two-dimensional shallow water model (SW2D-GPU) for processing in GPGPU. This chapter is structured in the form of an article, with the title "SW2D-GPU: A two-dimensional shallow water model accelerated by GPGPU" which was recently published in the journal *Environmental Modelling & Softwares*. Chapter 4 presents the coupling of the SW2D-GPU and EFDC-MPI models that resulted in the SW2D-EFDC coupled model. This chapter is structured in the form of an article, titled "A coupled 2D-3D Catchment-Lake model whith a parallel processing framework" which is under review in *Computers & Geosciences*. Chapter 5 presents the general conclusions of this dissertation.

1.1 OBJECTIVES

To develop a coupled 2D-3D Catchment-Lake model in multi-core and GPU architectures for hydrological-hydrodynamic modeling of lake ecosystems.

1.1.1 Specific objectives

1. To parallelize a 2D shallow water model (SW2D) for processing in GPU;
2. To couple the SW2D-GPU model and the EFDC-MPI hydrodynamic model for simulations using multi-core and GPU architectures;
3. To verify if the diffuse water inflows from the catchment influence the lake hydrodynamics;
4. To verify how the wind influences the water velocities in the lake and the transport of a virtual tracer.

2 LITERATURE REVIEW

2.1 MATHEMATICAL AND COMPUTATIONAL MODELING

One of the great challenges in hydrological science is to use advances in mathematical modeling to represent the complex processes that characterize hydrological systems that remain only partially known (PANICONI; PUTTI, 2015). One of these processes is the runoff generation, which involves surface and subsurface flows whose dynamics occur under different control factors that are still not well understood due to the lack of studies and comprehensive comparisons between different catchments with a variety of climatic, physiographic, hydrogeological and hydrological characteristics (CHIFFLARD *et al.*, 2019). Accurate simulations of catchment flows can provide important insights into water paths, residence times, and origin and magnitude of flows, playing an important role in estimating water and nutrient inputs into lakes (CHIFFLARD *et al.*, 2019; RUEDA; MACINTYRE, 2010).

Mathematical modeling has evolved rapidly in line with the rapid growth in computing power, as well as the development of more efficient and accurate numerical methods(AHN *et al.*, 2021a; O'DONNCHA *et al.*, 2019). Therefore, the development of new hydrological and hydrodynamic models has as a fundamental requirement the use of modern, fast, accurate and scalable numerical methods (ability to perform parallel processing in several processors) that provide the simulation of processes in different spatial and temporal scales (CLARK *et al.*, 2015; PANICONI; PUTTI, 2015).

Hydrological and hydrodynamic models are essential tools for formulating and testing scientific hypotheses, investigating spatio-temporal patterns and improving our understanding of catchment hydrology and their influence on lake hydrodynamics (FATICHI *et al.*, 2016; MUNAR *et al.*, 2018). According to Fatichi *et al.* (2016) process-based hydrological and hydrodynamic models are essentially one or more mathematical expressions that represent, and/or explicitly incorporate, the hydrological and hydrodynamic state variables that are observable and can be used together with laws of conservation of mass, energy, and momentum at different spatial and temporal scales to characterize the underlying physical processes. However, these models are composed by the description of a set of processes defined according to the objectives of the study, being able to describe the rain-runoff process, surface and groundwater flows, sediment transport or integrated processes that occur on the surface and in the subsurface at scales that can range from hillslopes to large catchments and lake ecosystems (HWANG *et al.*, 2021; MUNAR *et al.*, 2018; MUNAR *et al.*, 2019).

The way models have been developed are largely based on the decisions of modelers who use different criteria and assumptions, resulting in a great diversity of models, with different conceptions and structures even to represent the same processes (CLARK *et al.*, 2015). This has made it difficult to compare models and identify weaknesses and ways to make improvements. One of the challenges is to identify models with similar physi-

cal bases that can be combined to understand hydrological and hydrodynamic processes in catchments with different characteristics and at various spatial and temporal scales (FATICHI *et al.*, 2016; PANICONI; PUTTI, 2015; SOARES; CALIJURI, 2021).

2.1.1 Surface water flow modeling

Surface water flow modeling is often used in water flow simulations in catchments, lakes, lagoons and estuaries (HORVÁTH *et al.*, 2014; LEE *et al.*, 2016; VIERO *et al.*, 2014). Generally, surface water flow models are based on kinematic wave approximations or on a shallow water equation to simulate catchment flows and may also use more complex forms of the Navier-Stokes equations to simulate lake hydrodynamics (AHN *et al.*, 2021a; KIM *et al.*, 2012). Applications of shallow water models assume that water flows propagate with a much larger horizontal length scale than the vertical length scale, so they may not be suitable for simulations in deep water bodies (BRODTKORB; SÆTRA; ALTINAKAR, 2012; KAWAIKE; INOUE; TODA, 2000; KURGANOV; PETROVA, 2009).

Saint Venant's equations (also known as dynamic wave formulation) are used to describe the dynamics of shallow water in space and time with fluid motion occurring due to gravitational forces (gravitational potential energy) (KIM *et al.*, 2012). These equations are obtained from the integration of the Navier-Stokes equations over the vertical direction, assuming that there are no significant variations in the properties (e.g. temperature and density) of the fluid with depth (HORVÁTH *et al.*, 2014). If fluid properties vary with depth, multi-level stratified approaches can be used (KURGANOV; PETROVA, 2009). In the dynamic wave model, the momentum equation is balanced between the inertial, pressure, gravitational, frictional, and momentum terms, while in the kinematic wave model, the pressure, inertia, and local and convective acceleration terms are neglected (KIM *et al.*, 2012).

In the literature, there are numerous works that apply these theories or focus on developing improved methods to approximate the solution of these equations (BRODTKORB *et al.*, 2010; CARLOTTO *et al.*, 2021; FATICHI *et al.*, 2016; HORVÁTH *et al.*, 2014). A second-order semi-discrete upwind-centered scheme for one and two-dimensional systems of two-layer shallow water equations also was developed to represent fluids whose properties vary with depth, the scheme preserves equilibrium and momentum conditions (KURGANOV; PETROVA, 2009). A parallel implementation accelerated by Graphics Processing Units (GPU) with an explicit second-order finite volume scheme for the shallow water equations was developed considering inclined beds and the friction and shear components (BRODTKORB; SÆTRA; ALTINAKAR, 2012). Horváth *et al.* (2014) worked on solving discontinuity problems that prevent the solution of shallow wave equations close to dry areas. They developed a well-balanced scheme that preserves solution positivity across dry/wet boundaries. The method created is two-dimensional and can be applied in simulations of flooding and surface runoff in complex topographies. Acosta *et al.* (2015) identified that discretization of shallow water equations using Cartesian grids with fixed

cell sizes throughout the model domain can lead to the storage of a large amount of unnecessary dry cells for calculations. In medium or large computing domains this may require a lot of computer memory. To solve this problem, the authors developed an version of the Si3D model (SMITH, 2006) that saves memory using a nested grid that allows storing only the wet cells. In another study an approach based on Saint Venant's equations together with machine learning techniques with a random forest regression method was used to emulate infiltration predictions in an excessive flow scenario on a flat slope (CROMPTON; SYTSMA; THOMPSON, 2019).

2.1.2 Coupled hydrological and hydrodynamic modeling

Hydrodynamic modeling is a way of describing and interpreting water dynamics in lakes, rivers and wetlands from mathematical formulations that represent the spatio-temporal variation of physical, chemical and biological processes (KIM *et al.*, 2012). Hydrodynamic models can represent one, two or three spatial dimensions (1D, 2D, 3D) and are applied to quantify flows, determine residence times and interpret their influences on water quality and ecology as a result of variations in physical state of the system (e.g., water level, temperature, density, velocity and turbidity) (HODGES, 2014). Regarding the dimensionality of lake models Hodges (2014) points out that in many cases 3D hydrodynamic models can be replaced by reduced forms in 1D and 2D that demand less computational capacity, allowing the study of larger areas or in more detail, but the difficulties of applying reduced forms are not less, because despite facilitating the calculations and implementation, 1D and 2D models require more parameterization and calibration efforts. This characteristic in some cases motivates a greater use of 3D hydrodynamic models, since they are not more difficult to configure and apply compared to a 2D model and have the advantages of being able to represent non-uniform vertical distributions that are common in lakes.

Several hydrodynamic models were developed to contemplate different applications (MOOIJ *et al.*, 2010). In the category of 1D models, the GLM model (General Lake Model) is one of the most used, it is an open source vertical hydrodynamic model developed as an initiative of the Global Lake Ecological Observatory Network (GLEON), which calculates vertical profiles of temperature, salinity, density, mixing and surface heating/cooling and considers ice cover effects (BUECHE; HAMILTON; VETTER, 2017; BUECHE *et al.*, 2020; HIPSEY *et al.*, 2019). Despite being limited to one dimension, the GLM is ideal for long-term (seasonal and decades) vertical mixing and stratification studies (HIPSEY *et al.*, 2019). In the category of 3D models, some models have been widely used. This is the case of the Delft3D-FLOW model, which is a multidimensional (2D or 3D) hydrodynamic simulation program that calculates non-stable flow and transport phenomena that result from tidal and meteorological forces in a rectilinear or curvilinear boundary adjusted grid (DELTARES, 2019). The COHERENS model which is an open source three-dimensional hydrodynamic modeling system written in FORTRAN 90, is designed for a wide range

of applications in coastal seas, estuaries, lakes and reservoirs developed by the Management Unit of the North Sea Mathematical Models and the Scheldt estuary (MUMM) and is available at: <http://odnature.naturalsciences.be/coherens/>. The CH3D-WES (Curvilinear Hydrodynamic 3D) model is a 3D hydrodynamic salinity and temperature model that models the key physical processes that affect the circulation and vertical mixing of large water bodies (CHAPMAN *et al.*, 1996). The EFDC (Environmental Fluid Dynamics Code) model is a hydrodynamic model maintained by the United States Environmental Protection Agency (EPA) that can be used to simulate the hydrodynamics of surface aquatic systems in 2D and 3D, the EFDC model simulates fluids of varying density, turbulent flow, salinity and temperature. Recently, the EFDC model was parallelized to provide fast and efficient simulations in high-performance computing structures such as clusters with multiple processors and massively parallel devices (O'DONNCHA; RAGNOLI; SUITS, 2014; AHN *et al.*, 2021a). The IPH-TRIM3D-PCLake model is a three-dimensional hydrodynamic and water quality model developed by Fragoso *et al.* (2009) and maintained by the Institute of Hydraulic Research (IPH) of the Federal University of Rio Grande do Sul. This model has an innovative structure that couples a three-dimensional hydrodynamic module (TRIM3D) and an ecological lake model (PCLake) to describe hydrodynamic, biotic and abiotic components present in the water and sediments of an aquatic ecosystem.

Although the models described above combine efforts to make an accurate description of the hydrodynamics of lakes, lagoons, estuaries and wetlands, the hydrological components generated by catchments need to be calculated externally using hydrological models applied separately, with extensive and manual configurations (LOPES *et al.*, 2018). This compartmentalization makes it difficult to understand how catchment structure and river flows affect the lake hydrodynamic, including local circulation patterns, water levels, and large-scale water quality (RUEDA; MACINTYRE, 2010; MUNAR *et al.*, 2018), since the main water entry routes into the lake system are adjacent rivers whose flows depend on the catchment hydrology (FRASSL *et al.*, 2019; KIM *et al.*, 2012). According to Janssen *et al.* (2019) the catchment hydrology influences the spatial heterogeneity of nutrient loads, as the sources of water entering lakes can be local or widely dispersed, which determines the distribution of nutrients in the water body. In addition, in the nutrient transport process, high flow rates limit biological conversion, allowing greater nutrient spread, and low flows favor local retention, reducing nutrient contributions to the aquatic ecosystem. A way of representing the catchment hydrology together with the hydrodynamics of the lakes can be obtained by coupling hydrological and hydrodynamic models (KIM *et al.*, 2012; MUNAR *et al.*, 2018). The coupling of hydrological and hydrodynamic models has gained more attention in the last decade due to the growing importance of lake systems (HWANG *et al.*, 2021; LI *et al.*, 2014; TIAN *et al.*, 2019).

To explore the state of the art in "coupled hydrological and hydrodynamic modelling", in this dissertation a literature review was carried out that considered 90 publications

carefully selected from a total of more than 500 documents obtained from the Scopus and Web Of Science databases. Publications from 2010 to 2021 in English-language scientific journals, with peer review and impact factor greater than 2.5, were selected. Other filters for the selection of publications involved analysis of titles and abstracts. In which only works that had hydrodynamic and hydrological modeling applications in real cases involving lake ecosystems were kept.

Figure 1a shows the global distribution of hydrological and hydrodynamic modeling studies. The locations marked on the map correspond to the location of the lake, lagoon or estuary where the modeling studies were carried out, which corresponds to a total of 50 water bodies distributed in 22 countries on 5 continents. Figure 2 can be used in a complementary way to identify the name, scale and type of main water bodies. For this, it is necessary to look at the number of studies in parentheses, which coincide with the color scale of Figure 1a.

The numbers presented in Figure 1a correspond to the total number of studies that involved hydrodynamic modeling or coupled hydrological and hydrodynamic modeling. Figure 1b shows that most hydrological and hydrodynamic modeling studies took place in water bodies located in China (36 studies), followed by the United States (17 studies), Brazil (7 studies) , Italy (6 studies) and France (3 studies). Also in Figure 1b, the countries grouped into two categories are shown: (i) countries in which only hydrodynamic modeling studies were carried out; and (ii) countries in which coupled hydrological and hydrodynamic models are used. The bar plot shows the countries that had publications of hydrological and hydrodynamic modeling studies in the same case study. The number of applications of coupled models is also shown, because not necessarily all studies that had hydrological and hydrodynamic modeling involved the coupling of models. Only a small part of the studies involved the application of coupled hydrological and hydrodynamic models, which are distributed in lake ecosystems located in the following countries: China (6 studies), Brazil (4 studies), South Korea (3 studies), the United States (2 studies), Cambodia (1 study) and Norway (1 study).

Figure 1 – Global distribution of modeling studies in lake ecossistems. a) Number of hydrodynamic models applications. b) Number of hydrologic model aplications. c) Number of coupled hydrologic-hydrodynamic models applications. The legends show the number of models applications per lake and lagoon systems around the world. The sizes of the circles are proportional to the number of studies carried out in each location, which are also differentiated through the different colors.

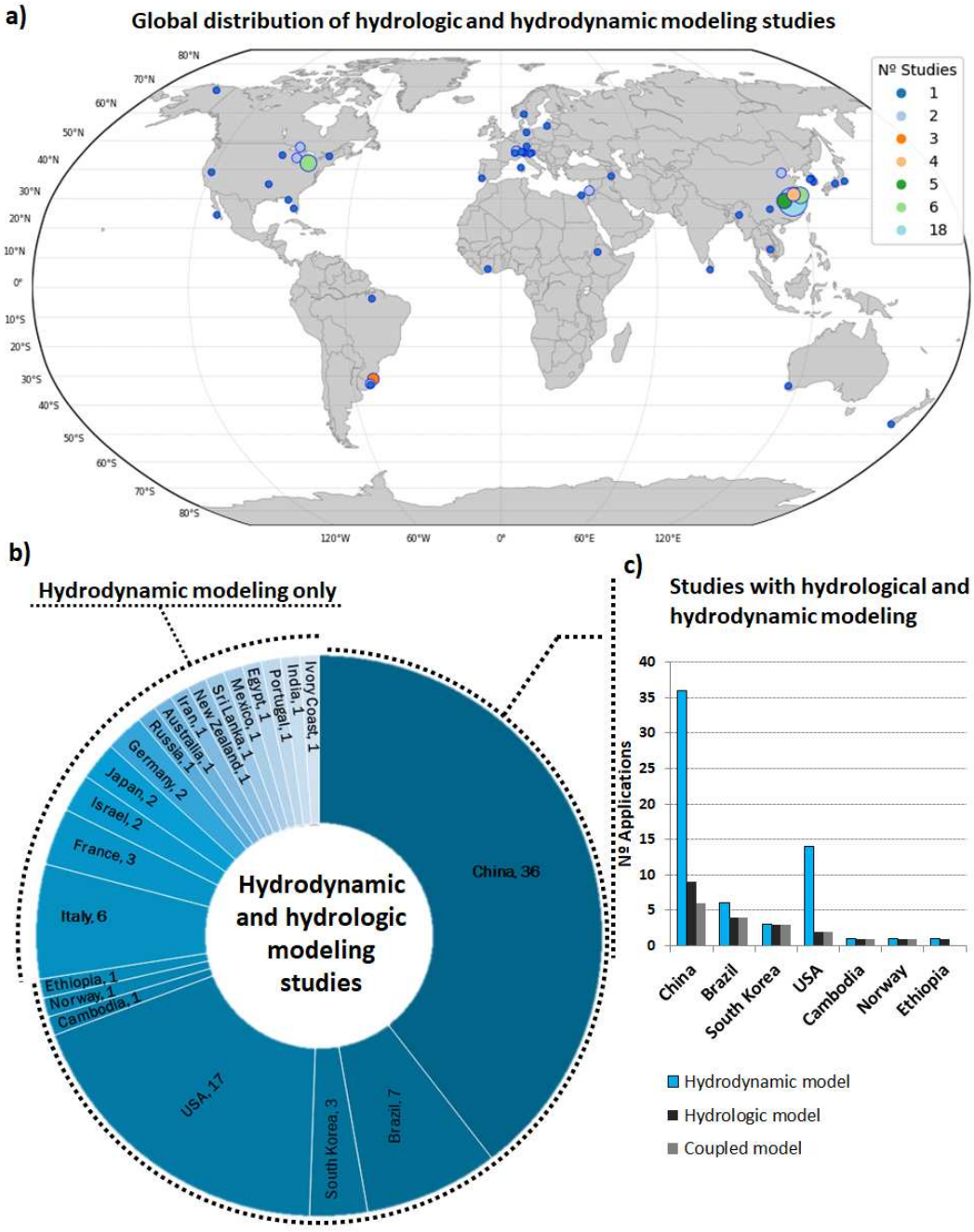

Source: Prepared by the author.

Figure 2 – Sunburst chart showing the names of water bodies (lakes, lagoons and estuaries) used as a study area in the publications reviewed. Shown here are the water bodies grouped into categories: Small scale, Medium scale and Large sacale according to the classification used by Messager *et al.* (2016). Within each group, the subdivision into types: Freshwater and Saltwater is shown. The number of times each water body served as a study area is shown in parentheses, those that do not have a number are those that appeared only once.

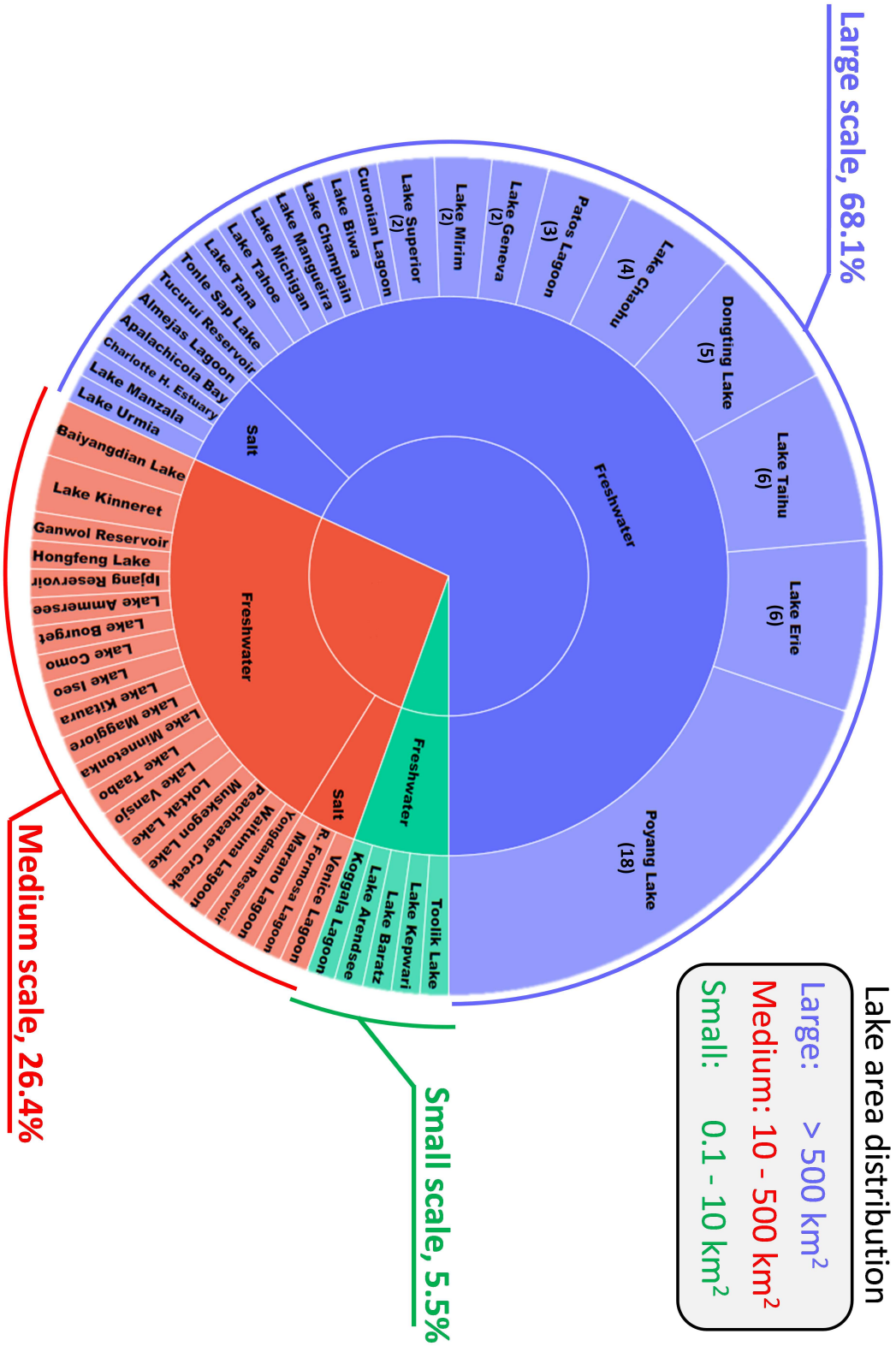

Source: Prepared by the author.

Table 1 shows the main coupled hydrological and hydrodynamic models found in

articles published from 2010 to 2021, the water bodies in which they were applied and the main scientific questions that are being investigated.

Table 1 – Some coupled/integrated hydrological and hydrodynamic models used in works published from 2010 to 2021. The first column contains authors names, the second column contains the names of the models, the third column contains the names of the water bodies and their respective countries and in the fourth column the main scientific questions investigated are presented.

Authors	**Coupled Models**	**Waterbody /Country**	**Main questions**
Hwang *et al.* (2021)	SWAT+EFDC	Ganwol reservoir/South Korea	How to assess whether water management measures are effective in improving water quality in estuarine reservoirs?
Munar *et al.* (2018), Munar *et al.* (2019)	MGB-IPH + IPH-ECO	Lake Mirim/Brazil	How can coupled hydrological-hydrodynamic modeling and satellite data help to understand the spatial and temporal variability of lake water surface temperature?
Shin *et al.* (2019)	SWAT+EFDC	Ipjang reservoir/South Korea	How to model sediment transport processes from loading in the catchment to mixing and sedimentation in the reservoir or lake?
Tian *et al.* (2019)	SWAT + MIKE 21	Hongfeng Lake/China	How to quantify the risk of pollution incidents in a lake catchment?
Lopes *et al.* (2018)	MGB-IPH (river-lake modeling)	Patos Lagoon/Brazil	Is it possible to simulate rivers, lakes and lagoons with one integrated hydrological-hydrodynamic model and coherently estimate water levels and inundated areas?

Continues on the next page

Table 1 - Continuation.

Authors	Coupled Models	Waterbody /Country	Main questions
Huang *et al.* (2016), Huang *et al.* (2018)	Xinanjiang model + EFDC	Lake Chaohu/China	(1) Whether one or both nutrients should be reduced for controlling harmful algal blooms (HABs)? (2) When and where to reduce nutrients for controlling harmful algal blooms (HABs)?
Zhang *et al.* (2017)	SWAT + Delft3D	Poyang Lake/China	How to estimate and verify stream flow at lake borders in ungauged zones?
Zia *et al.* (2016)	Integrated Assessment Model (IAM)	Lake Champlain/USA	How do the effects of global climate change combined with land cover changes influence hydrology and nutrient fluxes for freshwater lakes at catchment scale?
Couture *et al.* (2014)	Catchment-Lake model network	Lake Vansjo/Norway	How do climate change and land use influence river basin responses and lake water quality?
Kummu *et al.* (2014)	Analytical model +EIA 3D	Tonle Sap Lake/Cambodia	How do changes in hydrological regimes influence lake hydrodynamics?
Li *et al.* (2014)	WATLAC + MIKE 21	Poyang Lake/China	How can the coupling of hydrological and hydrodynamic models help to understand the relationship between lake water levels, catchment processes and the hydraulic connection between lakes and rivers?

Continues on the next page

Table 1 - Continuation.

Authors	Coupled Models	Waterbody /Country	Main questions
Kim *et al.* (2012)	tRIBS + OFM	Peacheater Creek/USA	How to predict the spatial and temporal hydrological response to imposed climate change scenarios, variations in land use, soil and vegetation types in small to large-scale catchments?
Lee *et al.* (2012)	GCM A2 + HSPF + CE-QUAL-W2	Yongdam reservoir/South Korea	How do the effects of climate change influence the thermal structure of the lake when interactions with catchment flows are considered?
Fragoso *et al.* (2011)	IPH-TRIM3D-PCLake	Lake Mangueira/Brazil	What are the effects of increased nutrient loadings in conjunction with climate changes on the trophic structure of a large subtropical lake?

A brief description of the studies listed in Table 1 is presented below. Hwang *et al.* (2021) used SWAT-Environmental Fluid Dynamics Code (EFDC) linkage to evaluate the water quality improvement scenarios considering the agricultural system and nonpoint source pollution of the upper Ganwol estuarine reservoir catchment located in South Korea. Munar *et al.* (2018) performed the coupling between a large-scale distributed hydrological model (MGB-IPH - Collischonn *et al.*, 2007) and a hydrodynamic model (IPH-ECO - Fragoso *et al.*, 2009). The coupled model was able to simulate the dynamics of a large lake in synergy with the hydrology of adjacent catchments using satellite altimetry and gauge data. The authors highlighted the importance of integrated hydrological-hydrodynamic modeling approaches to improve the understanding of the factors that control the hydrodynamic processes in lakes in the long term from simultaneous assessments of wet and dry periods or seasonal variations. In addition to quantifying the effects of external forcing on the lake's hydrodynamic processes, the approach used allowed the prediction of flows in ungauged areas, showing a better representation of the highest volumes of discharge. Shin *et al.* (2019) developed a framework that couples the Soil and Water Assessment Tool (SWAT) model with a hydrodynamic lake model, Environmental Fluid Dynamics Code (EFDC) to carry out the modeling of sediments in the catchment coupled with the

hydrodynamics of a receiving lake. They also demonstrated how to quantify uncertainty in integrated sediment modeling using the Generalized Likelihood Uncertainty Estimation (GLUE) approach. Tian *et al.* (2019) developed a coupled model composed of the Seveso III Directive (European Council's third revision of the Seveso Directive) and the SWAT and MIKE21 models to assess the environmental risk of pollution incidents in quantitative terms around Lake Hongfeng which is an important source of drinking water. Lopes *et al.* (2018) presented a modified version of the MGB-IPH model that includes wind effects. They performed modeling experiments in the Patos Lagoon catchment (integrated catchment-lagoon modeling) considering wind and no wind scenarios and tests with different input datasets. Huang *et al.* (2016) and Huang *et al.* (2018) coupled a 2D hydrological model (Xinanjiang) and the EFDC hydrodynamic model in which the Xinanjiang model simulate six inflow discharges for the boundary conditions of a hydrodynamic model to investigate the impacts of a water transfer project on the water transport pattern of Lake Chao, China. Zhang *et al.* (2017) coupled the soil and water assessment tool (SWAT) and the Delft3D model to simulate the interactions between water flows in ungauged zones of the catchment and Lake Poyang in China. Zia *et al.* (2016) developed an cascading integrated assessment model (IAM) to quantify the impact of temperature variability and precipitation as well as changes in land cover on nutrient load and frequency of harmful algal blooms (HABs) in Lake Champlain. To develop this study they used Global Circulation Models (GCMs) and a distributed hydrological model RHESSys (TAGUE; BAND, 2004) to estimate the flows and nutrient loads of the Lake Champlain catchment. Subsequently, the nutrient dynamics in Lake Champlain were simulated by hydrodynamic (EFDC - Hamrick, 1992) and biogeochemical (Row Column AESOP (RCA)) models. Couture *et al.* (2014) developed a framework of linked models to integrate climatic, hydrological, and hydrodynamic processes. First, a Global Climate Model (GCM) is used to estimate daily temperatures, precipitation and other regional hydroclimatic variables. These results are used as inputs for the rainfall-runoff hydrological model (PERSiST - Futter *et al.*, 2014) which calculates the daily flow values in the catchment to be used as inputs in the INCA-P model (WADE; WHITEHEAD; BUTTERFIELD, 2002) used to simulate the daily flows of suspended sediments and P for the lake. In the end the MyLake model (SALORANTA; ANDERSEN, 2007) calculates the hydrodynamic processes in the lake. They used this modeling framework to simulate total phosphorus loads and chlorophyll concentrations in Lake Vansjo, southern Norway. Li *et al.* (2014) coupled the water flow model for lake catchments (WATLAC) with the MIKE 21 hydrodynamic model to develop a physical model for Lake Poyang and its catchment in order to investigate the effects of catchment hydrology on lake hydrodynamics. Kim *et al.* (2012) coupled a distributed hydrological model that represents surface and subsurface water flows in catchments called tRIBS (TIN (Triangulated Irregular Network)-Based Real Time Integrated Basin Simulator) (IVANOV *et al.*, 2004) with the OFM hydrodynamic model (Overland Flow Model) (BRADFORD; KATOPODES, 1999), resulting in the tRIBS-OFM model.

The model formulation uses unstructured triangular mesh that allows dealing with complex topographies to represent partially wet areas and low flow conditions providing a seamless transition between hydrometeorological boundary conditions and those necessary for hydrodynamic simulation at the catchment scale. Lee *et al.* (2012) coupled the HSPF hydrological model (BICKNELL *et al.*, 2001) and the CE-QUAL-W2 hydrodynamic water quality model (COLE; BUCHAK, 1995) in a framework that also includes the global climate model (GCM A2). In this way they were able to study the effects of climate change on the Yongdam Reservoir lake with respect to variability in epilimnetic temperature, thermocline magnitude, and lake stratification. Fragoso *et al.* (2009) developed the coupled model IPH-TRIM3D-PCLake, which represents in an integrated way the hydrodynamic, water quality and biological processes of a lake. This model consists of a three-dimensional hydrodynamic module coupled to an ecosystem module. Fragoso *et al.* (2011) also applied this model to simulate the potential effects of nutrient enrichment and climate change on the trophic structure of Lake Mangueira.

Based on Figure 1b it is clear that few studies consider coupled hydrological and hydrodynamic modeling. One possible reason is that coupled hydrological and hydrodynamic models present a high computational demand and, consequently, result in time-consuming simulations (LOPES *et al.*, 2018; SHIN *et al.*, 2019). The use of high-performance computing in coupled models still remains an understudied topic and has hardly been explored in the models presented in Table 1. Such studies indicate that the coupling of hydrological and hydrodynamic models is a promising way to study lake ecosystems and becomes increasingly viable. However, the applicability of coupled hydrological and hydrodynamic models can be improved when high-performance computing methods and techniques are used (CARLOTTO; SILVA; GRZYBOWSKI, 2019; CARLOTTO *et al.*, 2021; O'DONNCHA; RAGNOLI; SUITS, 2014; O'DONNCHA *et al.*, 2019).

2.2 HIGH PERFORMANCE COMPUTING

According to the report by the National Energy Research Scientific Computing Center (NERSC), to explore problems that require large computational processing capacity, it is often necessary to use high performance computing (HPC), through structured computational models to take advantage of the capacity of multiple computers simultaneously, employing parallel computing techniques (NERSC, 2013).

The concept of parallel computing refers to the idea that large problems can be divided into smaller problems to be solved independently and on different processors that operate simultaneously to perform a large amount of calculations in reduced time (BARNEY, 2016). The main interest of using these techniques is to obtain an increase in the speed of numerical solutions of equations that represent real phenomena and with that to obtain a better representation of the physical systems, using larger and more refined grids, calibration and uncertainty analysis with several simulations and tests with large amounts

of data, conditions and parameters (VANKA, 2013). In this context, several publications have shown the advantages of parallel computing structures applied in simulations of environmental phenomena related to hydrodynamics (LE *et al.*, 2015; CARLOTTO *et al.*, 2021; O'DONNCHA; RAGNOLI; SUITS, 2014; O'DONNCHA *et al.*, 2019). In addition, high-performance computational models play a key role in reducing scientific problem solving time and broadening the prospects of finding effective engineering strategies to contain or minimize the consequences of environmental disasters (BRODTKORB; SÆTRA; ALTINAKAR, 2012; HORVÁTH *et al.*, 2014).

2.2.1 Parallel computing in MPI

Message Passing Interface (MPI) is one of the most used option to enable the programming of parallel scientific applications. MPI enables a large number of applications in scientific research in the most varied fields of knowledge, ranging from medical sciences to geosciences and engineering (BALAJI; CASAS, 2019). MPI emerged between 1992 and 1994 for use in C and Fortran codes. It has since been refined and expanded to most programming languages, including Perl, Python, Ruby, and Java (FARBER, 2011). MPI consists of a set of routines and libraries to be called in programs implemented in a compatible programming language. MPI programs generally use a type of communication called single-program, multiple-data (SPMD) in which multiple MPI instances of the same program run simultaneously. In programs implemented with MPI, usually a large problem is broken into several smaller problems that are solved at different ranks using MPI for data communication (JEFFERS; REINDERS, 2013). The rapid development of large computational structures for parallel processing has allowed the resolution of problems of increasing size and complexity in which MPI is generally used as the main form of communication between the various processors (nodes) (QUARANTA; MADDEGEDARA, 2021).

2.2.2 Parallel Computing in GPGPU

General purpose graphics processing units GPGPU feature great parallel processing power and have been increasingly used to solve scientific problems (BRODTKORB; SÆTRA; ALTINAKAR, 2012; HORVÁTH *et al.*, 2014; LE *et al.*, 2015). Consequently, systems adapted to the use of languages, libraries and tools (e.g., CUDA) for computing on GPUs have evolved a lot in the last decade, as these devices are found in most desktops and laptops and are used in supercomputers to accelerate computations in many real world applications (BRODTKORB; HAGEN; SÆTRA, 2013).

The demand for high-performance parallel computing has led to the exploration of GPGPUs, which prove to be powerful to accelerate numerical applications, have low cost and are developed with a massively parallel architecture composed of several processing cores, ideal for applications that demand parallel computing (TRISTRAM; HUGHES; BRADSHAW, 2014). According to (NVIDIA, 2016) GPU-accelerated computing allows

to obtain high performance for applications and computational code by transferring the compute-intensive parts to the GPU which will execute them in parallel by thousands of processing cores while the rest of the code continues to be executed by the CPU sequentially.

The main difference between a GPU and a CPU is in the way they process tasks. A CPU has a few cores optimized for serial (sequential) processing, while a GPU has a massively parallel architecture consisting of thousands of more efficient cores designed to handle multiple tasks simultaneously. In addition, they provide large memory bandwidths, are designed to accelerate image processing applications and to perform intensive computation across a large number of processing cores, and generally require less hardware resources (SMARI *et al.*, 2016). These characteristics allow a great capacity for GPUs to perform parallel computation in intensive numerical operations, which has driven the development of ways to exploit them to perform general-purpose computational tasks in solving real world problems.

2.2.2.1 The CUDA architecture

In GPUs developed by the company NVIDIA, access to resources to accelerate numerical applications occurs through the Compute Unified Device Architecture (CUDA). This is the architecture by which NVIDIA has developed GPUs that can perform both traditional graphics rendering tasks and general-purpose tasks (scientific computing, engineering, among others) using a programming language called CUDA C/C++ which is essentially the C or C++ programming language with various extensions that allow programming on massively parallel devices such as GPUs (NVIDIA, 2016).

3 SW2D-GPU: A TWO-DIMENSIONAL SHALLOW WATER MODEL ACCELERATED BY GPGPU

ABSTRACT[1]

Shallow water models are used for simulating flood and lake hydrodynamics. However, the computational cost of those models is often high and require high performance computing. We present the SW2D-GPU: a two-dimensional shallow water model accelerated by General Purpose Graphics Processing Unit. The model is implemented in parallel using CUDA C/C++. We exemplify the use of the model with two case studies: (i) Flood simulation in an urban area and (ii) water level simulation in a lake catchment. We have included potential evaporation in the formulation which expands its application to water level simulations in lakes and reservoirs. The SW2D-GPU model is approximately 34 times faster than its equivalent sequential version. The model can be run in any computer equipped with a NVIDIA GPU. Integrated simulations of surface waters in lake catchment and simulations of floods caused by dam break are some of the potential applications.

3.1 INTRODUCTION

The shallow water equations are the mathematical basis for many hydrodynamic models. Their applications ranging from the estimation of water level in rivers and lakes to the spatiotemporal evolution of floods (YU *et al.*, 2019; LIU; ZHANG; LIANG, 2019; FERRARIN; BAJO; UMGIESSER, 2020). However, model instability in complex topographies and long simulation times hinder their application in real cases studies (HORVÁTH *et al.*, 2014; LIU; QIN; LI, 2018). A common way to reduce simulation time is to use the two-dimensional (2D) formulation of the shallow water equations (THANG *et al.*, 2004; LEE *et al.*, 2014; LEE *et al.*, 2016). Yet, even 2D formulations might be prohibitive in computational domains typical of hydrological applications (LIU; ZHANG; LIANG, 2019; ECHEVERRIBAR *et al.*, 2019).

High performance computing (HPC) and codes suitable for parallel processing are the best alternative for accelerating numerical solutions (SMARI *et al.*, 2016). Most codes that approximate the solution to the shallow water equations are developed using sequential processing or parallelization schemes based on Message Passing Interface (MPI) or Open Multi-Processing (OpenMP) compatible with clusters composed of several Central Processing Units (CPU) (O'DONNCHA; RAGNOLI; SUITS, 2014; ANGUITA *et al.*, 2015; NOH *et al.*, 2018; NOH *et al.*, 2019; O'DONNCHA *et al.*, 2019). Recently, massively parallel devices such as the General Purpose Graphics Processing Unit (GPGPU) have been shown highly efficient to accelerate the solution of shallow water equations and environmental models with application in real world phenomena (BRODTKORB *et al.*, 2010; RANSOM; YOUNIS, 2016; VACONDIO *et al.*, 2017; CARLOTTO; SILVA; GRZYBOWSKI, 2019; DAZZI; VACONDIO; MIGNOSA, 2020).

GPUs are found on most personal computers and offer great computing power with thousands of processing cores (BRODTKORB; HAGEN; SÆTRA, 2013; SMARI *et al.*,

[1] This Chapter is adapted from: Carlotto *et al.* (2021).

2016). Consequently, systems adapted for the use of languages, libraries, and tools (e.g. CUDA C/C++, CUDA-Fortran) for computing in GPUs have evolved considerably in the last decade (BRODTKORB; HAGEN; SÆTRA, 2013; XIA; LIANG; MING, 2019). CUDA technology facilitates code parallelization and use of GPGPU to accelerate numerical solutions. Equally important are the unified API for HPC code development such as the one presented by O'Donncha *et al.* (2019) used for parallelization and development of complex code in large computational domains. However, each parallelization method has positive and negative aspects. OpenMP is simple to implement, but has limited scalability due to the size of shared memory; MPI is highly scalable for large problems, but increased communication between CPUs reduces computational performance; CUDA language for GPU computing is easy to implement and provides great parallel computing power at low cost, but processing on GPU is limited by memory constraints (NOH *et al.*, 2018; XIA; LIANG; MING, 2019).

Several model implementations harness the computing power of the GPU to approximate the solution of equations that govern the water flow in Earth system. An implementation of the 2D diffusive wave model was developed using CUDA-Fortran resulting in a speed-up of approximately 150 times (PARK; KIM; KIM, 2019). Hybrid CPU-GPU parallel computing was used to develop the Dhara model (LE; KUMAR, 2017) that couples an integrated surface and subsurface flow model numerically resolved by the Alternating Direction Implicit (ADI) scheme (GCS-flow - Le *et al.*, 2015) implemented in CUDA C/C++ and an Ecophysiological Multilayer Canopy Model (MLCan - Drewry *et al.*, 2010) implemented in MPI for parallel processing in CPU. The Dhara model combines the effects of microtopography and climate change on small-scale eco-hydrological dynamics using the advantages of MPI and GPU parallel computing for high performance in large-scale simulations. Ming *et al.* (2020) developed a real-time flood prediction system by coupling a numerical weather prediction model with a hydrodynamic model based on 2D shallow water equations solved using Godunov-type finite volume scheme with GPU implementation. In their approach, parallel computing on multiple GPUs was used to overcome the physical memory limitations of a single GPU (XIA; LIANG; MING, 2019).

In hydrological and hydrodynamic modeling, GPGPU-accelerated models allow high-resolution simulations which can lead to better process representation. In the case of lake ecosystems, for example, rainfall-runoff is usually modeled separate from lake hydrodynamics and it is imposed as boundary conditions due to computational constraints (ACOSTA *et al.*, 2015; JANSSEN *et al.*, 2019). In flood inundation forecasting, high-resolution computational grids are necessary (NOH *et al.*, 2018; NOH *et al.*, 2019); however, simplifications adopted to reduce the computational cost usually neglect the need for high spatial resolution to simulate flooding in complex terrains (KIM *et al.*, 2012). With the significant gain in processing power offered by GPU, such simplifications may no longer be necessary. The adaptation of models based on shallow water equations that can account for meteorological variables and the interaction of surface water dynamics

between hillslopes, streams, and lakes are a valuable tool for water resources management, especially in catchments with limited data (GU; MA; LI, 2016; MUNAR *et al.*, 2018; JIANG *et al.*, 2019). Moreover, these solutions are relevant for problems such as parallelizing and updating models with thousands of lines of code (e.g., Weather Research and Forecasting - WRF model) and to improve the representation of hydrological process in Earth System Models (SCHNEIDER *et al.*, 2017). Despite the advances in computing technologies that provide great parallel processing power at low cost, effort is still needed to update and develop hydrological and hydrodynamic model codes compatible with multiple processors and massively parallel devices (O'DONNCHA; RAGNOLI; SUITS, 2014; LE *et al.*, 2015; KUFFOUR *et al.*, 2020).

In order to obtain a high performance 2D shallow water model that simulates hydrological processes in realistic systems using low cost computers, we have developed SW2D-GPU: a two-dimensional shallow water model accelerated by GPGPU. The accelerated model is based on a sequential version previously implemented in Fortran (LEE, 2013; NOH *et al.*, 2016). The new version is suitable for processing in massively parallel devices with CUDA technology. We highlight the applicability and performance of the model using two case studies: (i) flood simulation in an urban area; and (ii) simulation of integrated catchment and lake water levels in response to meteorological data and human interferences. Performance analysis is based on: (i) comparison between the total time that each version of the model (parallel and sequential) takes to complete the test simulations; and (ii) comparison of the computation time of the CUDA kernels processed in the GPU with the equivalent functions of the sequential model executed in the CPU.

3.2 MODEL IMPLEMENTATION

We base our parallel model on a sequential version of a two-dimensional shallow water model previously implemented in Fortran (LEE, 2013; NOH *et al.*, 2016). We have parallelized and completely rewritten the numerical code in the CUDA C/C++ programming language. The parallel version of the model maintains the same order of tasks as the original sequential implementation to provide a performance comparison between the two versions. We propose and implement a formulation to estimate potential evaporation as a function of temperature and solar radiation. Moreover, we include the option of adding an unlimited number of streamflow time series in different locations of the drainage network.

3.2.1 The numerical model

The numerical model is based on the 2D shallow water equations (LEE *et al.*, 2014; NOH *et al.*, 2016). In this formulation the Coriolis strength, the wind resistance, and the viscosity terms are neglected, so that the continuity equation of the two-dimensional shallow water model are:

$$\frac{\partial h}{\partial t} + \frac{\partial M}{\partial x} + \frac{\partial N}{\partial y} = r_{\mathrm{e}} + q_{\mathrm{ex}} - E, \tag{3.1}$$

$$r_{\mathrm{e}} = r - r \times (INF + INT + LWL), \tag{3.2}$$

the momentum equations are:

$$\frac{\partial M}{\partial t} + \frac{\partial (uM)}{\partial x} + \frac{\partial (vM)}{\partial y} = -gh\frac{\partial H}{\partial x} - f_1, \tag{3.3}$$

$$\frac{\partial N}{\partial t} + \frac{\partial (uN)}{\partial x} + \frac{\partial (vN)}{\partial y} = -gh\frac{\partial H}{\partial y} - f_2, \tag{3.4}$$

and the friction terms are:

$$f_1 = \frac{gn^2 M\sqrt{u^2+v^2}}{h^{4/3}}, \tag{3.5}$$

$$f_2 = \frac{gn^2 N\sqrt{u^2+v^2}}{h^{4/3}}, \tag{3.6}$$

where h is the water depth; $H = h + z_{\mathrm{b}}$, where z_{b} is the topographic elevation; $M = uh$ and $N = vh$, where u and v are the velocities in the x and y directions respectively; r_{e} is the effective rainfall; r is the rainfall; INF is the percentage of rainfall infiltration loss; INT is the percentage of rainfall interception loss; LWL is the lake water loses (only in the cells in the lake area and water bodies); q_{ex} is the term that defines the flow into the drainage network; E is the potential evaporation; t is the time; f_1 and f_2 are the friction components where g is the acceleration of gravity and n is Manning's roughness

coefficient. In Equation 3.1 the terms on the right are time-dependent (time series of gauged or calculated data).

The height of water (h_d) that drains in a given section of the channel (i.e., an inlet or outlet of the system) is defined by the following equation:

$$\frac{\partial h_\mathrm{d}}{\partial t} = \frac{Q_\mathrm{d}}{A} = q_\mathrm{ex}, \tag{3.7}$$

where Q_d is accumulated flow at the entrance to the channel and A is the area of the receiving cell.

Potential evaporation is calculated at each time step based on the energy balance method as a function of temperature and solar radiation (CHOW; MAIDMENT; MAYS, 1988), written as follows:

$$E = \begin{cases} \frac{R_\mathrm{s}}{l_\mathrm{v}\rho_\mathrm{w}} \times t_\mathrm{k} \times 1000, & h \geq h_\mathrm{min} \\ 0, & h < h_\mathrm{min} \end{cases}, \tag{3.8}$$

where:

$$R_s = (1-\alpha)R_g,$$

where R_s is net radiation [$\mathrm{Wm^{-2}}$]; R_g is global solar radiation [$\mathrm{Wm^{-2}}$]; α is albedo; l_v is the latent heat of vaporization [$\mathrm{Jkg^{-1}}$]; ρ_w is the density of the water [$\mathrm{kgm^{-3}}$], t_k is the monitoring time interval of the data [s] and h_min is the minimum water depth to activate potential evaporation. The constant 1000 is used to convert the results to millimeters, and t_k adjusts the results to the time interval of the input data.

To estimate the latent heat of vaporization as a function of temperature we use the equation presented in the work of Sellers (1984) written as follows:

$$l_\mathrm{v} = 1.91846 \times 10^6 \times ((T(t) + 273.15)/((T(t) + 273.15) - 33.91))^2, \tag{3.9}$$

where $T(t)$ is the air temperature [°C] observed in time t.

The density of water is calculated as a function of temperature this way (JONES; HARRIS, 1992):

$$\rho_\mathrm{w} = 999.85308 + 6.32693 \times 10^{-2} T(t) - 8.523829 \times 10^{-3} T(t)^2 + \cdots$$

$$+6.943248 \times 10^{-5} T(t)^3 - 3.821216 \times 10^{-7} T(t)^4, \tag{3.10}$$

The Equations 3.8, 3.9 and 3.10 allow estimating potential evaporation as a function of temperature and solar radiation.

The formulation of the model is suitable for simulating the dynamics of surface waters in order to:

Figure 3 – Leapfrog method time-space discretization scheme. $M = uh$ and $N = vh$, where h is the water depth. i and j are the spatial variation indexes in the x and y directions, respectively. t is the time axis and $\triangle t$ is the time interval.

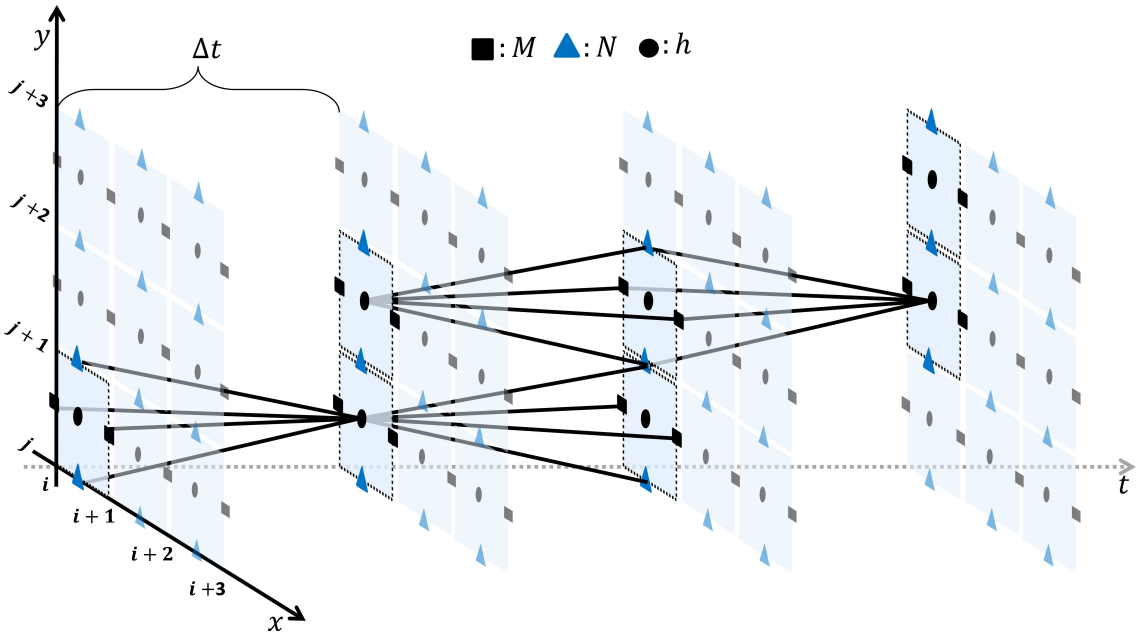

Source: Carlotto *et al.* (2021)

- Study the interactions between the dynamics of surface waters in the catchment and the variation of the water level in the water bodies (e.g. streams, lakes and lagoons);
- Study the influences of the evaporation process on the water level;
- Verify in a simplified way how restrictions on water availability due infiltration losses, interception, and processes within the lake affect the hydrodynamics of the lake.
- Study surface water runoff phenomena (e.g., floods) where this 2D formulation of shallow water equations is valid.

3.2.1.1 Time-space discretization scheme

The time-space discretization of the model uses the Leapfrog method and a finite difference scheme (LEE, 2013; NOH *et al.*, 2016). Figure 3 shows the alternate calculation procedure in which the water depth is calculated at the center of the cell and the flows at the boundaries of the adjacent cells.

Through this scheme the continuity equation (Equation 4.1) can be written as follows:

$$\frac{h^{t+3}_{i+1/2,j+1/2} - h^{t+1}_{i+1/2,j+1/2}}{2\triangle t} + \frac{M^{t+2}_{i+1,j+1/2} - M^{t+2}_{i,j+1/2}}{\triangle x} + \cdots$$

$$+ \frac{N^{t+2}_{i+1/2,j+1} - N^{t+2}_{i+1/2,j}}{\triangle y} = r^{t+2}_{\mathrm{e}_{i+1/2,j+1/2}} + q^{t+2}_{\mathrm{ex}_{\mathrm{i+1/2,j+1/2}}} - E^{t+2}_{i+1/2,j+1/2}, \tag{3.11}$$

where i and j are the spatial variation indexes in the x and y directions, respectively.

A detailed description of the discretization of momentum equations and friction terms can be found in Lee (2013) and Noh *et al.* (2016).

3.2.2 Parallel implementation in GPGPU

We use parallel computing in GPGPU with the CUDA C/C++ programming language and implement in the Visual Studio Community 2013 software programming environment with CUDA toolkit version 8.0. We test the model using a GeForce GTX 1060 graphic card with 1280 CUDA cores and 6 GB of memory running in an Intel *core*® i7 - 7700K CPU with 16 GB of memory. An implementation of the SW2D-GPU model is also available for use with the Linux operational system.

3.2.2.1 Code structure in CUDA C/C++

The main steps of the code in CUDA C/C++ are shown in Figure 4. The parts of the code that demand massive calculations are performed on the GPU with parallel processing and the other parts are performed on the CPU with sequential processing. The sequential version of the model has the same sequence of operations, but all steps are processed in the CPU. To enable the performance comparison with the sequential version that uses double precision, the SW2D-GPU model was also implemented with double precision.

Figure 4 – Model structure implemented in CUDA C/C++. Where t is the time; t_{max} is the maximum time for the simulation and t_{out} it is the time to write the results.

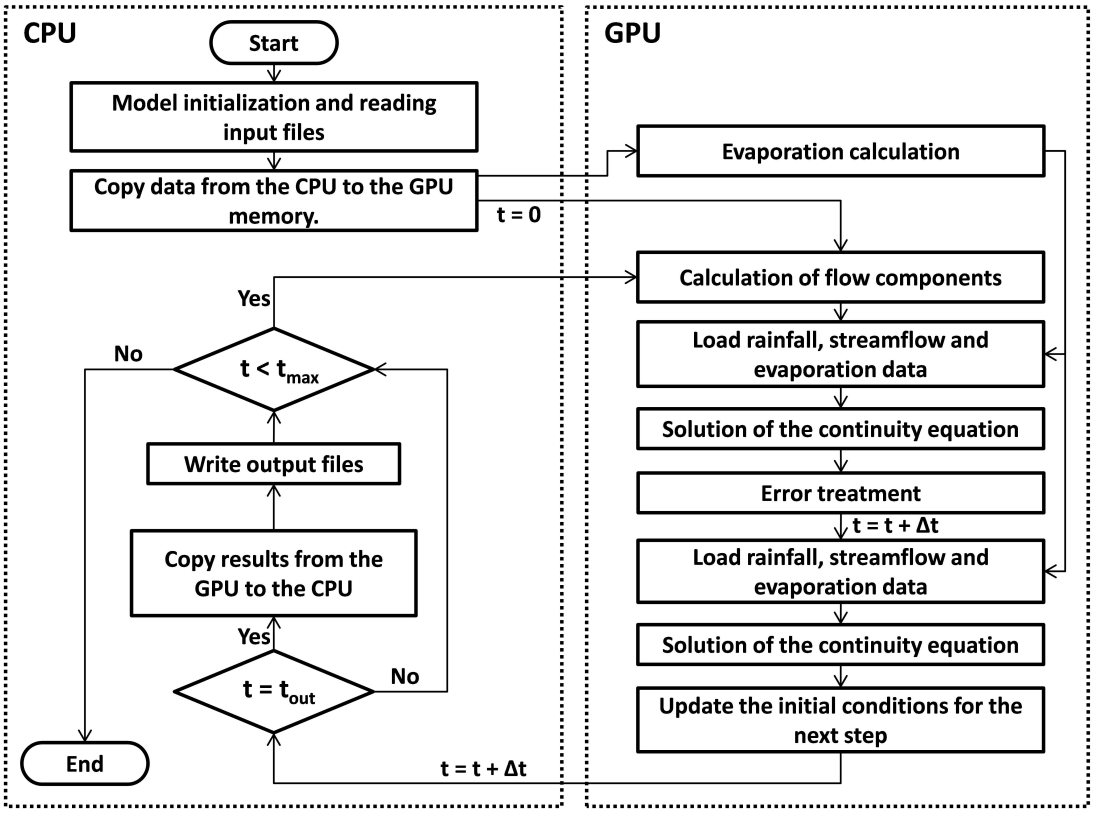

Source: Carlotto *et al.* (2021)

The diagram in Figure 4 illustrates the model structure and the sequence of operations to approximate the solution of the shallow water equations using the Leapfrog method. First, the input data is read and stored in the CPU memory, and then data used in parallel processing in the kernels implemented in CUDA C/C++ is copied to GPU memory. Next, the solution of the shallow water equations is approached iteratively in which the calculations distributed in space are performed in parallel on the GPU, but the temporal evolution occurs sequentially on the CPU, so that the calculations of u, v, and h are performed for all matrix positions alternately according to the Leapfrog method. In this procedure, the CUDA kernels processed on the GPU are called successive times from the CPU iteratively until the solution is approximated using $^1/_{(2\triangle t)}$ iterations for each second of numerical integration, as in each iteration the calculations are performed on $t+\triangle t$ and $t+2\triangle t$ to enable alternate calculations of the Leapfrog method, according to Figure 3. For this, the continuity equation is calculated twice, according to Figure 4. A Courant-Friedrichs-Levy (CFL) condition is required to define the time step ($\triangle t$) that provides the stability of the numerical solution. According to Altaie (2016), for the 2D shallow water equations assuming a Courant number (C) less than 1, the stability condition can be defined according to the following Equation 3.12:

$$\triangle t < \frac{1}{\left(V_{\max} + \sqrt{gh}\right)\left(\triangle x^{-1} + \triangle y^{-1}\right)}, \tag{3.12}$$

where g is the acceleration of gravity, h is the water depth, $\triangle t$ is the time step, $\triangle x$ and $\triangle y$ are the spatial resolutions in the x and y directions, respectively.

Parallel calculations are performed by CUDA kernels through processing entities organized in grids, blocks, and threads. The grid size is equal to the number of blocks needed to cover the entire computational domain. Each block contains multiple threads (e.g., 512, 1024, depending on the GPU). Each thread on the GPU is associated with a specific index so it can access memory locations in an array. In the CUDA kernels of the SW2D-GPU model, we use a 1D indexing scheme in which 2D matrices of m rows and n columns receive linear indexing in row-major order and are treated as vectors of $m \times n$ elements. The linear row-major indexing structure favors the transfer of coalesced memory in which consecutive threads access consecutive memory addresses so that all threads in a warp access global memory at the same time. The linear row-major indexing structure of a 2D array and the distribution of blocks and threads in the parallel code are illustrated in Figure 5.

Figure 5 – Distribution of blocks and threads used in SW2D-GPU code implemented in CUDA C/C++. The block and thread division structure is illustrated for a 4×4 array. Where m is the number of rows and n is the number of columns.

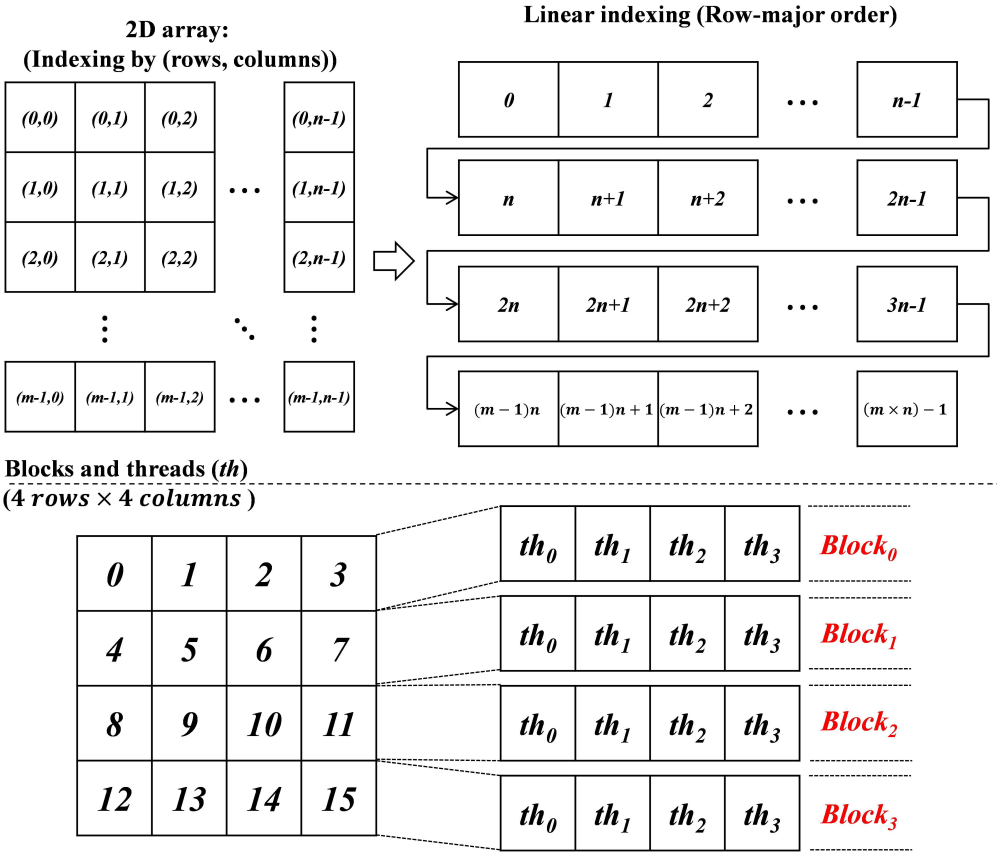

Source: Carlotto *et al.* (2021)

In the GPU used in this work, each block can have a maximum of 1024 threads. Therefore, for an array with less than 1024 elements, a single block with the number of threads equivalent to the number of elements in the array is used. For arrays with more than 1024

elements, multiple blocks with 1024 threads each can be used. The determination of the number of blocks and threads and the calling of a CUDA kernel are exemplified in the pseudo code shown in Figure 6a.

Figure 6 – Structure of a CUDA kernel and calculation of the number of blocks and threads. a) Code for determining the number of blocks and threads and calling the CUDA kernel. b) Structure of a CUDA kernel with 1D indexing. Where TPB is the number of threads per block, NB is the number of blocks, N is the number of elements in the array, and thr_id is the thread index.

a)

Determining the number of threads and blocks

```
if (N < maxThreadsPerBlock){
    TPB = N;
    NB = (N + N - 1) / N;
}
else{
    TPB = maxThreadsPerBlock;
     NB = (N + maxThreadsPerBlock - 1) /
     maxThreadsPerBlock;
}
//Call CUDA Kernel
CUDA_kernel<<< NB,TPB>>>(gpu variables...,N);
```

b)

CUDA Kernel Structure

```
__global__ void CUDA_kernel( gpu variables... ,int N){

int thr_id = blockDim.x*blockIdx.x + threadIdx.x;

      while (thr_id < N){
      //=======
         PROGRAM CODE;
      //=======
      thr_id += gridDim.x * blockDim.x;
      }
}
```

Source: Carlotto *et al.* (2021)

The structure of a CUDA kernel with 1D indexing used in the implementation of the SW2D-GPU model kernels is presented in Figure 6b. Thread indices are calculated as:

$$thr\_id = blockDim.x \times blockIdx.x + threadIdx.x, \tag{3.13}$$

where blockDim.x is the x dimension of the block dimension; blockIdx.x is the x dimension block identifier and threadIdx.x is the x dimension thread identifier. The while loop shown in Figure 6b is used to increment the threads index one grid size ($gridDim.x \times blockDim.x$) at a time, this procedure is called a grid-stride loop which guarantees the uniform distribution of work to the threads and obtaining maximum memory coalescence.

The steps with parallel processing are shown on the right side of the Figure 4. The main CUDA kernels involved in each stage are:

- gpu_evaporation_calc: calculates the potential evaporation from temperature and solar radiation data;
- Flux: calculates flows by approximating the solution of the momentum equations;
- Continuity: performs the solution of the continuity equation;
- Treat_error: performs the correction of small errors in the flow components at the dry/wet boundaries;

- hm_hn, uu1_vv1, uua_vva: perform the calculation of depth values and water velocity components in the x and y directions;
- Forward: updates the initial conditions for solving the shallow water equation in the next time step.

3.2.2.2 Input and output data

The SW2D-GPU has four categories of input data:

- Topographic data: a file containing the elevations of the terrain is a mandatory entry for the model, bathymetry must be included in areas where there are lakes or water bodies.
  - digital elevation model (DEM) [m]: model works with DEM in a wide range of spatial resolutions.
- Hydrometeorological data: temperature and solar radiation data is necessary if evaporation process is considered.
  - rainfall [mm]: the duration of the simulation and the temporal resolution will be defined based on the period and the temporal resolution of the rainfall data series.
  - temperatures [°C]: temperature data is only needed when the evaporation process is active.
  - solar radiation [Wm^{-2}]: solar radiation data is only needed when the evaporation process is active.
  - inflow and outflow [m^3s^{-1}]: the model allows to inform water inlet or outlet at points where monitored data are available. Water flows entering the computational domain are defined as positive and water flows exiting the domain are negative.
- Initial and boundary conditions:
  - initial water level [m]: to start the simulation it is necessary to inform the initial water level in the lake. This entry is made using a raster map with the same dimensions as the DEM.
  - Boundary condition of known value (Dirichlet boundary condition) [m]: a known water level value is reported in a given location, which can be a point where the water level remains constant after reaching a threshold. Usually at the outlet of the catchment or at some point of interest with a specified value.
- Parameters:

- manning roughness coefficient: this coefficient controls the friction terms of the shallow water model, it can be a value chosen according to the characteristics of the catchment, aspects of the channel through which the water flows and the soil cover.
- albedo: this parameter is variable according to the ability of the medium to reflect incident radiation. The albedo is less than 1 and depends not only on the characteristics of the surface but also on the angle of incidence of light.
- lake water losses [%]: percentage of water losses inside the lake during rainfall events (e.g. seepage or evaporation during rainfall).
- rainfall interception loss [%]: percentage of evaporation loss due to rainfall intercepted by vegetation.
- infiltration [%]: percentage of rainfall that infiltrates into the catchment and does not contribute to overland flow or the inflow of water into the lake.

The outputs of the 2D shallow water model are saved in the .vtk format (data file format used in the Visualization Toolkit - VTK, https://vtk.org/ which is designed to provide a consistent data representation scheme for a variety of data set types). The main outputs are:

- Velocity in the x direction [m]: matrix that stores velocity values in the x direction.
- Velocity in the y direction [m]: matrix that stores velocity values in the y direction.
- Water level [m]: matrix that stores the values of the water level (h) above the soil surface.

The results are saved in a sequence of files called Results_ "file number" .vtk. File numbering is sequential and unitary (0,1,2,3 ... n). The real time is obtained by the product between the file number and the time interval defined for saving the results.

3.2.2.3 Post-processing

Post-processing and visualization of model results saved in .vtk files can be performed with any open source software that offers high performance features for viewing large data sets such as VisIt (https://wci.llnl.gov/simulation/computer-codes/visit/) or ParaView software (https://www.paraview.org/).

3.3 CASE STUDY 1: URBAN INUNDATION

We applied the SW2D-GPU model for the simulation of flooding in the urban area (hatched area in Figure 7c) of the Federal University of Santa Catarina (UFSC). The UFSC catchment is approximately 4.09 km^2 with eight contributing sub-basins ranging from 0.07 km^2 to 1.19 km^2. In the study area, the concentration time is approximately 28

min, and the largest drainage channel is approximately 4 km long (MONTEIRO *et al.*, 2021). The low area of the catchment is urbanized with main drainage channels rectified with concrete walls and bottom. In this application, the SW2D-GPU model was configured to consider a precipitation event homogeneously distributed in space and eight points with known streamflows over the drainage network that supplies the UFSC campus area.

Figure 7 – Federal University of Santa Catarina (UFSC) catchment and Peri Lake catchment. a) Geographical position of the city of Florianópolis on a map of South America and position of the Peri Lake catchment and UFSC catchment on the map of the Florianópolis. b) Elevation map of the UFSC catchment. c) Land cover map in which the hatched region corresponds to the UFSC campus area. Points P1, P2, P3, P4, P5, P6, P7 and P8 mark the locations with known streamflows. d) Elevation map of the Peri Lake catchment and stream network. e) Land use map where the location of the weather station, rainfall interception plot, and the location of the water extraction point for urban supply are shown.

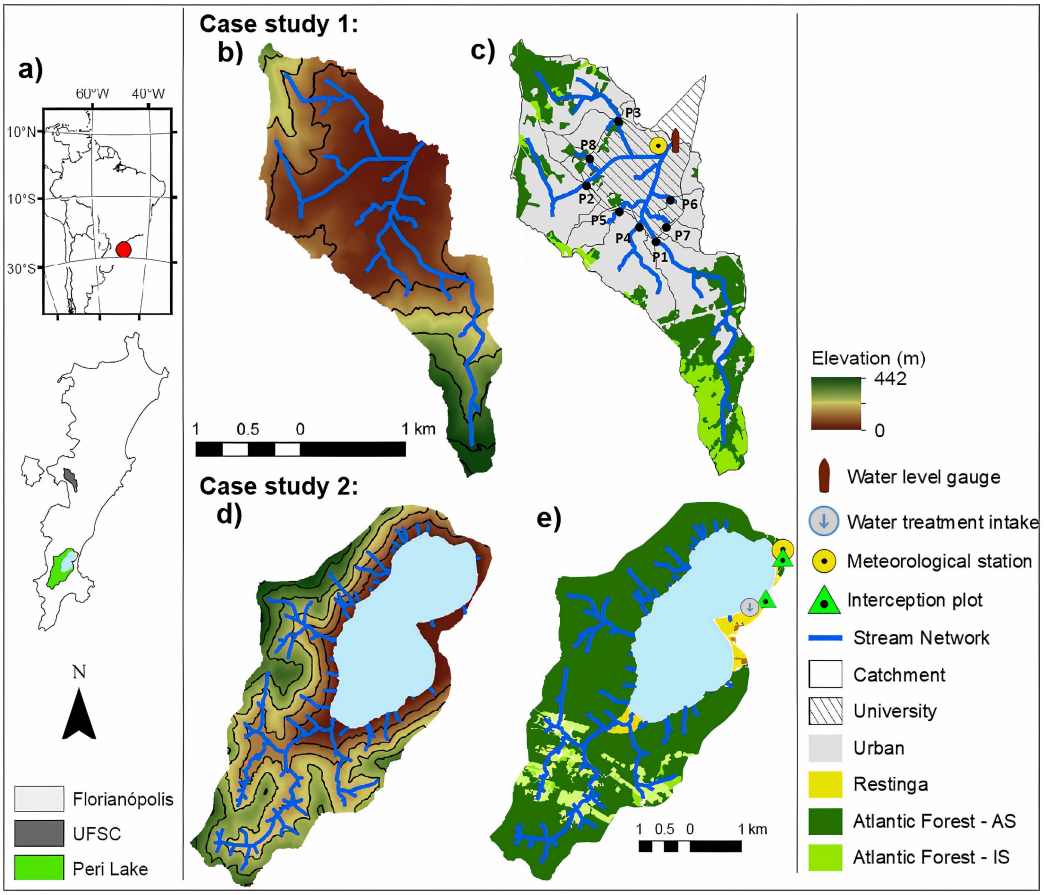

Source: Carlotto *et al.* (2021)

3.3.1 Input data

The digital elevation model (DEM) in this case study (Figure 8a) has a spatial resolution of 1 meter (*Sistema de Informações Geográficas de Santa Catarina*-SIGSC; SDS, 2016). Figure 8a shows the DEM for the active cells that define the computational domain with 893330 grid points in a matrix of 1588 rows and 1189 columns.

To obtain the initial condition of the water levels in the study area, we perform a simulation of a period of 1 hour with constant baseflow values in the 8 points distributed according to Figure 8a. For the simulation of the flooding process, we use the unit hy-

drograph to derive the streamflow for the eight sub-basins that drain to the study area (Figure 8b).

Figure 8 – Model inputs for the flood simulation. a) Digital elevation model (DEM) and points with observed streamflows used as model inputs (P1, P2, P3, P4, P5, P6, P7 and P8) and points for recording the variation of water levels during the simulation (WL1, WL2, WL3). b) Graph showing the amounts of rainfall and the inflows of the model at each point over time.

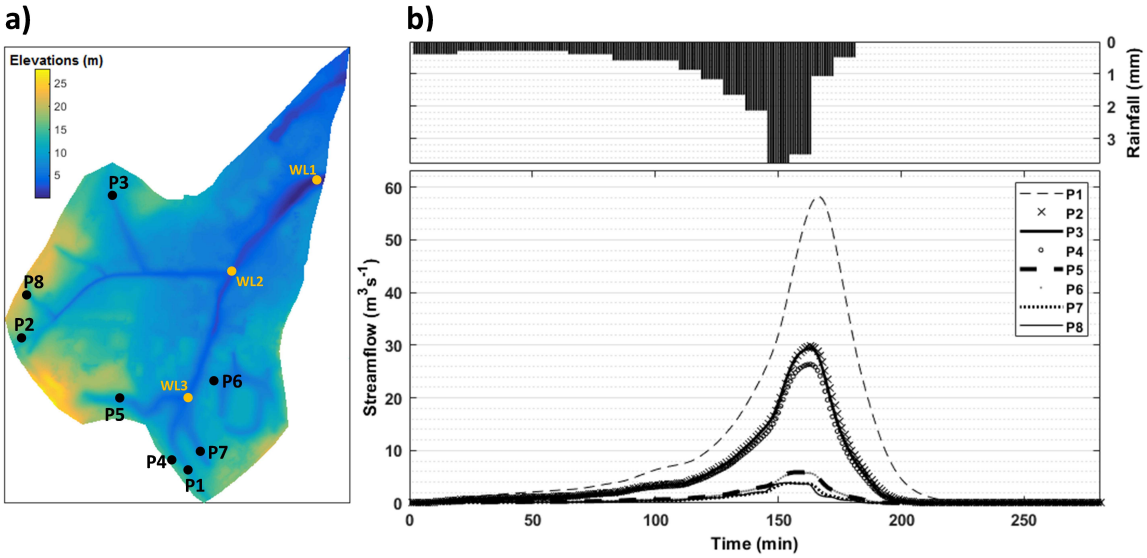

Source: Carlotto *et al.* (2021)

The rainfall and streamflow in Figure 8b are the main inputs for this case study. Streamflow is inserted into the system at the locations defined by points P1, P2, P3, P4, P5, P6, P7 and P8 (Figure 8a). At locations near the junctions of the channels we define points WL1, WL2 and WL3 to record changes in water level during the simulation. At the outlet of the drainage network near point WL1, we define a boundary in which all the water comes out of the system. As the channels walls and bottom is concrete, we adopt the Manning's coefficient of 0.012. The data is of a period of 4 hours and 41 minutes with rainfall homogeneously distributed in the study area during the first 180 minutes. We use a digital elevation model with a spatial resolution of 1 m for the simulation. To satisfy the Courant-Friedrichs-Levy condition we use a time step of 0.01 s.

3.3.2 Results

The results of the flood simulation in the UFSC campus area are in Figure 9. The SW2D-GPU model simulates the variation of water levels in response to the contribution of eight sub-basins that drain to the study area. Figure 9a shows the simulated water level at points WL1, WL2 and WL3. Choosing the positions of these points (Figure 8a) helps to show how the water level varies along the main channel of the drainage network. For example, point WL1 near the channel outlet reaches higher levels than the intermediate point WL2 and the point WL3 located near the entrance of the channel. These values can help to predict the time when flooding is likely to occur in these regions. The spatio-temporal variation of water levels is shown in Figures 9b to Figure 9g beginning with the

spatial distribution of water levels after 90 minutes of simulation with low intensity rainfall at which the maximum water level reaches 1.30 meters. In Figure 9a small oscillations in the simulated levels are observed, which is a normal behavior for a shallow water simulation. As the rainfall becomes more intense, there is an increase in water levels, as shown in Figure 9. After 165 minutes of simulation, the most critical situation occurs in which some regions of the UFSC campus would be inundated.

Figure 9 – Results of the flood simulation in the UFSC campus area. a) Rainfall and water levels at points WL1, WL2 and WL3. b), c), d), e), f), and g) Water levels after 90, 120, 150, 165, 180 and 195 minutes, respectively. The color map is shown in the upper left corner and represents the water level in meters.

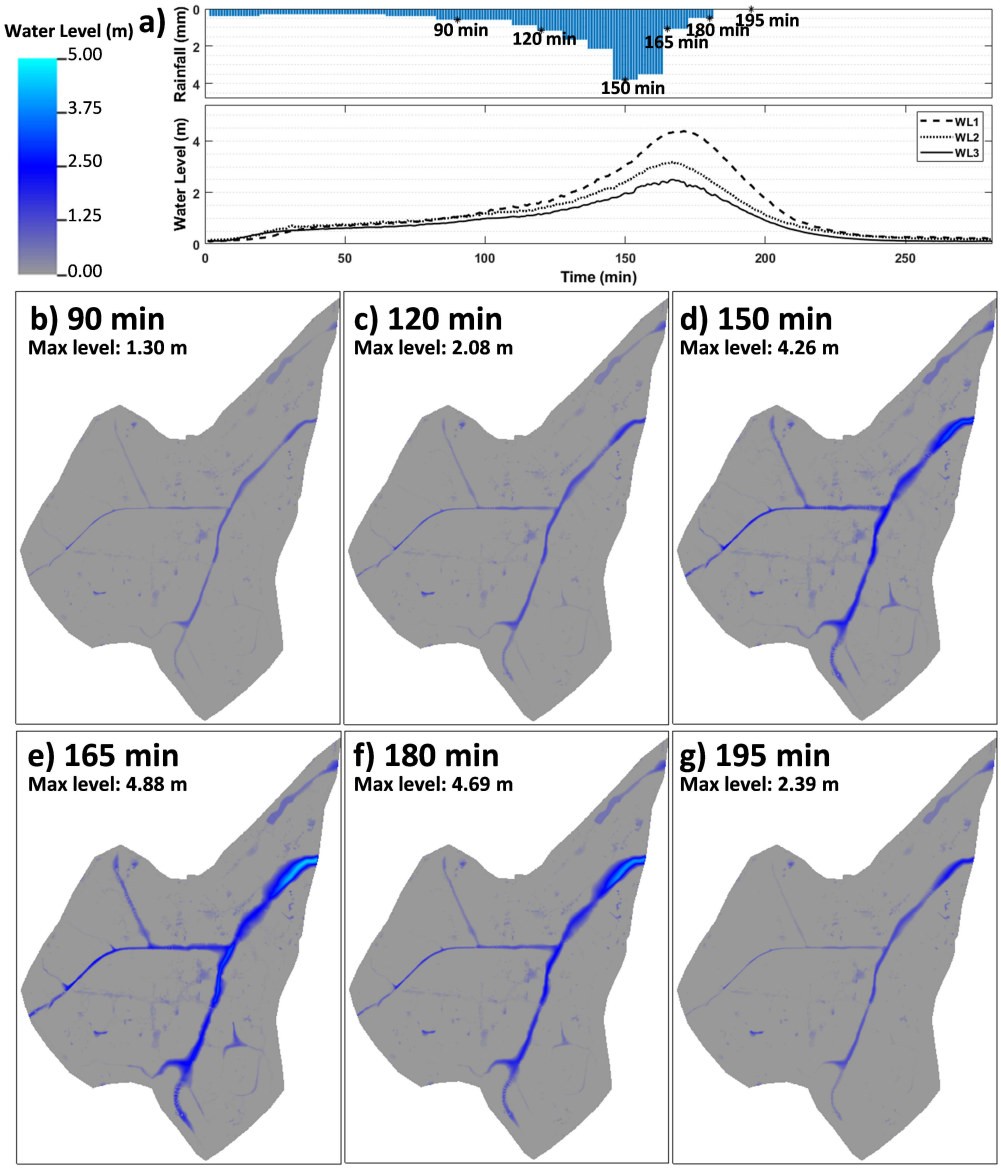

Source: Carlotto *et al.* (2021)

3.4 CASE STUDY 2: INTEGRATED LAKE WATER LEVEL SIMULATION

The Peri Lake catchment is located in Santa Catarina Island (PEREZ *et al.*, 2020; CHAFFE *et al.*, 2021; SANTOS *et al.*, 2021), southern Brazil (Figure 7d) is the largest

source of water supply on the Island and an important ecosystem for biodiversity preservation (SBROGLIA; BELTRAME, 2012). It is located in the transition between tropical and temperate climates, with hot summer, no dry season, with average annual precipitation of 1500 mm. Peri Lake catchment is surrounded by hillslopes covered by some of the remains of Subtropical Atlantic Rain Forest and a sandy Restinga, with a coastal lake with a surface area of 5.7 km^2. The maximum depth of the lake is approximately 11.0 m in the central portion and an average depth of 7.0 m, and no direct seawater influence (HENNEMANN; PETRUCIO, 2011; CHAFFE *et al.*, 2021). The only outflow communication between the Lake and the Atlantic Ocean is via the Sangradouro river, in which the main freshwater is collected to supply the Florianópolis Island (OLIVEIRA, 2002).

In this case study, the SW2D-GPU is used to model the water level variation in Peri Lake. We consider six main fluxes in the water balance: (i) rainfall (R); (ii) evaporation (Ev); (iii) water abstraction for human consumption (WA); (iv) forest interception (INT); (v) infiltration (INF); (vi) lake water losses (LWL). Figure 10 presents a conceptual model of the main processes and hydrometeorological variables in this case study.

Figure 10 – Conceptual model of the processes and variables involved in modeling water levels in the Peri Lake.

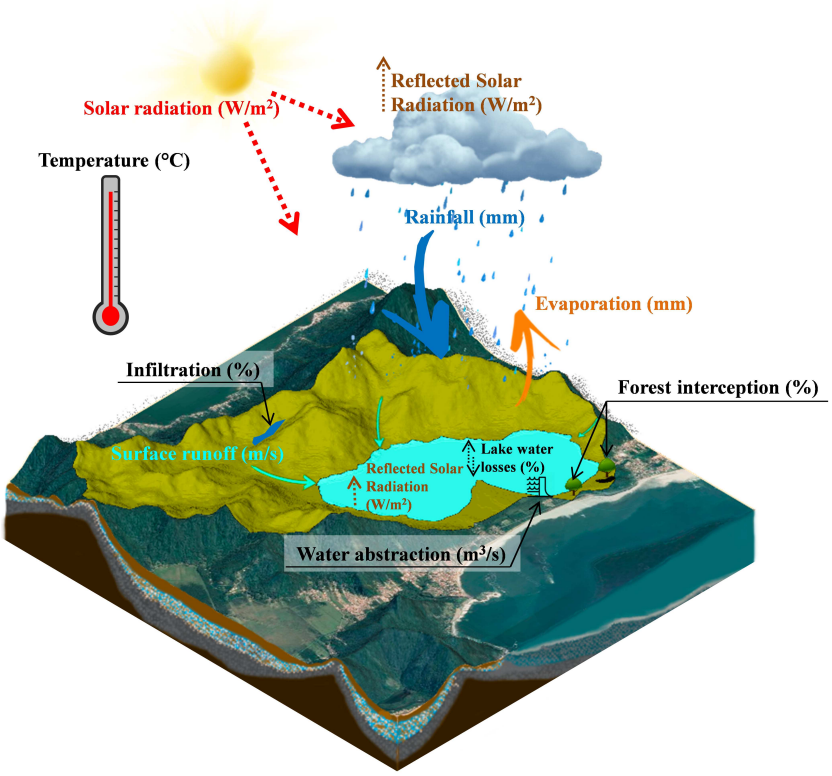

Source: Carlotto *et al.* (2021)

In the energy balance, part of the solar radiation is reflected by the surface depending on the albedo, the rest composes the net radiation that combined with the temperature provides the potential evaporation estimate in the lake. Part of the rainfall is intercepted by forest, part is retained in the catchment and infiltrates the soil and the difference

becomes runoff flowing into the lake (Figure 10). Water output from the lake is due to evaporation process and water abstraction for the water treatment plant. Next, we use the SW2D-GPU model to simulate the influence of each of these factors on the variation of the water level in the Peri Lake.

3.4.1 Input data

The terrain elevation data in the catchment and the bathymetry of the lake area are merged into the same raster map Figure 11a. The digital elevation model has a spatial resolution of 12.5 m (Dataset: ASF DAAC, 2018). The bathymetry of Peri Lake is provided by the Sanitation Company - CASAN. The Rainfall, temperature and solar radiation data are monitored in a meteorological station installed in the Peri Lake catchment (Figure 7c). The data period used starts on 02/01/2020 and ends on 05/02/2020 as shown in Figure 11b. Lake level data is provided by CASAN and the evaporation is estimated using the Equations 3.8, 3.9 and 3.10.

Figure 11 – Input data for the 2D shallow water model applied in the Peri Lake catchment. a) Elevation data and bathymetry. The color scheme represents the terrain elevations and contour lines show the water depths (initial conditions) above the bathymetric surface in meters. b) Meteorological data of the Peri Lake catchment. Solar radiation, temperatures and rainfall are the main meteorological inputs.

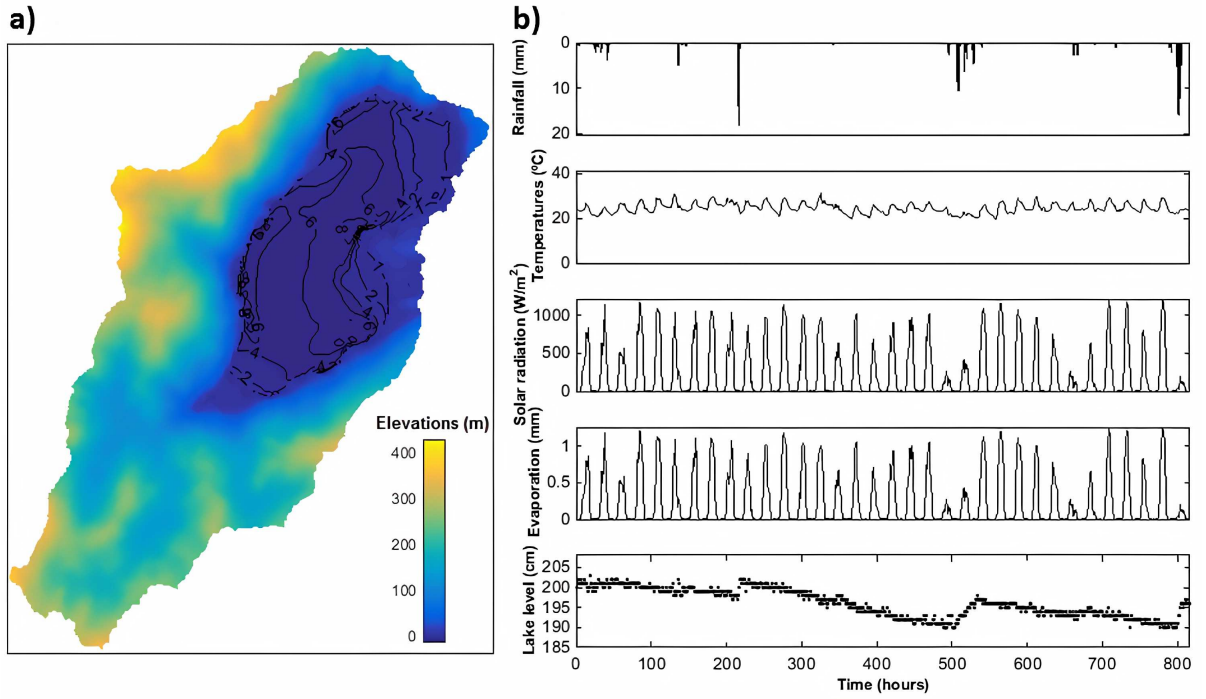

Source: Carlotto *et al.* (2021)

We adopted a water abstraction from the Peri Lake of 0.12 m^3s^{-1}. The Manning coefficient is defined as 0.12 (distributed homogeneously in space) considering the presence of boulders (Manning's coefficient: 0.040 - 0.070) with correction for channels covered by forests (correction value for the Manning's coefficient: 0.025 - 0.050) (ARCEMENT; SCHNEIDER, 1989). To satisfy the Courant-Friedrichs-Levy condition we use a time

step of 0.04 s. We assume that about 30% of the direct rainfall in the lake is lost due to different mechanisms (transformation into water vapor, infiltration in the hyporheic zone, and others) here called lake water losses (LWL) and about 20% of the rainfall in the catchment is retained through the infiltration process (INF), not contributing to the lake supply. Quantities of water intercepted by the forest during the rainfall event and the albedo were estimated using a trial and error calibration procedure. A manual calibration procedure was used to eliminate the need for a very large number of repetitions and to be able to test defined values based on knowledge of the study area (SÁ *et al.*, 2019; PEREZ *et al.*, 2020). For the interception of water by the forest we tested values around 40% and 45% (SÁ *et al.*, 2019). Albedo values can vary considerably during the day (RUTAN; Louis Smith; WONG, 2014), and values between 0.20 and 0.30 are reasonable for a coastal lake in latitude 27 S. The Nash–Sutcliffe model efficiency coefficient (NSE) values corresponding to each combination of forest interceptation and albedo values are shown in the Table 2.

Table 2 – Combinations of parameters used in the calibration procedure and the respective values of Nash–Sutcliffe model efficiency coefficient (NSE).

Forest interception (%)	albedo	NSE
45	0.25	0.9320
40	0.20	0.9296
40	0.25	0.9269
45	0.30	0.9264

All combinations of parameters allowed to obtain an NSE greater than 0.9 demonstrating that the model can represent the variations in water levels observed in the lake. In calibration we assume that an NSE equal to 0.9320 was already good enough for the purpose of this case study. The solid red line shown in Figure 12a represents the model results with the best set of calibration parameters. The water intercepted by the forest during the rainfall event corresponds to 45% (SÁ *et al.*, 2019), and albedo to 0.25. Potential evaporation is applied to water in the lake and where the water level exceeded a defined threshold, which we define here as 5 cm.

3.4.2 Results

The SW2D-GPU model integrates modeling of the hillslope, streams and lake to consider the diffuse water inputs to the lake, as shown in Figure 12b and d. In this case study we evaluate the influence of the different processes and parameters that make up the model variation in the water level (Figure 12a). In the results of the simulation considering only the rainfall (R) and no water outlet from the system (black dotted line), it can be verified that the model satisfies the principle of conservation of the mass, since there are no gains or significant losses of water during dry periods. In the results of the simulation considering rainfall (R), lake water losses (LWL = 30%), infiltration (INF = 20%)

Figure 12 – Simulation of the water level in the Peri Lake for the period from 02/01/2020 to 05/02/2020. a) The black dots represent the level data monitored in the lake; the black dotted line represents the simulated water levels considering only the rainfall (R) with no water outlet from the system; the dash dot dash orange line represents the simulated water levels considering rainfall (R), lake water losses (LWL), infiltration (INF) and interception (INT); the dashed blue line represents simulated water levels considering rainfall (R), lake water losses (LWL), infiltration (INF), interception (INT) and evaporation (Ev) and the solid red line represents the simulated water levels considering rainfall (R), lake water losses (LWL), infiltration (INF), interception (INT), evaporation (Ev) and water abstraction (WA). b) Water levels during a 38.8 mm rainfall distributed over the catchment. c) Catchment after a period of drought. d) Water levels during a 4.8 mm rainfall distributed over the catchment. The color bar is on a logarithmic scale to show small water level values.

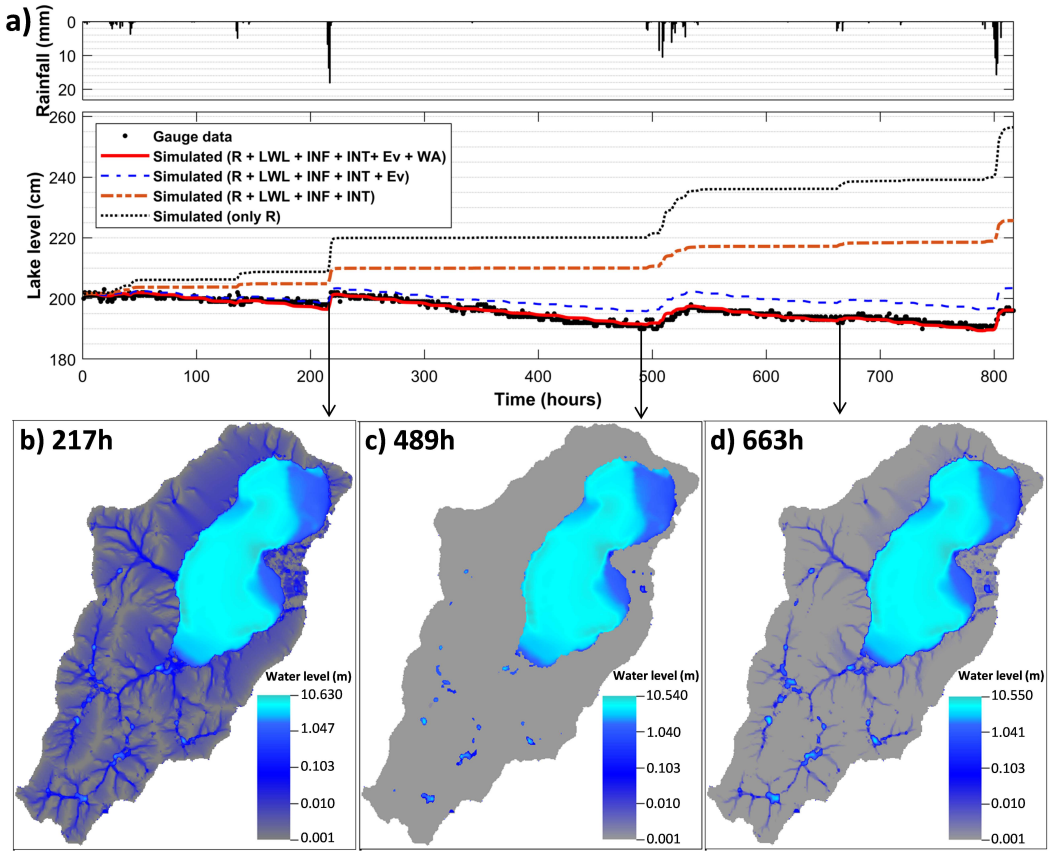

Source: Carlotto *et al.* (2021)

and interception (INT = 45%) it can be seen that these parameters define the amount of water that is available to supply the catchment and consequently the lake level during the rainfall. When evaporation (Ev) is included, the lake and the water balance depend on the temperature and solar radiation. Finally, the water abstraction for human consumption is activated. These results confirm the sensitivity of the model to the different parameters and variables, and how each of them influences the variation in lake water levels.

The diffuse characteristic of water inputs to the lake during an accumulated rainfall equal to 38.8 mm at the time of the simulation corresponding to 217h of the rainfall data can be seen in Figure 12b which also shows that the contributions to the level of water in the lake occur by main channels and also by the runoff on the hillslopes. The locations where the water remains stored in the catchment can be seen in Figure 12c

which shows the catchment after a dry period of approximately 11 days, the stored water will contribute to a faster response to the generation of runoff in the next rainfall as these spaces will already be filled with water. With an accumulated rain of approximately 4.8 mm there is generation of runoff in which the preferred paths are the main channels of the catchment as shown in Figure 12d.

In a scenario with no water outlet from the system (Figure 12a) the 187.4 mm of accumulated rainfall would provide an increase of approximately 55 cm in the water level in the lake. However, in a scenario considering lake water losses (LWL), infiltration (INF), interception (INT), evaporation (Ev) and water abstraction (WA), the water level in the lake decreases by 5 cm, in agreement with the level data monitored in the lake (Figure 12a).

3.5 PERFORMANCE OF THE PARALLEL AND SEQUENTIAL MODELS

Here, we compare the computation times of the SW2D-GPU model with the sequential version as a function of the increase in the number of grid points in the computational domain. The numerical tests were performed with one-minute simulations (just to obtain computation times). In all performance comparisons we consider double precision and the same time step for the two versions (CPU and GPU) of the model (Figure 13). The parallel model significantly decreases the simulation times of the 2D shallow water model. The speed-up comparing the two versions of the model increases as a function of the increase in the number of grid points in the computational domain (Figure 13). This is due not only to the proper use of memory space, but also to the large number of calculations that can be performed in parallel on the GPU. The sequential model needs to perform a large number of iterations to traverse the entire computational domain (a time-consuming process with calculations performed one after the other) repeatedly. However, in very small computational domains the time spent transferring data between the CPU and the GPU can make the model implemented in CUDA less advantageous compared to the sequential version processed in the CPU (i.e., the advantages gained from faster calculations done in parallel are lost when transferring data between CPU and GPU). The speed-up in Case study 1 (Figure 13b) is between 10 and 32 times with the number of grid points of 5×10^4 to 6×10^6 and the speed-up in Case study 2 is between 19 and 34 times with the number of grid points of 1×10^5 to 7×10^6 (Figure 13d).

The performance gains in the simulations are a result of the parallel processing performed in the CUDA kernels. To show the computation times of the main CUDA kernels implemented in the SW2D-GPU model compared to the computation times of the equivalent functions of the sequential model processed in the CPU, we use the original domains of Case studies 1 (with 893330 grid points) and 2 (with 122307 grid points), the results are shown in Figure 14.

Figure 13 – Model performance (CPU and GPU versions) as a function of the increase in the number of grid points. a) and b) correspond to Case study 1. c) and d) correspond to Case study 2.

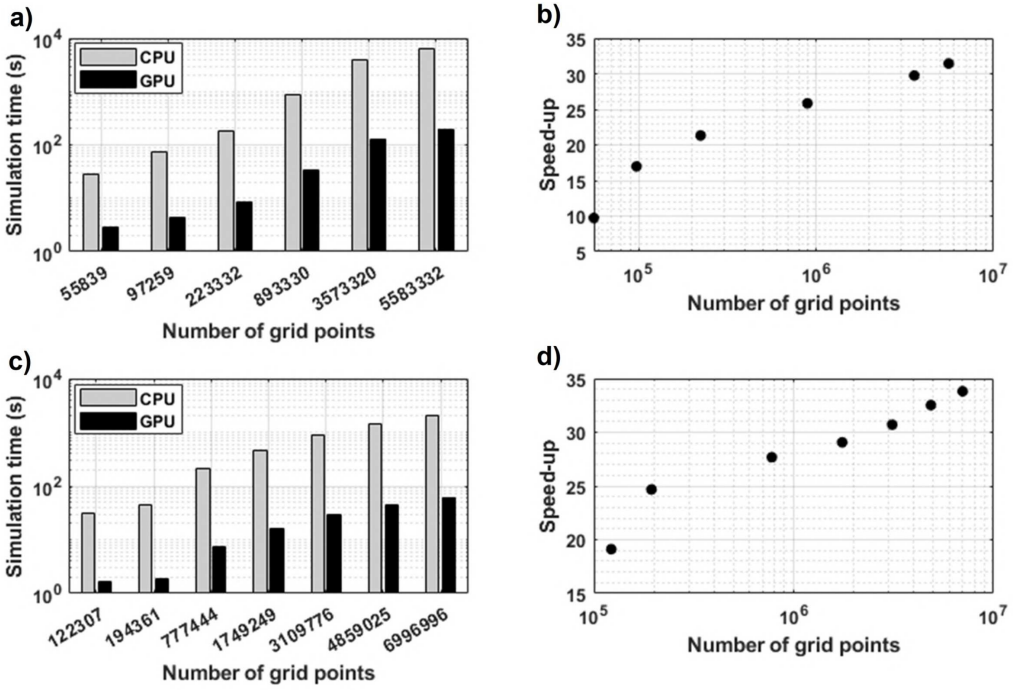

Source: Carlotto *et al.* (2021)

Figure 14 – Computation times of the main CUDA kernels and functions of the sequential model. The square and triangle markers correspond to the computation times obtained for the domain with 893330 grid points of Case study 1 and for the domain with 122307 grid points of Case study 2, respectively. The filled markers are the computation times of the sequential model and empty markers are the computation times of the SW2D-GPU model

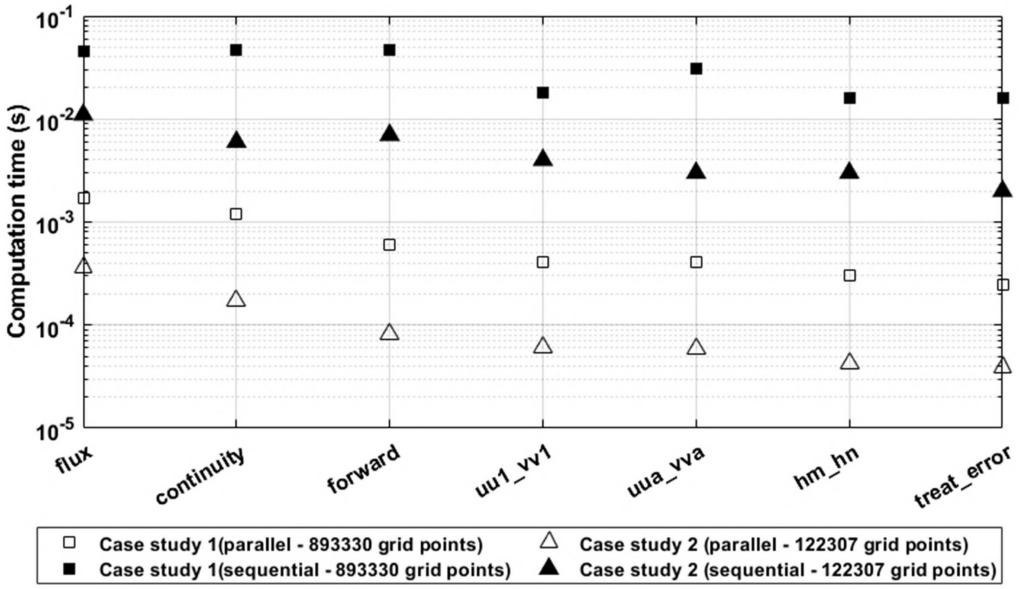

Source: Carlotto *et al.* (2021)

The “flux”, “continuity” and “forward” CUDA kernels have the greatest computational demands (Figure 14). These are the functions in which the greatest amount of calculations occur to approximate the solution of 2D shallow water equations. The performance gain is homogeneous compared to the different CUDA kernels, but “flux”, “continuity” and

"forward" are more time consuming.

3.6 MAIN LIMITATIONS

The GPGPU-accelerated 2D shallow water model (SW2D-GPU) was developed and tested in simulations of urban flooding and water flow in a catchment containing a lake. Although the SW2D-GPU model showed good functioning and good computational performance in both cases, it is important to know the limitations caused both by its conceptual and mathematical bases that involve simplifications, as well as numerical and computational ones that have restrictions of use for being dependent on devices (GPU).

Regarding the mathematical bases, the limitations of the SW2D-GPU model are mainly due to simplifications that disregard wind resistance, viscosity terms, Coriolis forces and transport of solutes and particles. As a two-dimensional model, the SW2D-GPU assumes that water flows propagate with a much larger horizontal length scale than the vertical length scale, which makes it unsuitable for applications in deep water bodies. By disregarding wind velocities, the model is also unsuitable for applications in problems where the wind significantly influences water flows. The transport of solutes and particles is also disregarded, so the model can only represent variations in water levels and velocities, which is a disadvantage when it is desired to study the hydrodynamics of lakes.

The ability to consider lake water losses (LWL), infiltration (INF), interception (INT) was added to the model by means of percentage values that must be previously estimated for the catchment. Water abstraction (WA) can also be considered as a constant or variable value in time and space.Also included in the model was a mathematical formulation to consider the process of potential evaporation that varies over time using the energy balance method combined with equations that determine the variation of the latent heat of vaporization and the density of water as a function of temperature and solar radiation.

The model was adapted to provide hydrological modeling in ecosystems with little data availability, therefore, it must be considered that the model has some limitations, such as: (i) the use of percentage values for water losses (INT, INF, LWL) that act only as limiters of the amount of rainfall that becomes available to supply surface waters in the catchment and in the lake, therefore they only act during the rainfall. Although this is a convenient way to make the model applicable in places with little availability of measured data, it has the disadvantage of depending on the modeler experience and previous knowledge about the study area (sufficient to estimate INT, INF and LWL in terms of percentages); (ii) rainfall and Manning coefficient are homogeneously distributed in space, which can be a problem for applications in large catchments with spatial variations in rainfall or in conditions where the land cover is highly heterogeneous; (iii) water movements induced by the wind are neglected; and (iv) interactions with subsurface or groundwater are not considered (but the model allows the use of time series of flows to represent the base flows). Despite the limitations, the parallel formulation presented in this work can be easily

integrated with other models or receive new modules for the calculation of subsurface and groundwater flows.

The main hardware requirement to use the SW2D-GPU model is that the computer is equipped with a Graphics Processing Unit (GPU) with CUDA technology, which is exclusively provided by the company NVIDIA. Another important point is the amount of memory available on the GPU, this is usually one of the main problems of GPU-accelerated computing, as all the data that participates in the parallel calculations must be allocated in the GPU memory. For applications of the model, it is desirable that the GPU has at least 3 GB of memory.

3.7 CONCLUSIONS

In this chapter we parallelize and implement a 2D shallow water model using CUDA C/C++ and show that parallel computing in the General Purpose Graphics Processing Unit (GPGPU) is a powerful way to accelerate this model. The SW2D-GPU model was able to perform the simulations 34 times faster than the sequential model. In addition to having a significant improvement in performance, the model can now also represent the evaporation process in water bodies.

The model can simulate flood inundation in urban areas and can consider water inputs from different sub-basins. The model simulates in an integrated manner the surface water dynamics in the hillslope, streams, and lake as well as human interference through water abstraction. This model allows diffuse inflows of water in the lake and is an interesting option especially to study the hydrology of lake ecosystems with little availability of hydrological data using low-cost computers equipped with GPU with CUDA technology. While the interactions between surface and subsurface waters and the water movement induced by the wind were neglected, the parallel formulation presented in this chapter can be easily integrated with other models or receive new modules for the calculation of those processes. The SW2D-GPU model code is simple and short, so it can be used for learning activities and programming studies in CUDA language, and it can also help with planning for larger code parallelization.

4 A COUPLED 2D-3D CATCHMENT-LAKE MODEL WITH A PARALLEL PROCESSING FRAMEWORK

ABSTRACT[1]

The interdependence between the hydrodynamics of the lakes and the water inflows from the catchments is a determining factor in understanding how physical, chemical and biological processes develop in lake ecosystems. However, the computational cost to simulate these coupled processes in large domains may demand parallel processing capabilities. In this chapter, we develop a coupled 2D-3D model for lake ecosystems using a parallelized version of the Environmental Fluid Dynamics Code (EFDC) and a two-dimensional model based on shallow water equations (SW2D). The EFDC uses Message Passing Interface while we implement the SW2D in CUDA C/C++ language for parallel processing in Graphics Processing Unit. The coupled SW2D-EFDC model simulates catchment hydrology and several hydrodynamic features of the lake, such as transport of solutes and sediments, thermal processes, and water quality. As a case study, the SW2D-EFDC model is applied to the hydrodynamic modeling of the Peri Lake catchment considering the interactions between the lake and the surface water inflows during a rainfall event. The SW2D-EFDC combines high-performance computing technologies to provide parallel processing, good scalability and usability.

4.1 INTRODUCTION

The interaction between lake and catchment water flows determines the physical, chemical, and biological aspects of lake circulation (RUEDA; MACINTYRE, 2010; LOPES *et al.*, 2018). Point and diffuse water inputs from the catchment influence the spread of nutrients and the way that local flow regime changes propagate in the aquatic systems (JANSSEN *et al.*, 2019). Therefore, coupled hydrological and hydrodynamic models are a valuable tool for water resources management and understanding of lake systems (HUANG *et al.*, 2016). While most coupling approaches generally consider point inlets between the lake and the main rivers (LI *et al.*, 2014; XIE; YANG; FU, 2012), diffuse water inputs that occur at the catchment-lake boundaries are more challenging to model.

Distributed hydrological models often use two-dimensional (2D) formulations of shallow water equations to simulate surface water flows in catchments (ECHEVERRIBAR *et al.*, 2019). These models are also used to calculate the amounts of water entering lakes and lagoons. Therefore, they are an alternative to generate flow inputs for hydrodynamic models that simulate variations in the physical, chemical and biological characteristics of water in lakes (SOARES; CALIJURI, 2021). Hydrodynamic modeling in lakes in most cases involves representing changes that occur not only in the horizontal plane, but also in the vertical profile of the water, requiring the use of 3D models. As an example, Bocaniov *et al.* (2016) used the 3D model ELCOM-CAEDYM to relate the external phosphorus loads to the space-time dynamics of hypoxia in Lake Erie. Another study also considered the SI3D model (SMITH, 2006) to explore the behavior of storm water flows in small lakes of complex bathymetry with interconnected catchments, showing that the 3D hy-

[1] This Chapter has been submitted to Computer & Geosciences and is under review.

drodynamic models can accurately describe the evolution of the thermal structure and the ways of inflowing rivers in lakes (RUEDA; MACINTYRE, 2010).

The hydrodynamic modeling in lakes is usually preceded by data pre-processing and creation of model input files, this task requires advanced knowledge in some programming language and the realization of manual procedures with the application of several softwares (SHIN *et al.*, 2019). When inputs (flows, concentrations, sediment load, among others) are obtained through numerical modeling with hydrological model in the catchment, a common approach essentially involves the following steps: (i) application of a hydrological model; (ii) selection of the variable to be used in the hydrodynamic model; (iii) definition of the positions in which the variable will be inserted in the boundary between catchment and lake (boundary conditions); (iv) creation of the input files, and (v) execution of the hydrodynamic model. Performing each of these steps manually is time-consuming and prone to data manipulation errors, in addition to being a limitation for real-time modeling. Therefore, it is necessary to develop automated ways to provide the coupling of hydrological and hydrodynamic models for applications in lake ecosystems modeling (ALARCON *et al.*, 2014; HWANG *et al.*, 2021; SHIN *et al.*, 2019; ZHANG *et al.*, 2017). For example, Huang *et al.* (2016) coupled a 2D hydrological model (Xinanjiang) and the EFDC hydrodynamic model in which the Xinanjiang model simulate six inflow discharges for the boundary conditions of a hydrodynamic model to investigate the impacts of a water transfer project on the water transport pattern of Lake Chao, China. Zhang *et al.* (2017) coupled the Soil and Water Assessment Tool (SWAT) and the Delft3D model to simulate the interactions between water flows in ungauged zones of the catchment and Lake Poyang in China. Hwang *et al.* (2021) used SWAT-Environmental Fluid Dynamics Code (EFDC) linkage to evaluate the water quality improvement scenarios considering the agricultural system and nonpoint source pollution of the upper Ganwol estuarine reservoir catchment located in South Korea.

While the coupling of hydrological and hydrodynamic models may eliminate the need for human interference in transferring data between models, it may result in long computational time. This problem can be minimized by using models adapted for parallel processing using Message Passing Interface (MPI) or massively parallel devices such as GPUs. Among the options of hydrodynamic models that offer high performance is the Environmental Fluid Dynamics Code (EFDC) model originally developed by Virginia Institute of Marine Science (HAMRICK, 1992) and parallelized using MPI (O'DONNCHA; RAGNOLI; SUITS, 2014). The EFDC-MPI model is open source and can simulate three-dimensional flows, transport, mixing dynamics, thermal, and biogeochemical processes in rivers, lakes, estuaries, and coastal regions.

In this chapter, we couple the EFDC-MPI model with a 2D shallow water model (SW2D-GPU - Carlotto *et al.*, 2021) for the simulation of catchment-lake interactions. The coupled SW2D-EFDC model uses parallel computing with hybrid processing in which water flows in the catchment are calculated on the GPU and the 3D simulation of the lake

hydrodynamics is performed on a computer cluster using MPI. The SW2D-EFDC model can simulate diffuse water input from the catchment and the hydrodynamics of the lake considering atmospheric forcing and particle transport.

4.2 METHODS

4.2.1 Shallow water model (SW2D-GPU)

The SW2D-GPU model is based on 2D shallow water equations (CARLOTTO *et al.*, 2021; NOH *et al.*, 2016). In this formulation the Coriolis strength, the wind resistance, and the viscosity terms are neglected, so that the equations of the two-dimensional shallow water model are written as follows:

Continuity equation:

$$\frac{\partial h}{\partial t} + \frac{\partial M}{\partial x} + \frac{\partial N}{\partial y} = r_{\mathrm{e}} + q_{\mathrm{ex}} - E, \tag{4.1}$$

$$r_{\mathrm{e}} = r(1 - (INF + INT + LWL)) \tag{4.2}$$

Momentum equations:

$$\frac{\partial M}{\partial t} + \frac{\partial (uM)}{\partial x} + \frac{\partial (vM)}{\partial y} = -gh\frac{\partial H}{\partial x} - f_1, \tag{4.3}$$

$$\frac{\partial N}{\partial t} + \frac{\partial (uN)}{\partial x} + \frac{\partial (vN)}{\partial y} = -gh\frac{\partial H}{\partial y} - f_2, \tag{4.4}$$

Friction terms:

$$f_1 = \frac{gn^2 M\sqrt{u^2 + v^2}}{h^{4/3}}, \tag{4.5}$$

$$f_2 = \frac{gn^2 N\sqrt{u^2 + v^2}}{h^{4/3}}, \tag{4.6}$$

where h is the water depth; $H = h + z_{\mathrm{b}}$ where z_{b} is the topographic elevation; $M = uh$ and $N = vh$, where u and v are the velocities in the x and y directions respectively; r_{e} is the effective rainfall; r is the rainfall; INF is the percentage of rainfall infiltration loss; INT is the percentage of rainfall interception loss; LWL is the lake water looses (only in the cells in the lake area and water bodies); q_{ex} is the term that defines the flow into the drainage network (height of water per unit time in a given network cell); E is the potential evaporation; t is the time; f_1 and f_2 are the friction components where g is the acceleration of gravity and n is Manning's roughness coefficient.

The space-time discretization of the model uses the Leapfrog method and a finite difference scheme in which water depths are calculated at the cell centers and fluxes are calculated at the boundaries with adjacent cells (CARLOTTO *et al.*, 2021; NOH *et al.*, 2016). The numerical solution of the momentum and continuity equations is done with

parallel processing in the GPU for the x, y space and the temporal evolution is performed iteratively with a sequential code processed in the CPU (Figure 16). More details on the numerical and computational formulation of the model can be found in Carlotto *et al.* (2021).

4.2.2 Environmental Fluid Dynamics Code (EFDC-MPI)

The EFDC-MPI model is based on Reynolds-averaged Navier-Stokes equations. When Boussinesq approximation for variable density fluid is used, the continuity and momentum equations can be written as follows (HAMRICK, 1992).

Three-dimensional continuity equation:

$$\partial_t \left(m\eta\right) + \partial_x \left(m_{\mathrm{y}} h u\right) + \partial_y \left(m_{\mathrm{x}} h v\right) + \partial_z \left(m w\right) = 0, \tag{4.7}$$

$$\partial_t \left(m\eta\right) + \partial_x \left(m_{\mathrm{y}} h \int_0^1 u dz\right) + \partial_y \left(m_{\mathrm{x}} h \int_0^1 v dz\right) = 0, \tag{4.8}$$

Momentum equations:

$$\begin{aligned} \partial_t \left(mhu\right) + \partial_x \left(m_{\mathrm{y}} huu\right) + \partial_y \left(m_{\mathrm{x}} hvu\right) + \partial_z \left(mwu\right) - \left(mf + v\partial_x m_{\mathrm{y}} - u\partial_y m_{\mathrm{x}}\right) hv \\ = -m_{\mathrm{y}} h\partial_x \left(g\eta + p\right) - m_{\mathrm{y}} \left(\partial_x z_{\mathrm{b}} - z\partial_x h\right) \partial_z p + \partial_z \left(mh^{-1} A_{\mathrm{v}} \partial_z u\right) + Q_{\mathrm{u}}, \end{aligned} \tag{4.9}$$

$$\begin{aligned} \partial_t \left(mhv\right) + \partial_x \left(m_{\mathrm{y}} huv\right) + \partial_y \left(m_{\mathrm{x}} hvv\right) + \partial_z \left(mwv\right) - \left(mf + v\partial_x m_{\mathrm{y}} - u\partial_y m_{\mathrm{x}}\right) hu \\ = -m_{\mathrm{x}} h\partial_y \left(g\eta + p\right) - m_{\mathrm{x}} \left(\partial_y z_{\mathrm{b}} - z\partial_y h\right) \partial_z p + \partial_z \left(mh^{-1} A_{\mathrm{v}} \partial_z v\right) + Q_{\mathrm{v}}, \end{aligned} \tag{4.10}$$

$$\partial_z p = -gh\left(\rho - \rho_0\right) \rho_0^{-1} = -ghb \tag{4.11}$$

The vertical velocity is w, and is related to the physical vertical velocity w^* by:

$$w = w^* - z\left(\partial_t \eta + m_{\mathrm{x}}^{-1} u\partial_x \eta + m_{\mathrm{y}}^{-1} v\partial_y \eta\right) + \left(1 - z\right)\left(m_{\mathrm{x}}^{-1} u\partial_x z_{\mathrm{b}} + m_{\mathrm{y}}^{-1} v\partial_y z_{\mathrm{b}}\right), \tag{4.12}$$

where w is the vertical velocity in the z direction; f is the Coriolis parameter; A_{v} is the vertical diffusivity; m_{x} and m_{y} are the square roots of the diagonal components; $m = m_{\mathrm{x}} m_{\mathrm{y}}$ is the Jacobian root; p is the pressure; Q_{u} and Q_{y}, are the affluent–effluent movement terms and g the gravity acceleration. Figure 15 shows the relationship between lake bed elevation (z_b), water level (η), and water depth (h).

To provide uniform resolution in the vertical direction EFDC model uses a time variable stretching transformation. The stretching transformation is given by:

$$z = \frac{\left(z^* + z_{\mathrm{b}}(x,y)\right)}{\left(\eta(x,y,t) + z_{\mathrm{b}}(x,y)\right)}, \tag{4.13}$$

Figure 15 – Lake bed elevation (z_b), water level (η), and water depth (h) in the Cartesian coordinate system.

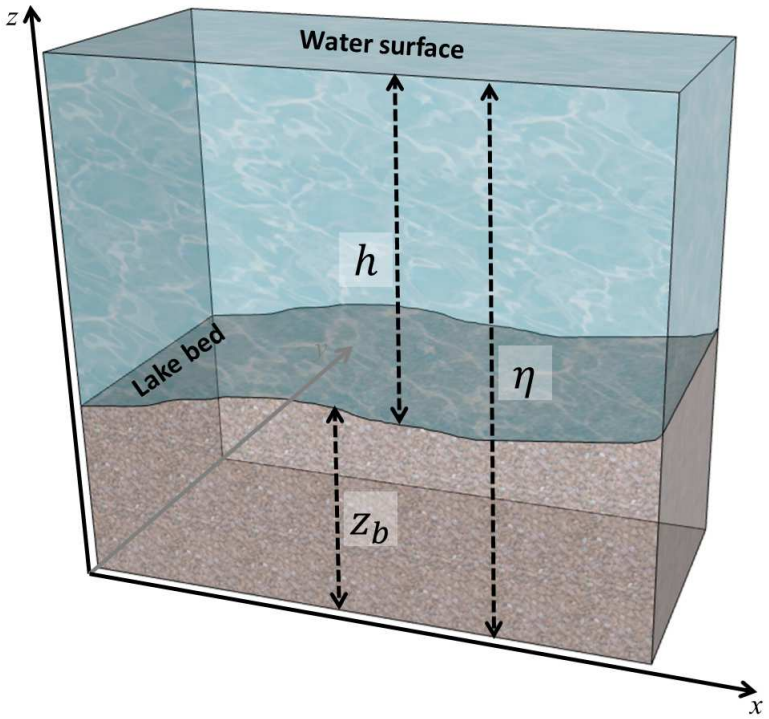

Source: Prepared by the author.

where z^* denotes the original physical vertical coordinates and z_b and η are the physical vertical coordinates of the bottom topography and the free surface respectively. The EFDC model has an extensive mathematical formulation that includes water quality model, particle tracking model, temperature, sediment transport, among others. More details about the model and its formulation can be found in Hamrick (1992).

To solve the equations of motion, the EFDC model uses a second order finite difference method in a staggered or orthogonal curvilinear grid (HAMRICK, 1996). A three-time Leapfrog numerical integration scheme with periodic trapezoidal corrections is used for the temporal integration of the model (HAMRICK, 1992; HAMRICK, 1996). The finite difference scheme is divided into external mode (barotropic mode) and internal mode (baroclinic mode). The external mode solution is semi-implicit and calculates the two-dimensional field of water surface elevations with the pre-conditioned conjugate gradients method (HAMRICK, 1996). The new surface elevation field is used to calculate the depth averaged barotropic velocities. In external mode it is possible to simultaneously define surface elevations, wave characteristics, or volumetric flow to be used as boundary conditions (HAMRICK, 1996). The internal scheme for solving the momentum equations uses the same time step as the external solution and is implicit with respect to vertical diffusion (HAMRICK, 1996).

4.2.3 Coupling

The SW2D-EFDC model uses parallel hybrid processing that leverages the processing power of the GPU and multiple CPUs (cluster). The structure of the codes implemented in CUDA C and MPI are illustrated in Figure 16. The coupling module is implemented in the SW2D-GPU model, comprising functions to map lake-catchment boundaries and automate the process of creating the computational domain grid and the necessary inputs for coupled simulations (Figure 16).

Here, an off-line coupling was used in which the models communicate through external files. The coupling scheme used contains functions that automate the process of creating EFDC-MPI model inputs while running the SW2D-GPU model. Inputs that do not depend on the solution of the shallow water equation or the identification of the lake-catchment boundary (such as: the files that define the grid, the computational domain decomposition and the initial conditions of temperature, salinity and dye concentrations) are created at the initialization of the SW2D-GPU model. The salinity, temperature, and dye concentration time series that are boundary conditions applied only at the lake-catchment boundaries and the flow time series that depend on the solution of the shallow water equations are created at the end of the SW2D-GPU model run. The files with general simulation settings (EFDC.INP and SHOW.INP) are also created. The functions that make up the coupling module and the main generated files are described below.

4.2.3.1 Computational grid

The EFDC model uses a stretched or sigma vertical coordinate. The horizontal coordinate system can be curvilinear or orthogonal, allowing for different grid configurations. In the SW2D-GPU model the computational domain is discretized with square cells and cartesian grid, therefore, the EFDC-MPI model is also configured to use a grid that maintains the same characteristics.

- Grid specification files: The grid generating preprocessor code, *gefdc.f*, is used to generate the horizontal grid and the DXDY.INP and LXLY.INP files. This code is provided with the original version of the EFDC model. However, to use *gefdc.f* the input files CELL.INP, DEPDAT.INP, GRIDEXT.INP, GEFDC.INP are required. Here we developed a code called *make_grid_inputs.c* to automate the creation of these files using the digital elevations model with bathymetry coupled from the SW2D-GPU model and a mask that defines the lake region, both are files in Esri ASCII raster format.
  - CELL.INP: file containing computational domain definition and horizontal cell type identifier.
  - CELLLT.INP: file containing horizontal cell type identifier for saving mean mass transport. The file CELLLT.INP may be equal CELL.INP file or define a subset of the water cells in the computational domain.

Figure 16 – Flowchart of the SW2D-EFDC model. The SW2D-GPU model, the coupling module and a single time step of the EFDC-MPI model are illustrated. t is time, $\triangle$t is time step, $t_{max}$is simulation time, t_{out} is output time, u and v are velocities in x and y directions and h is water depth. The functions and input files (*.INP) are explained in Sections 4.2.3.1-4.2.3.4.

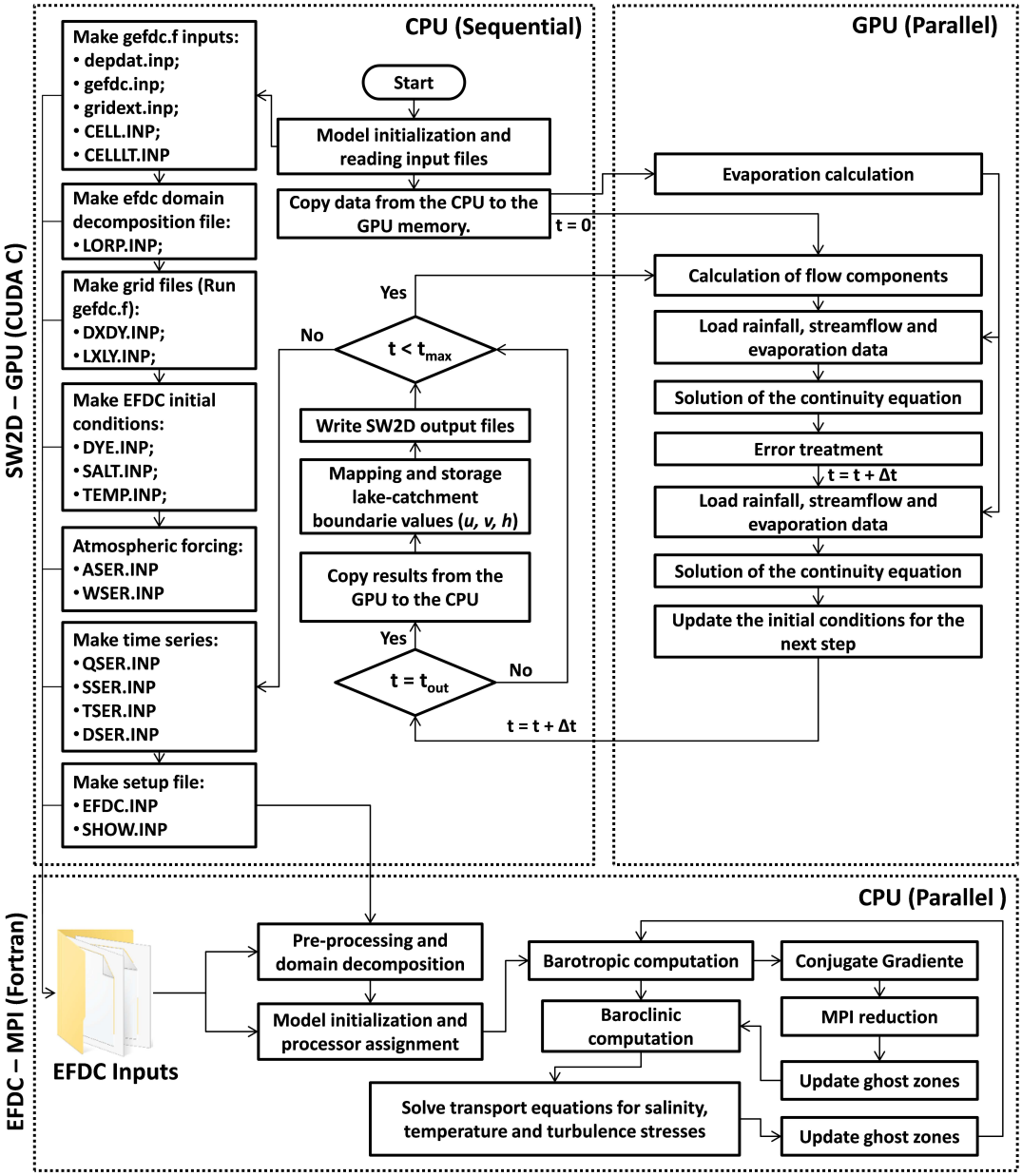

Source: Prepared by the author.

  - DEPDAT.INP: file containing depth or bottom topography (based on lake bathymetry).
  - GRIDEXT.INP: file of water cell corner coordinates.
  - GEFDC.INP: master input file for *gefdc.f*.

- When running *gefdc.f* the following files are created:
  - DXDY.INP: provides the spatial resolution dx and dy, the initial water depth, the bottom elevations, and the roughness coefficient.
  - LXLY.INP: provides geometric properties of the computational domain (cell center coordinates and the components of a rotation matrix).

- Domain decomposition file: The computational domain grid is decomposed into Locally Optimal Rectilinear Partition (LORP) using an optimal partition calculation code (O'DONNCHA; RAGNOLI; SUITS, 2014). The code was adapted to run automatically in the SW2D-EFDC coupled model, requiring only the information on the number of processors and the CELL.INP file as input.
  - LORP.INP: contains the information for domain decomposition with load balanced among a defined number of processors.

4.2.3.2 The initial conditions and time series input files

- Dye, salinity and temperature initial conditions: these files contain values corresponding to all cells of the lake domain, distributed in the horizontal (x, y) and in each vertical layer.
  - DYE.INP: initial concentrations of a dye.
  - SALT.INP: initial salinity values.
  - TEMP.INP: initial temperature values.

- Atmospheric forcings:
  - ASER.INP: contains the time series of atmospheric pressure, air temperatures, rainfall, evaporation and solar radiation. It also includes unit conversion parameters.
  - WSER.INP: time series of wind velocities and wind directions. It can be used to specify the convention used for wind directions.

- Time series forcing and boundary condition files: Each file can contain multiple time series. In the SW2D-EFDC model these files contain a time series for each lake-catchment boundary cell.
  - QSER.INP: volume flows time series.

  - SSER.INP: water salinity time series.
  - TSER.INP: water temperatures time series.
  - DSER.INP: time series of dye concentrations.

4.2.3.3 General parameters and run control files

- EFDC.INP: run control parameters and information about model domain, external forcings and output controls.
- SHOW.INP: control screen writing of information (i.e., water surface elevation, surface and bottom salinity) at the horizontal location specified by the horizontal cell indices.

The input files (.INP) of the EFDC model presented above are described in detail in Hamrick (1996) and Tetra Tech (2007).

4.2.3.4 Mapping lake-catchment boundaries

The flows calculated by the SW2D-GPU model are inserted in the EFDC-MPI model through the catchment-lake boundaries. The determination of the i and j positions of the cells that belong to the lake-catchment boundary is determined with a mapping algorithm that uses as input a lake mask composed of values 1 in the lake region and 0 elsewhere (Figure 17a). The code in Figure 17c identifies the differences in lake mask values whenever a lake-catchment boundary cell is reached. At the boundary positions belonging to the catchment domain, the values of flows in the south (S), north (N), east (E), and west (W) directions are calculated. These values are used as boundary conditions written in the QSER.INP file to be applied to the boundary cells belonging to the lake domain (i.e., BC in Figure 17b). Flow values are grouped according to the directions from which they enter the lake and recorded along with simulation times and BC positions (Figure 17b). The values of u, v e h are dynamically updated with the results of the SW2D-GPU model at each time interval of the simulation and the water velocities in BC are internally calculated by the EFDC-MPI model with the values of h of the boundaries belonging to the lake domain.

Figure 17 – Mapping of lake-catchment boundaries. a) Mask in which the cells belonging to the lake region are set to 1 and the other cells to 0. b) Illustrates lake-catchment boundary cell positions where boundary cells (BC) belong to the lake domain and catchment cells are identified with directions from which flows entering the lake are coming (south - S, north - N, east -E, and west - W). On the right, the records of times (t), flows (Q_{yn}, Q_{ys}, Q_{xe}, and Q_{xw}) and x and y positions are presented, grouped according to the direction from which the flows come. c) Code for mapping the i and j coordinates of lake-catchment boundaries and calculating volume flows. Where s_bc, n_bc, w_bc and e_bc store the i and j coordinate values at the south, north, west, and east boundaries, respectively. s_val, n_val, w_val and e_val store the calculated flow values at the south, north, west and east boundaries, respectively. N is the number of time intervals in the simulation.

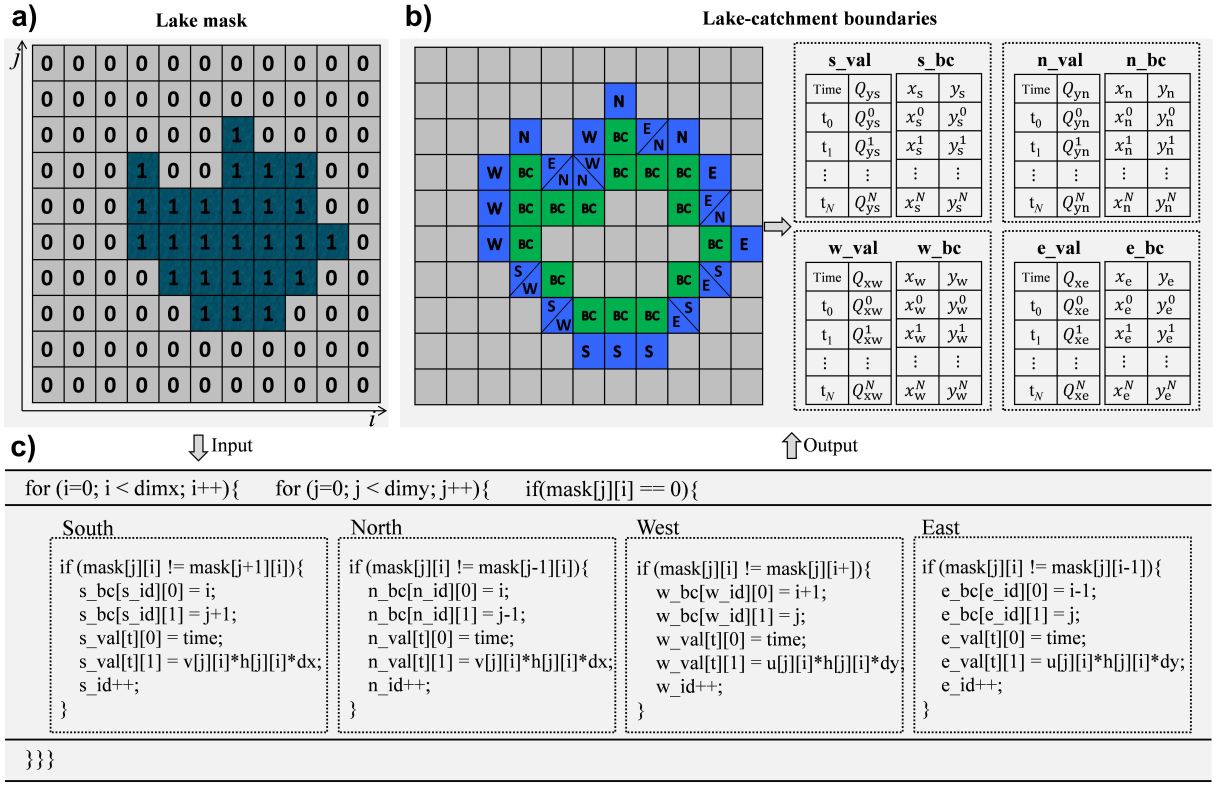

Source: Prepared by the author.

4.2.3.5 Flow coupling

The SW2D-EFDC model couples the water flows in the catchment and the lake (Figure 18a) and also establishes a link with the heat exchange (Figure 18b) and transport processes.

The SW2D-EFDC model simulates the 2D-3D hydrodynamics of the lake system and provides a detailed view of the vertical profiles of velocity, temperature and chemical composition of water in the lake (Figure 18c). In the lake domain a vertical Sigma Stretch Grid is used in which the vertical resolution is distributed according to the number of layers and the height of the water above the lake bottom in each cell. The calculation to determine the vertical resolution of each layer is performed internally by the EFDC model based on the number of layers and proportions defined in the EFDC.INP file.

For the coupling of the SW2D-GPU and EFDC-MPI models, the vertical resolution of each lake cell is divided equally between the layers. Likewise, the water flows entering

the lake are divided by the number of layers and distributed evenly in each layer of cells at the lake-catchment boundaries (Figure 18e).

The Figure 18d shows the horizontal coupling between the catchment and lake domains. The flows calculated by the SW2D-GPU model are stored and related according to the orientation of the faces at the boundaries of the EFDC-MPI model and the direction of the flows coming from the catchment so that we have flows from the north (Q_{yn}) entering faces facing north, flows from south (Q_{ys}) entering faces facing south, flows from east (Q_{xe}) entering faces facing east and flows from west (Q_{xw}) entering faces facing to the west. Flow values are written to the QSER.INP file and entered into the lake domain as a volume flow boundary condition.

Figure 18 – Illustration of the SW2D-EFDC coupled model. a) Ilustration of the Catchment-Lake coupling. b) 3D model of the lake showing the distribution of simulated temperatures. c) Vertical temperature profiles. d) Illustration of the horizontal coupling in which the arrows indicate the direction of the flows Q_{yn}, Q_{ys}, Q_{xe} and Q_{xw} (flows from north, south, east, and west, respectively). e) 3D view of the coupling interface in a section in which the 3D lake model has 3 vertical layers that receive flows Q_{L1}, Q_{L2} and Q_{L3}. Where k is the number of layers.

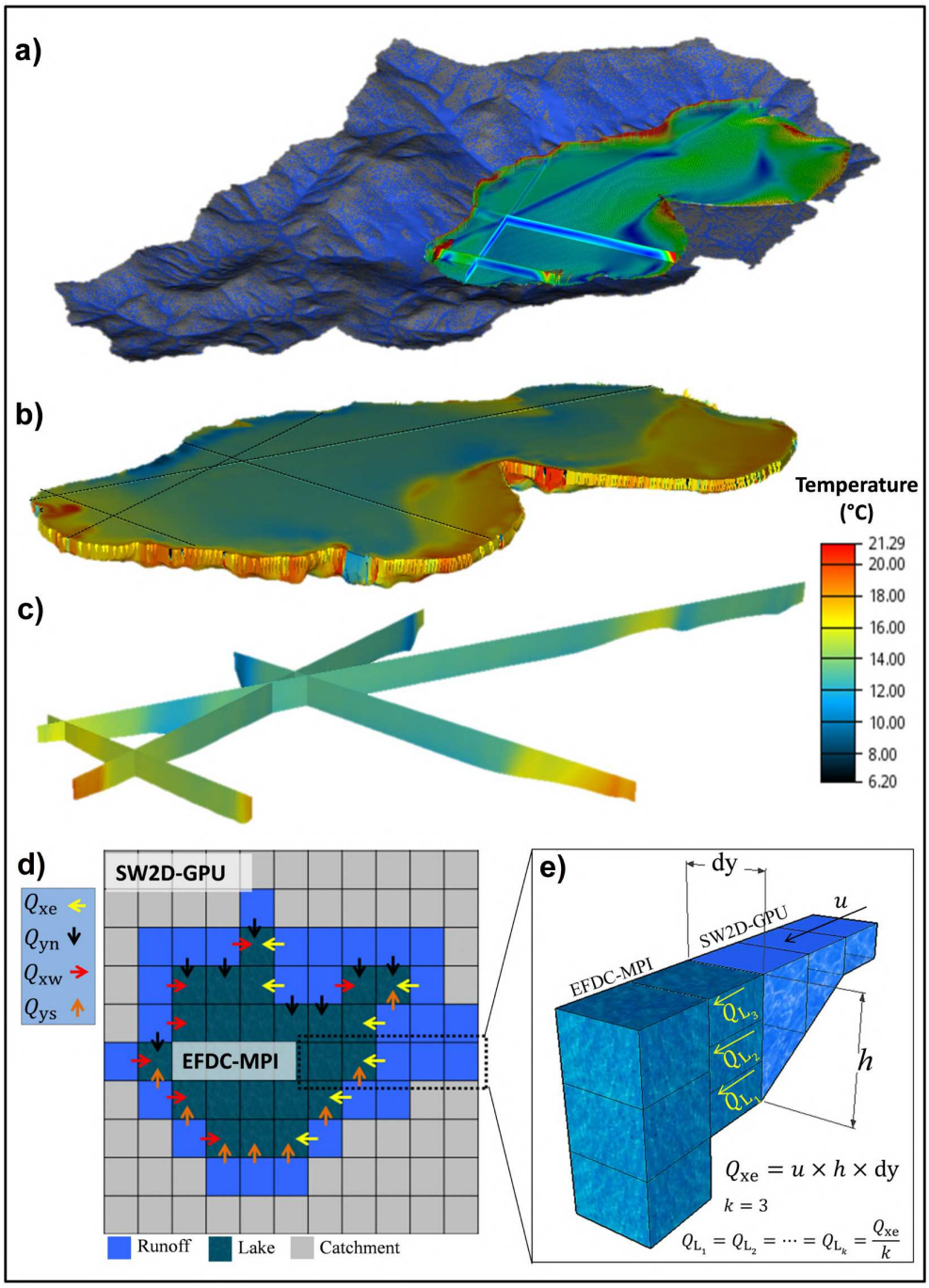

Source: Prepared by the author.

4.2.4 Study area

The Peri Lake catchment is located in Santa Catarina Island, southern Brazil (Figure 19) in the of transition between tropical and temperate climates, with average annual precipitation of 1500 mm (CHAFFE *et al.*, 2021; HENNEMANN; PETRUCIO, 2011). The lake surface area is 5 km^2 with average depth of 7.0 m and maximum depth of 11.0

m. The surrounding hillslopes are covered by remains of Subtropical Atlantic Rain Forest and sandy Restinga (PEREZ *et al.*, 2020; SANTOS *et al.*, 2021). It is the largest source of water supply on the Island and an important ecosystem for biodiversity preservation. The lake supplies water to the local population through the Water and Sanitation Company (CASAN), which is authorized to abstract up to 200 Ls^{-1} of water. In Figure 19, the location of the water abstraction is marked with a triangle.

Figure 19 – Study area. (a) Shows the location of the Peri Lake catchment on the map of Florianópolis Island in Southern Brazil. (b) Peri Lake catchment in which the elevations, drainage network and the bathymetry of the lake (contour lines) are shown. The color bar represents the topographic elevations. The triangle represents the location of the water abstraction.

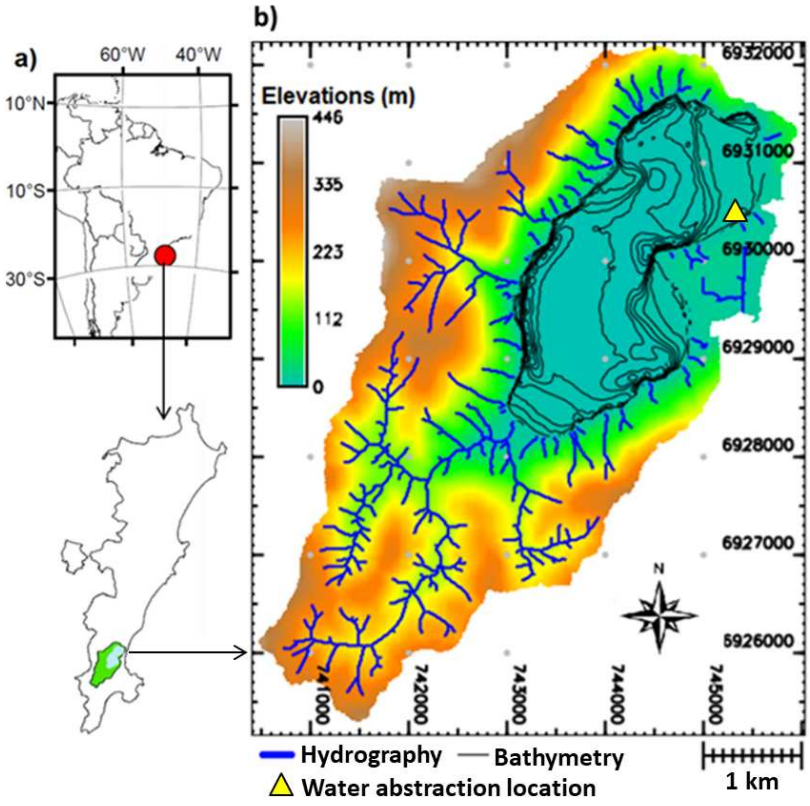

Source: Prepared by the author.

4.2.5 Catchment-lake simulation using SW2D-EFDC model

The SW2D-EFDC model is applied in the simulation of the hydrodynamics of Peri Lake considering the inflows of water coming from the catchment. The computational domain consists of a grid with 701 rows and 556 columns of rectangular cells with spatial resolution of 10 m. The catchment domain has 143723 active cells and the lake domain has 50638 active cells of which 1394 cells belong to the catchment-lake coupling interface.

In the simulations we use a manning coefficient of 0.012 and a time step of 0.04 seconds for the 2D model. For the 3D model, a coefficient of roughness of the bottom is 0.00025 and a time step of the numerical solver is 0.5 seconds. The time series of the meteorological data were discretized with a temporal resolution of 1 hour (Figure 20).

Figure 20 – Weather data for the period from 22/01/2020-09:00 to 29/01/2020-09:00 with temporal resolution of 1 hour. (a) Distribution of wind velocities and wind directions. (b) Rainfall, solar radiation and temperature data

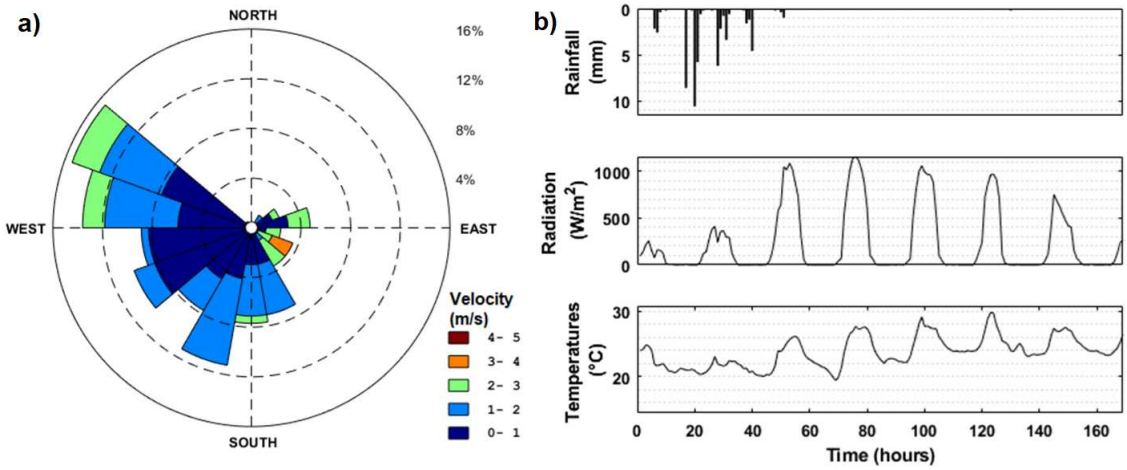

Source: Prepared by the author.

The simulations were carried out for two scenarios: (i) without wind; and (ii) including the wind (only in the lake area). To help visualize the water inputs and hydrodynamics in the lake, the dye transport has been included in the simulation. The water that comes from the catchment is represented by the concentration 10.00 mgL^{-1} and the initial concentration in the lake is equal to 0.00 mgL^{-1} (Figure 22). We assume that 45% of rainfall is lost by interception, 20% is lost by infiltration in the catchment. In the lake area, a water loss equivalent to 30% is considered. In order to represent the water treatment plant abstractions, a water collection point that extracts about 120 Ls^{-1} was included.

During the simulations, water level variations in the lake are recorded. First, only the SW2D-GPU model is used to verify whether the parameters used would provide a good representation of the water level variations in the lake. Then the coupled version SW2D-EFDC is applied and again we verify the water level variation. In this way, it is possible to compare the two models and verify the conservation of mass and that the water inlets in the lake are compatible with those of the SW2D-GPU using the SW2D-EFDC model.

4.3 RESULTS

The lake level is well represented by both the SW2D-GPU model and the coupled SW2D-EFDC version (Figure 21). In the first 60 hours (period in which the catchment has the greatest contributions to the water inputs in the lake), the coupling between the two models is well established so that there are no significant water losses at the catchment-lake interface. A small difference in the simulated levels is verified after 80 h, in which the levels of the coupled model SW2D-EFDC are slightly higher due to differences in the ways in which water is extracted (by evaporation and water abstraction) in the 3D model lake domain.

After verifying that the coupling was successful with respect to the representation of the level variation, we can explore other aspects of the lake hydrodynamics and visualize

Figure 21 – Simulated water levels and gauge data. The black dots represent the gauged level data. The red dashed line represents the lake level simulated by the SW2D-GPU model and the blue line represents the lake level simulated by the SW2D-EFDC model.

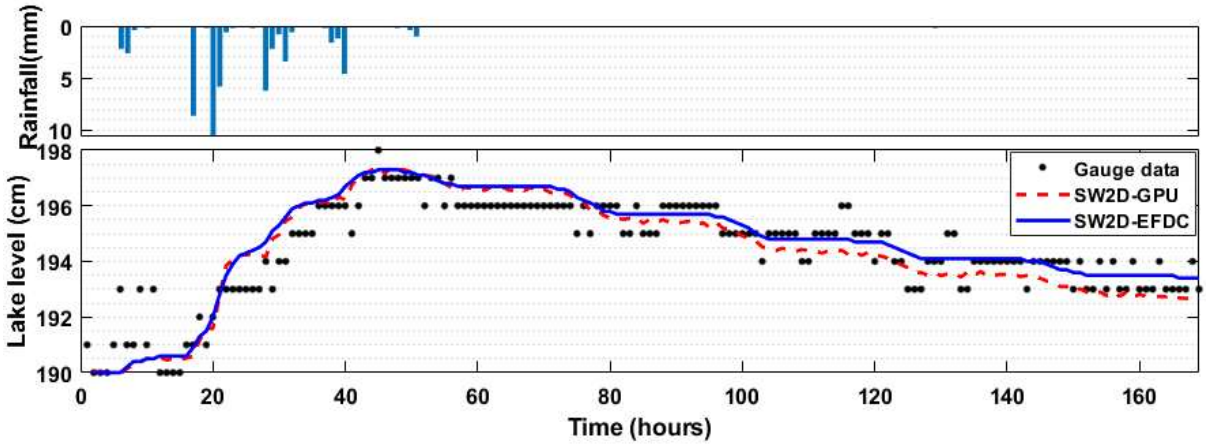

Source: Prepared by the author.

where the main water inlets occur and how the dye concentration (tracer) propagate inside the lake. The Figure 22 presents the results of simulations of water flows in the catchment and the hydrodynamics of the lake in wind-on and wind-off scenarios in which, in addition to the water velocities, the dynamics of a dye (tracer) are also simulated. It can be seen that water enters through rivers that have the largest drainage network, and in the period of the most intense rainfall the water velocities coming from the main river cause velocities of up to 0.036 m/s in the inner part of the lake. However, there are also several smaller water inlets across the catchment-lake boundary (Figure 22i–l). In a scenario that includes wind speeds and directions we can see the hydrodynamic behavior of the lake, estimate how the water velocities in the lake behave (Figure 22m–p) or estimate how the transport of a dye or solutes would enter from the catchment (Figure 22q–t).

Figure 22 – Interactions between water flows in the catchment and the lake. a–d) Water depth variation in the catchment. e–h) Water velocities in the lake in a wind-off setting. i–l) The dynamics of a dye in the lake in a wind-off scenario. m–p) Water velocities in the lake in a wind-on scenario. q–t) Dynamics of a dye in the lake in a wind-on scenario. The columns represent the results at 24, 48, 72 and 96 hours, respectively.

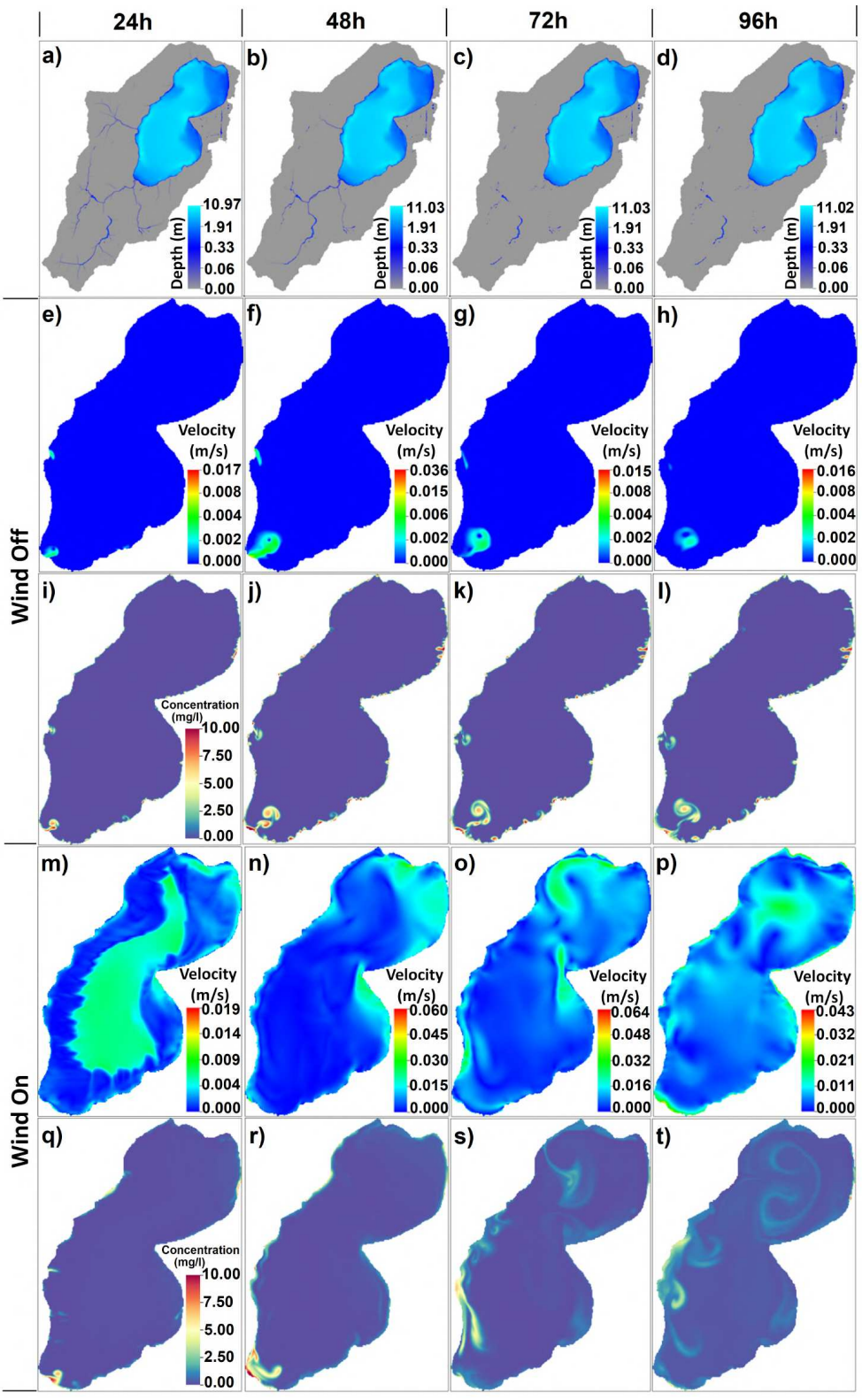

Source: Prepared by the author.

In the simulation, the waters entering the catchment are mixed with a virtual tracer

that facilitates the visualization of diffuse water inflows into the lake. In the wind-off scenario, it is easier to perceive the water inflows coming from the two main rivers, which with higher velocities transport the virtual tracer towards the central area of the lake, whereas the diffuse inflows distributed along the entire catchment-lake boundary have lower velocities and the virtual tracer remains on the lake shores. When wind velocities and directions are considered, the hydrodynamics of the lake is modified, with the wind as the main controller of water movement. In this scenario, the effect of the mixing of the virtual tracer that enters through the catchment-lake boundary becomes visible, since now the tracer concentrations that were retained on the lake shores are carried by the water towards the central region. This behavior, in addition to showing that wind velocities are of great importance for lake hydrodynamics, also reveals that diffuse water inflows across catchment-lake boundaries can significantly influence lake water composition. Although this case study shows a way to use virtual tracer concentrations (Dye) to visualize diffuse water inflows into the lake, it can also be a good way to infer possible entry points for nutrients and solutes from the catchment, estimate for which regions of the lake are transported, and possibly define where the highest concentrations can be found.

4.4 MAIN LIMITATIONS

In this chapter, the coupling between the SW2D-GPU model and the EFDC-MPI hydrodynamic model was carried out. In this way, the SW2D-GPU model calculates the water flows in the catchment and the results are inserted into the EFDC-MPI hydrodynamic model in the form of a boundary condition. Here, an off-line coupling was used in which the models communicate through external files. For this I developed a coupling module that transfers data from the SW2D-GPU model to the EFDC-MPI model in a fully automated way. The main limitations of the SW2D-EFDC model are: (i) it does not represent return flows, that is, flows occur only from the catchment to the lake; (ii) the computational domain of the lake is fixed (does not consider the increase of the lake area); (iii) tracer (dye) concentration, salinity and water temperature are considered in the model, but for simplification they are defined with homogeneous initial conditions for the entire lake, which over time are modified by inputs from the catchment; (iv) the water quality module has not been tested in the current version of the SW2D-EFDC model, and (v) the coupling does not consider interactions with subsurface water and groundwater.

4.5 CONCLUSIONS

In this chapter, an efficient coupling of the SW2D-EFDC model is presented for the simulation of water flows between catchment and lake. Through an application of the coupled model in the simulation of water flow in the Peri lake catchment, we verify that the coupled model correctly simulates the lake water levels during a precipitation event. The 3D simulation of the lake hydrodynamics are consistent in the representation of the

water velocities in the lake in wind-off and wind-on settings, as well as in the representation of the transport of a virtual tracer in these same scenarios. The SW2D-EFDC is a useful tool to study the hydrodynamics of lakes considering the contributions of the catchment. As a consequence of our coupling of these models it is possible to make efficient simulations of water flows in the catchment together with several hydrodynamic modeling features of the lake, such as transport of solutes and sediments, thermal processes and water quality.

5 GENERAL CONCLUSIONS

In this dissertation, the coupling between a two-dimensional surface runoff model based on the shallow water equations (SW2D-GPU) and the three-dimensional hydrodynamic model EFDC-MPI was carried out. The coupled model was developed to provide fast and efficient hydrodynamic simulations exploring the parallelism of computing structures that can range from desktops to clusters with multiple processors, massively parallel devices such as GPUs (Graphics Processing Unit) and supercomputers.

The first step to carry out this work was the implementation and parallelization of the two-dimensional shallow water model in CUDA C language for high performance computing on GPU, the model was called SW2D-GPU. Through two case studies: (i) simulation of flooding in the urban area; and (ii) integrated catchment-lake simulation, it was shown that the model can simulate flooding in urban areas considering water inflows from different sub-basins and can also be applied to simulate in an integrated way the dynamics of surface waters on hillslopes, streams and shallow lakes, as well as human interference with the extraction of water for public supply. The main potentialities of the SW2D-GPU model are: (i) the ability to simulate the interactions between the lake and its catchment, which makes it an interesting option to study the hydrology of lake ecosystems, even in ungauged areas; (ii) the high computational performance, with simulations that are up to 34 times faster than those performed with the sequential version of the model implemented in Fortran, when applied in domains with up to 7 million grid points; and (iii) high-resolution simulations can be performed on low-cost computers equipped with a GPU with CUDA technology. Although the SW2D-GPU model provides an integrated simulation of surface flows between the lake and the catchment, important aspects of lake hydrodynamics are neglected, such as: water quality, nutrient transport, wind influences, water temperature and processes that depend on the vertical dimension.

The second step adopted in this dissertation was the coupling of the SW2D-GPU model with the EFDC-MPI hydrodynamic model to provide a 3D hydrodynamic modeling of the lake considering the diffuse water inflows from the catchment, solute transport and wind influences. This coupling resulted in the SW2D-EFDC model that uses parallel processing in multi-core and GPU architectures. Thus, it minimizes the problem of long computational time, which is one of the main obstacles for the application of coupled models in real-world simulations. Another problem inherent to the complexity of the models is the preparation of the inputs to start the simulation, mainly in the part of the 3D hydrodynamic model. Therefore, in the coupling, the processes of creating the inputs and the configuration of the 3D hydrodynamic model were automated to ensure the continuity of the solution and the exchange of data between the SW2D-GPU model and the EFDC-MPI model without the need for human intervention. The SW2D-EFDC model has the following potentialities: (i) it allows hydrological and hydrodynamic simulations in large areas and with high spatial resolution; (ii) it simulates hydrodynamics in lake ecosystems

with little availability of measured data; (iii) it simulates catchment and lake interactions; (iv) it is ideal for simulations using GPUs and clusters with multiple processors (CPUs) and can also be used in common office computers.

In this dissertation it was shown that the coupled model is able to represent the exchange of water and concentrations of solutes (tracer) between the catchment and the lake. The tests and application of the coupled model SW2D-EFDC were developed in the Peri Lake catchment, which is a lake ecosystem with a tropical climate located in southern Brazil. First, it was verified that the coupled model correctly simulated lake water levels during a precipitation event without significant losses in water exchange between catchment and lake. Then the SW2D-EFDC model was applied to simulate the lake hydrodynamics considering the transport of a virtual tracer in wind-off and wind-on scenarios. This application showed that the model remained stable for water velocities induced by wind velocities measured in the catchment. The transport of a virtual tracer showed the model ability to represent the inputs and dynamics of chemical compounds coming from the catchment. In view of this, it is understood that the SW2D-EFDC model can be a useful tool to study water flows in the catchment and its influences on water levels and hydrodynamic of lakes at a catchment scale.

Lakes are present in different parts of the world and hydrological and hydrodynamic studies in these ecosystems require approaches and tools capable of reconciling three main activities: (i) obtaining data in field studies; (ii) computational modeling; and (iii) interpretation of results and hydrological processes. The development of the SW2D-EFDC model is a first effort to provide simultaneous communication between these activities. On the one hand, the modeling can help in the planning of field studies and, on the other hand, the SW2D-EFDC model can be constantly improved and tested as the catchment is being instrumented. Regarding usability, the SW2D-EFDC model significantly reduces the difficulties commonly encountered in the hydrological-hydrodynamic modeling of lake ecosystems, since most of the configuration procedures were automated.

The coupling of the SW2D-GPU model and the EFDC-MPI model allowed us to take an important step towards studying the influence of catchment flows on lake hydrodynamics, in an automated way and with high-performance computational resources. However, a number of limitations still remain and offer opportunities for future studies.

One of the challenges for coupled hydrological-hydrodynamic modeling is the bidirectional representation of flows (catchment $\rightarrow$ lake; lake $\rightarrow$catchment). In the SW2D-EFDC model the flows occur only from the catchment to the lake, this was a simple way adopted to test how the EFDC-MPI model would behave in the face of a coupling involving the entire boundary between catchment and lake. The test results showed good computational performance and there was no loss of numerical stability, indicating that a more complex coupling scheme involving the bidirectional representation of the flows is viable and recommended for future studies. This improvement, in addition to enabling return flows from the lake to rivers in the catchment, will also provide for addressing problems

where the lake area varies significantly.

The potential of the EFDC-MPI hydrodynamic model can be better explored and tested as data becomes more available. For this, the formulation of the coupling scheme and creation of the initial conditions can be improved to provide a more detailed approach to the spatio-temporal distribution of solute concentrations, salinity and water temperatures. Furthermore, in the continuity of the development of the SW2D-EFDC model, the consideration of the water quality module (which is already implemented in the EFDC-MPI model), is a necessary procedure to enable advanced studies of lake hydrodynamics, physicochemical and biological reactions.

The development of an integrated approach considering subsurface waters is also an opportunity for future research in the development of the SW2D-EFDC model. The EFDC model supports boundary conditions capable of interacting with groundwater flows which facilitates the task of coupling with an integrated surface and subsurface water flow model. At this point, the SW2D-EFDC model can be integrated with a subsurface flow model or new combinations of models can be tested. The SW2D-EFDC model is open source and available at: <https://github.com/LabHidro/SW2D-EFDC>.

REFERENCES

ACOSTA, M.; ANGUITA, M.; FERNÁNDEZ-BALDOMERO, F. J.; RAMÓN, C. L.; SCHLADOW, S. G.; RUEDA, F. J. Evaluation of a nested-grid implementation for 3D finite-difference semi-implicit hydrodynamic models. *Environmental Modelling and Software*, v. 64, p. 241–262, 2015. ISSN 13648152.

AHN, J. M.; KIM, H.; CHO, J. G.; KANG, T.; KIM, Y. S.; KIM, J. Parallelization of a 3-dimensional hydrodynamics model using a hybrid method with mpi and openmp. *Processes*, v. 9, n. 9, 2021. ISSN 22279717.

AHN, J. M.; KIM, J.; PARK, L. J.; JEON, J.; JONG, J.; MIN, J.-H.; KANG, T. Predicting cyanobacterial harmful algal blooms (Cyanohabs) in a regulated river using a revised efdc model. *Water (Switzerland)*, MDPI AG, v. 13, n. 4, 2021.

ALARCON, V. J.; JOHNSON, D.; MCANALLY, W. H.; ZWAAG, J. van der; IRBY, D.; CARTWRIGHT, J. Nested Hydrodynamic Modeling of a Coastal River Applying Dynamic-Coupling. *Water Resources Management*, Kluwer Academic Publishers, v. 28, p. 3227–3240, 2014.

ALTAIE, H. New Techniques Of Derivations for Shallow Water Equations. *International Journal of Advanced Scientific and Technical Research*, v. 3, n. 6, p. 131–150, 2016.

ANGUITA, M.; ACOSTA, M.; FERNÁNDEZ-BALDOMERO, F. J.; RUEDA, F. J. Scalable parallel implementation for 3D semi-implicit hydrodynamic models of shallow waters. *Environmental Modelling and Software*, v. 73, p. 201–217, 2015. ISSN 13648152.

ARCEMENT, G. J.; SCHNEIDER, V. R. *Guide for Selecting Manning's Roughness Coefficients for Natural Channels and Flood Plains*. Denver, Colorado, 1989. v. 2339, 1–38 p. Disponível em: <<https://pubs.usgs.gov/wsp/2339/report.pdf>>.

BALAJI, P.; CASAS, M. Special issue on the message passing interface. *Parallel Computing*, v. 86, p. 14–15, 2019. ISSN 0167-8191. Disponível em: <<https://www.sciencedirect.com/science/article/pii/S016781911930095X>>.

BARNEY, B. *Introduction to Parallel Computing*. 2016. Disponível em: <<https://computing.llnl.gov/tutorials/parallel_comp/>>.

BENNINGTON, V.; MCKINLEY, G. A.; KIMURA, N.; WU, C. H. General circulation of Lake Superior: Mean, variability, and trends from 1979 to 2006. *Journal of Geophysical Research*, Blackwell Publishing Ltd, v. 115, n. C12, p. C12015, dec 2010. ISSN 0148-0227.

BICKNELL, B.; IMHOFF, J.; KITTLE, J.; JOBES, T. J.; DONIGIAN, A. J. *Hydrological Simulation Program-Fortran, user's manual for version 12*. Athens, 2001.

BOCANIOV, S. A.; LEON, L. F.; RAO, Y. R.; SCHWAB, D. J.; SCAVIA, D. Simulating the effect of nutrient reduction on hypoxia in a large lake (Lake Erie, USA-Canada) with a three-dimensional lake model. *Journal of Great Lakes Research*, International Association of Great Lakes Research, v. 42, n. 6, p. 1228–1240, 2016. ISSN 03801330.

BRADFORD, S. F.; KATOPODES, N. D. Hydrodynamics of Turbid Underflows. I: Formulation and Numerical Analysis. *Journal of Hydraulic Engineering*, v. 125, n. 10, p. 1006–1015, 1999.

BRODTKORB, A. R.; HAGEN, T. R.; LIE, K. A.; NATVIG, J. R. Simulation and visualization of the Saint-Venant system using GPUs. *Computing and Visualization in Science*, v. 13, n. 7, p. 341–353, 2010. ISSN 14329360.

BRODTKORB, A. R.; HAGEN, T. R.; SÆTRA, M. L. Graphics processing unit (GPU) programming strategies and trends in GPU computing. *Journal of Parallel and Distributed Computing*, Elsevier Inc., v. 73, n. 1, p. 4–13, 2013. ISSN 07437315.

BRODTKORB, A. R.; SÆTRA, M. L.; ALTINAKAR, M. Efficient shallow water simulations on GPUs: Implementation, visualization, verification, and validation. *Computers and Fluids*, v. 55, p. 1–12, 2012. ISSN 00457930.

BUECHE, T.; HAMILTON, D. P.; VETTER, M. Using the General Lake Model (GLM) to simulate water temperatures and ice cover of a medium-sized lake: a case study of Lake Ammersee, Germany. *Environmental Earth Sciences*, Springer Verlag, 2017.

BUECHE, T.; WENK, M.; POSCHLOD, B.; GIADROSSICH, F.; PIRASTRU, M.; VETTER, M. GlmGUI v1.0: An R-based graphical user interface and toolbox for GLM (General Lake Model) simulations. *Geoscientific Model Development*, Copernicus GmbH, v. 13, n. 2, p. 565–580, 2020. ISSN 19919603.

CARLOTTO, T.; CHAFFE, P. L. B. Acoplamento de modelos 2D e 3D de alto desempenho para modelagem hidrológica e hidrodinâmica em ecossistemas lacustres. In: *Anais do XXIV Simpósio Brasileiro de Recursos Hídricos*. Belo Horizonte: ABRHidro, 2021. p. 1–9. Disponível em: <<https://anais.abrhidro.org.br/job.php?Job=13113>>.

CARLOTTO, T.; CHAFFE, P. L. B.; SANTOS, C. I. dos; LEE, S. SW2D-GPU: A two-dimensional shallow water model accelerated by GPGPU. *Environmental Modelling & Software*, v. 145, 2021.

CARLOTTO, T.; SILVA, R. da; GRZYBOWSKI, J. GPGPU-accelerated environmental modelling based on the 2D advection-reaction-diffusion equation. *Environmental Modelling & Software*, v. 116, p. 87–99, jun 2019. ISSN 13648152.

CARLOTTO, T.; SILVA, R. V. da; GRZYBOWSKI, J. M. A GPGPU-accelerated implementation of groundwater flow model in unconfined aquifers for heterogeneous and anisotropic media. *Environmental Modelling and Software*, Elsevier Ltd, v. 101, p. 64–72, 2018. ISSN 13648152.

CHAFFE, P. L. B.; Innocente dos Santos, C.; PEREZ, A. B. A.; SÁ, J. H. M.; CARLOTTO, T.; HOINASKI, L. Observing the critical zone on a critical budget: The Peri Lake experimental catchment. *Hydrological Processes*, v. 35, n. 3, 2021. ISSN 10991085.

CHAPMAN, R. S.; JOHNSON, B. H.; VEMULAKONDA, S. R.; WES. *User's Guide for the Sigma Stretched Version of CH3D-WES: A Three-Dimensional Numerical Hydrodynamic, Salinity, and Temperature Model*. Vicksburg, MS, 1996.

CHIFFLARD, P.; BLUME, T.; MAERKER, K.; HOPP, L.; MEERVELD, I.; GRAEF, T.; GRONZ, O.; HARTMANN, A.; KOHL, B.; MARTINI, E.; IMJELA, C. R.; REISS, M.; RINDERER, M.; ACHLEITNER, S. How can we model subsurface stormflow at the catchment scale if we cannot measure it? *Hydrological Processes*, John Wiley & Sons, Ltd, v. 33, n. 9, p. 1378–1385, apr 2019. ISSN 0885-6087.

CHOW, V.; MAIDMENT, D.; MAYS, L. *Applied Hydrology*. [S.l.]: McGraw-Hill, 1988. (Civil Engineering). ISBN 9780071001748.

CLARK, M. P.; NIJSSEN, B.; LUNDQUIST, J. D.; KAVETSKI, D.; RUPP, D. E.; WOODS, R. A.; FREER, J. E.; GUTMANN, E. D.; WOOD, A. W.; BREKKE, L. D.; ARNOLD, J. R.; GOCHIS, D. J.; RASMUSSEN, R. M. A unified approach for process-based hydrologicmodeling: 1. Modeling concept. *Water Resources Research*, p. 2498–2514, 2015.

COLE, T.; BUCHAK, E. *CE-QUAL-W2: A two dimensional, laterally averaged, hydrodynamic and water quality model, Version 2.0 user's manual*. Vicksburg, MS, 1995.

COLLISCHONN, W.; ALLASIA, D.; SILVA, B. C. D. A.; CARLOS, E. M. The MGB-IPH model for large-scale rainfall-runoff modelling. *Hydrological Sciences Journal*, v. 5, n. 52, p. 878–895, 2007.

COUTURE, R. M.; TOMINAGA, K.; STARRFELT, J.; MOE, S. J.; KASTE, Y.; WRIGHT, R. F. Modelling phosphorus loading and algal blooms in a Nordic agricultural catchment-lake system under changing land-use and climate. *Environmental Sciences: Processes and Impacts*, Royal Society of Chemistry, v. 16, n. 7, p. 1588–1599, 2014. ISSN 20507895.

CROMPTON, O.; SYTSMA, A.; THOMPSON, S. Emulation of the Saint Venant Equations Enables Rapid and Accurate Predictions of Infiltration and Overland Flow Velocity on Spatially Heterogeneous Surfaces. *Water Resources Research*, John Wiley & Sons, Ltd, v. 55, n. 8, p. 7108–7129, aug 2019. ISSN 0043-1397.

DARGAHI, B.; SETEGN, S. G. Combined 3D hydrodynamic and watershed modelling of Lake Tana, Ethiopia. *Journal of Hydrology*, v. 398, n. 1-2, p. 44–64, 2011. ISSN 00221694.

Dataset: ASF DAAC. *ALOS PALSAR_ Radiometric_ Terrain_ Corrected_ high_ res*. ASF DAAC, 2018. Disponível em: <<https://search.asf.alaska.edu/{#}/>>.

DAZZI, S.; VACONDIO, R.; MIGNOSA, P. Internal boundary conditions for a GPU-accelerated 2D shallow water model: Implementation and applications. *Advances in Water Resources*, Elsevier Ltd, v. 137, p. 103525, 2020.

DELTARES. *Delft3D-FLOW Simulation of multi-dimensional hydrodynamic flows and transport phenomena, including sediments - User Manual*. Netherlands: Deltares, 2019.

DREWRY, D. T.; KUMAR, P.; LONG, S.; BERNACCHI, C.; LIANG, X. Z.; SIVAPALAN, M. Ecohydrological responses of dense canopies to environmental variability: 1. Interplay between vertical structure and photosynthetic pathway. *Journal of Geophysical Research: Biogeosciences*, v. 115, n. 4, p. 1–25, 2010. ISSN 01480227.

ECHEVERRIBAR, I.; MORALES-HERNÁNDEZ, M.; BRUFAU, P.; GARCÍA-NAVARRO, P. 2D numerical simulation of unsteady flows for large scale floods prediction in real time. *Advances in Water Resources*, v. 134, 2019. ISSN 03091708.

Chapter 10 - cuda in a cloud and cluster environments. In: FARBER, R. (Ed.). *CUDA Application Design and Development*. Boston: Morgan Kaufmann, 2011. p. 241–264. ISBN 978-0-12-388426-8. Disponível em: <<https://www.sciencedirect.com/science/article/pii/B9780123884268000100>>.

FATICHI, S.; VIVONI, E. R.; OGDEN, F. L.; IVANOV, V. Y.; MIRUS, B.; GOCHIS, D.; DOWNER, C. W.; CAMPORESE, M.; DAVISON, J. H.; EBEL, B.; JONES, N.; KIM, J.; MASCARO, G.; NISWONGER, R.; RESTREPO, P.; RIGON, R.; SHEN, C.; SULIS, M.; TARBOTON, D. An overview of current applications, challenges, and future trends in distributed process-based models in hydrology. *Journal of Hydrology*, Elsevier, v. 537, p. 45–60, jun 2016. ISSN 0022-1694.

FERRARIN, C.; BAJO, M.; UMGIESSER, G. Model-driven optimization of coastal sea observatories through data assimilation in a finite element hydrodynamic model (SHYFEM v.7_5_65). *Geoscientific Model Development Discussions*, p. 1–28, 2020. ISSN 1991-959X.

FRAGOSO, C. R.; Motta Marques, D. M.; FERREIRA, T. F.; JANSE, J. H.; NES, E. H. van. Potential effects of climate change and eutrophication on a large subtropical shallow lake. *Environmental Modelling & Software*, v. 26, n. 11, p. 1337–1348, nov 2011. ISSN 13648152.

FRAGOSO, C. R.; NES, E. H. V.; JANSE, J. H.; MARQUES, M. IPH-TRIM3D-PCLake : A three-dimensional complex dynamic model for subtropical aquatic ecosystems. *Environmental Modelling and Software*, Elsevier Ltd, v. 24, n. 11, p. 1347–1348, 2009. ISSN 1364-8152.

FRASSL, M. A.; ABELL, J. M.; BOTELHO, D. A.; CINQUE, K.; GIBBES, B. R.; JÖHNK, K. D.; MURAOKA, K.; ROBSON, B. J.; WOLSKI, M.; XIAO, M.; HAMILTON, D. P. A short review of contemporary developments in aquatic ecosystem modelling of lakes and reservoirs. *Environmental Modelling & Software*, v. 117, n. June 2018, p. 181–187, 2019.

FUTTER, M. N.; ERLANDSSON, M. A.; BUTTERFIELD, D.; WHITEHEAD, P. G.; ONI, S. K.; WADE, A. J. PERSiST: A flexible rainfall-runoff modelling toolkit for use with the INCA family of models. *Hydrology and Earth System Sciences*, v. 18, n. 2, p. 855–873, 2014. ISSN 16077938.

GETIRANA, A.; LIBONATI, R.; CATALDI, M. Brazil is in water crisis - it needs a drought plan. *Nature*, v. 600, n. 7888, p. 218–220, 2021. ISSN 14764687.

GU, H.; MA, Z.; LI, M. Effect of a large and very shallow lake on local summer precipitation over the Lake Taihu basin in China. *Journal of Geophysical Research: Atmospheres*, Wiley-Blackwell, v. 121, n. 15, p. 8832–8848, aug 2016. ISSN 2169897X.

HAMRICK, J. User's Manual for the Environmental Fluid Dynamics Computer Code. *Special Reports in Applied Marine Science and Ocean Engineering (SRAMSOE)*, v. 331, 1996. Disponível em: <<https://doi.org/10.21220/V5M74W>>.

HAMRICK, J. M. *A Three-Dimensional Environmental Fluid Dynamics Computer Code : Theoretical and computational aspects.* [S.l.], 1992.

HENNEMANN, M. C.; PETRUCIO, M. M. Spatial and temporal dynamic of trophic relevant parameters in a subtropical coastal lagoon in Brazil. *Environmental Monitoring and Assessment*, v. 181, n. 1-4, p. 347–361, 2011. ISSN 01676369.

HIPSEY, M. R.; BRUCE, L. C.; BOON, C.; BUSCH, B.; CAREY, C. C.; HAMILTON, D. P.; HANSON, P. C.; READ, J. S.; SOUSA, E. de; WEBER, M.; WINSLOW,

L. A. A General Lake Model (GLM 3.0) for linking with high-frequency sensor data from the Global Lake Ecological Observatory Network (GLEON). *Geoscientific Model Development*, Copernicus GmbH, v. 12, n. 1, p. 473–523, jan 2019. ISSN 1991-9603.

HODGES, B. Hydrodynamical Modeling. In: *Reference Module in Earth Systems and Environmental Sciences*. [S.l.]: Elsevier, 2014. ISBN 9780124095489.

HORVÁTH, Z.; WASER, J.; PERDIGÃO, R. A. P.; KONEV, A.; BLOSCHL, G. A two-dimensional numerical scheme of dry/wet fronts for the Saint-Venant system of shallow water equations. *International Journal for Numerical Methods in Fluids*, p. 601–629, 2014.

HUANG, J.; YAN, R.; GAO, J.; ZHANG, Z.; QI, L. Modeling the impacts of water transfer on water transport pattern in Lake Chao, China. *Ecological Engineering*, Elsevier B.V., v. 95, p. 271–279, 2016. ISSN 0925-8574.

HUANG, J.; ZHANG, Y.; HUANG, Q.; GAO, J. When and where to reduce nutrient for controlling harmful algal blooms in large eutrophic lake Chaohu, China? *Ecological Indicators*, Elsevier B.V., v. 89, p. 808–817, 2018. ISSN 1470160X.

HUI, Y.; FARNHAM, D. J.; ATKINSON, J. F.; ZHU, Z.; FENG, Y. Circulation in Lake Ontario: Numerical and Physical Model Analysis. *Journal of Hydraulic Engineering*, American Society of Civil Engineers (ASCE), v. 147, n. 8, 2021.

HWANG, S.; JUN, S. M.; SONG, J. H.; KIM, K.; KIM, H.; KANG, M. S. Application of the swat-efdc linkage model for assessing water quality management in an Estuarine reservoir separated by levees. *Applied Sciences (Switzerland)*, v. 11, n. 9, p. 1–16, 2021. ISSN 20763417.

IVANOV, V. Y.; VIVONI, E. R.; BRAS, R. L.; ENTEKHABI, D. Catchment hydrologic response with a fully distributed triangulated irregular network model. *Water Resouces Research*, v. 40, p. 1–23, 2004.

JANSSEN, A. B.; WIJK, D. van; GERVEN, L. P. van; BAKKER, E. S.; BREDERVELD, R. J.; DEANGELIS, D. L.; JANSE, J. H.; MOOIJ, W. M. Success of lake restoration depends on spatial aspects of nutrient loading and hydrology. *Science of The Total Environment*, v. 679, p. 248–259, aug 2019. ISSN 00489697.

JEFFERS, J.; REINDERS, J. Chapter 12 - mpi. In: JEFFERS, J.; REINDERS, J. (Ed.). *Intel Xeon Phi Coprocessor High Performance Programming*. Boston: Morgan Kaufmann, 2013. p. 343–362. ISBN 978-0-12-410414-3. Disponível em: <<https://www.sciencedirect.com/science/article/pii/B9780124104143000128>>.

JIANG, C.; ZHOU, Q.; YU, W.; YANG, C.; LIN, B. A Dynamic Bidirectional Coupled Hydrologic-Hydrodynamic Model for Flood Prediction. *Natural Hazards and Earth System Sciences*, n. December, p. 1–32, 2019. ISSN 1561-8633.

JONES, F. E.; HARRIS, G. L. ITS-90 density of water formulation for volumetric standards calibration. *Journal of Research of the National Institute of Standards and Technology*, v. 97, n. 3, p. 335–340, 1992. ISSN 1044677X.

KAWAIKE, K.; INOUE, K.; TODA, K. Inundation flow modeling in urban area based on the unstructured meshes. *Hydraulic Engineering Software*, 2000.

KIM, J.; WARNOCK, A.; IVANOV, V. Y.; KATOPODES, N. D. Coupled modeling of hydrologic and hydrodynamic processes including overland and channel flow. *Advances in Water Resources*, v. 37, p. 104–126, mar 2012. ISSN 03091708.

KUFFOUR, B.; ENGDAHL, N.; WOODWARD, C.; CONDON, L.; KOLLET, S.; MAXWELL, R. Simulating Coupled Surface-Subsurface Flows with ParFlow v3.5.0: Capabilities, applications, and ongoing developmentof an open-source, massively parallel, integrated hydrologic model. *Geoscientific Model Development Discussions*, p. 1–66, 2020. ISSN 1991-959X.

KUMMU, M.; TES, S.; YIN, S.; ADAMSON, P.; JÓZSA, J.; KOPONEN, J.; RICHEY, J.; SARKKULA, J. Water balance analysis for the Tonle Sap Lake-floodplain system. *Hydrological Processes*, John Wiley and Sons Ltd, v. 28, n. 4, p. 1722–1733, feb 2014. ISSN 08856087.

KURGANOV, A.; PETROVA, G. Central-Upwind Schemes for Two-Layers Shallow Water Equations. *SIAM Journal on Scientific Computing*, v. 31, n. 3, p. 1742–1773, 2009.

LAI, G.; WANG, P.; LI, L. Possible impacts of the Poyang Lake (China) hydraulic project on lake hydrology and hydrodynamics. *Hydrology Research*, Nordic Association for Hydrology, v. 47, n. S1, p. 187–205, dec 2016. ISSN 0029-1277.

LE, P. V.; KUMAR, P.; VALOCCHI, A. J.; DANG, H. V. GPU-based high-performance computing for integrated surface-sub-surface flow modeling. *Environmental Modelling and Software*, Elsevier Ltd, v. 73, p. 1–13, 2015. ISSN 13648152.

LE, P. V. V.; KUMAR, P. Interaction Between Ecohydrologic Dynamics and Microtopographic Variability Under Climate Change. *Water Resources Research*, John Wiley & Sons, Ltd, v. 53, n. 10, p. 8383–8403, oct 2017. ISSN 00431397.

LEE, H. W.; KIM, E. J.; PARK, S. S.; CHOI, J. H. Effects of climate change on the thermal structure of lakes in the Asian Monsoon Area. *Climatic Change*, v. 112, n. 3-4, p. 859–880, 2012. ISSN 01650009.

LEE, S. *Study on Development of Integrated Urban Inundation Model Incorporating Drainage Systems*. 126 p. Tese (Dissertação) — Kyoto University, 2013.

LEE, S.; NAKAGAWA, H.; KAWAIKE, K.; ZHANG, H. Urban Inundation Simulation Incorporating Sewerage System without Structure Effect. *Annuals of Disaster Prevention Res. Inst., Kyoto University., No. 57 B*, n. 57, p. 407–414, 2014.

LEE, S.; NAKAGAWA, H.; KAWAIKE, K.; ZHANG, H. Urban inundation simulation considering road network and building configurations. *Journal of Flood Risk Management*, v. 9, n. 3, p. 224–233, 2016. ISSN 1753318X.

LEON, L. F.; SMITH, R. E.; HIPSEY, M. R.; BOCANIOV, S. A.; HIGGINS, S. N.; HECKY, R. E.; ANTENUCCI, J. P.; IMBERGER, J. A.; GUILDFORD, S. J. Application of a 3D hydrodynamic-biological model for seasonal and spatial dynamics of water quality and phytoplankton in Lake Erie. *Journal of Great Lakes Research*, International Association of Great Lakes Research, v. 37, n. 1, p. 41–53, mar 2011. ISSN 03801330.

LI, M.; ZHANG, Q.; LI, Y.; YAO, J.; TAN, Z. Inter-annual variations of Poyang Lake area during dry seasons: characteristics and implications. *Hydrology Research*, Nordic Association for Hydrology, v. 47, n. S1, p. 40–50, dec 2016. ISSN 0029-1277.

LI, Y.; ZHANG, Q.; YAO, J.; WERNER, A. D.; LI, X. Hydrodynamic and Hydrological Modeling of the Poyang Lake Catchment System in China. *Journal of Hydrologic Engineering*, ASCE-AMER SOC CIVIL ENGINEERS, v. 19, n. 3, p. 607–616, mar 2014. ISSN 1084-0699.

LIU, Q.; QIN, Y.; LI, G. Fast Simulation of Large-Scale Floods Based on GPU Parallel Computing. *Water*, MDPI AG, v. 10, n. 5, p. 589, may 2018. ISSN 2073-4441.

LIU, Z.; ZHANG, H.; LIANG, Q. A coupled hydrological and hydrodynamic model for flood simulation. *Hydrology Research*, v. 2, n. 50, p. 589–606, 2019.

LOPES, V. A.; FAN, F. M.; PONTES, P. R.; SIQUEIRA, V. A.; COLLISCHONN, W.; MARQUES, D. d. M. A first integrated modelling of a river-lagoon large-scale hydrological system for forecasting purposes. *Journal of Hydrology*, Elsevier, v. 565, p. 177–196, 2018. ISSN 0022-1694.

MAURICIO, A.; CAVALCANTI, J. R.; MARTIN, J.; MAINARDI, F.; MOTTA-MARQUES, D.; RUBERTO, C.; JR, F. Coupling large-scale hydrological and hydrodynamic modeling : Toward a better comprehension of watershed-shallow lake processes. *Journal of Hydrology*, Elsevier, v. 564, n. July, p. 424–441, 2018. ISSN 0022-1694.

MESSAGER, M. L.; LEHNER, B.; GRILL, G.; NEDEVA, I.; SCHMITT, O. Estimating the volume and age of water stored in global lakes using a geo-statistical approach. *Nature Communications*, v. 7, p. 1–11, 2016. ISSN 20411723.

MING, X.; LIANG, Q.; XIA, X.; LI, D.; FOWLER, H. J. Real-Time Flood Forecasting Based on a High-Performance 2-D Hydrodynamic Model and Numerical Weather Predictions. *Water Resources Research*, v. 56, n. 7, p. 1–22, 2020. ISSN 19447973.

MONTANARI, A.; YOUNG, G.; SAVENIJE, H. H.; HUGHES, D.; WAGENER, T.; REN, L. L.; KOUTSOYIANNIS, D.; CUDENNEC, C.; TOTH, E.; GRIMALDI, S.; BLÖSCHL, G.; SIVAPALAN, M.; BEVEN, K.; GUPTA, H.; HIPSEY, M.; SCHAEFLI, B.; ARHEIMER, B.; BOEGH, E.; SCHYMANSKI, S. J.; Di Baldassarre, G.; YU, B.; HUBERT, P.; HUANG, Y.; SCHUMANN, A.; POST, D. A.; SRINIVASAN, V.; HARMAN, C.; THOMPSON, S.; ROGGER, M.; VIGLIONE, A.; MCMILLAN, H.; CHARACKLIS, G.; PANG, Z.; BELYAEV, V. "Panta Rhei-Everything Flows": Change in hydrology and society-The IAHS Scientific Decade 2013-2022. *Hydrological Sciences Journal*, v. 58, n. 6, p. 1256–1275, 2013. ISSN 02626667.

MONTEIRO, L. R.; Dos Santos, C. I.; KOBIYAMA, M.; CORSEUIL, C. W.; CHAFFE, P. L. B. Effects of return periods on flood hazard mapping: An analysis of the ufsc campus basin, florianópolis city, brazil. *Revista Brasileira de Recursos Hidricos*, v. 26, 2021. ISSN 23180331.

MOOIJ, W. M.; TROLLE, D.; JEPPESEN, E.; ARHONDITSIS, G.; BELOLIPETSKY, P. V.; NES, E. H. V.; WELLS, S. A.; JANSE, J. H. Challenges and opportunities for integrating lake ecosystem modelling approaches. *Aquatic Ecology*, n. 44, p. 633–667, 2010.

MUNAR, A. M.; CAVALCANTI, J. R.; BRAVO, J. M.; FAN, F. M.; MOTTA-MARQUES, D. da; FRAGOSO, C. R. Coupling large-scale hydrological and hydrodynamic modeling: Toward a better comprehension of watershed-shallow lake processes. *Journal of Hydrology*, Elsevier B.V., v. 564, p. 424–441, sep 2018. ISSN 00221694.

MUNAR, A. M.; CAVALCANTI, J. R.; BRAVO, J. M.; MOTTA-MARQUES, D. da; FRAGOSO, C. R. Assessing the large-scale variation of heat budget in poorly gauged watershed-shallow lake system using a novel integrated modeling approach. *Journal of Hydrology*, Elsevier B.V., v. 575, p. 244–256, 2019. ISSN 00221694.

NERSC. *Large Scale Computing and Storage Requirements for Biological and Environmental Science: Target 2017*. Berkeley, 2013.

NOH, S. J.; LEE, J. H.; LEE, S.; KAWAIKE, K.; SEO, D. J. Hyper-resolution 1D-2D urban flood modelling using LiDAR data and hybrid parallelization. *Environmental Modelling and Software*, Elsevier Ltd, v. 103, p. 131–145, 2018. ISSN 13648152.

NOH, S. J.; LEE, J. H.; LEE, S.; SEO, D. J. Retrospective dynamic inundation mapping of hurricane harvey flooding in the Houston metropolitan area using high-resolution modeling and high-performance computing. *Water (Switzerland)*, v. 11, n. 3, 2019. ISSN 20734441.

NOH, S. J.; LEE, S.; AN, H.; KAWAIKE, K.; NAKAGAWA, H. Ensemble urban flood simulation in comparison with laboratory-scale experiments: Impact of interaction models for manhole, sewer pipe, and surface flow. *Advances in Water Resources*, Elsevier Ltd, v. 97, p. 25–37, 2016. ISSN 03091708.

NVIDIA. *Computação com GPU NVIDIA*. 2016. Disponível em: <<http://www.nvidia.com.br/object/gpu-accelerated-computing-br.html>>.

O'DONNCHA, F.; IAKYMCHUK, R.; AKHRIEV, A.; GSCHWANDTNER, P.; THOMAN, P.; HELLER, T.; AGUILAR, X.; DICHEV, K.; GILLAN, C.; MARKIDIS, S.; LAURE, E.; RAGNOLI, E.; VASSILIADIS, V.; JOHNSTON, M.; JORDAN, H.; FAHRINGER, T. AllScale toolchain pilot applications: PDE based solvers using a parallel development environment. *Computer Physics Communications*, Elsevier B.V., v. 251, p. 107089, 2019. ISSN 00104655.

O'DONNCHA, F.; RAGNOLI, E.; SUITS, F. Parallelisation study of a three-dimensional environmental flow model. *Computers and Geosciences*, Elsevier, v. 64, p. 96–103, 2014. ISSN 00983004.

OLIVEIRA, J. S. *Análise Sedimentar Em Zonas Costeiras: Subsídio Ao Diagnóstico Ambiental Da Lagoa Do Peri-Ilha De Santa Catarina-Sc, Brasil*. 154 p. Tese (Dissertação de Mestrado) — Universidade Federal de Santa Catarina, 2002.

PANICONI, C.; PUTTI, M. Physically based modeling in catchment hydrology at 50: Survey and outlook. *Water Resources Research*, v. 51, n. 9, p. 7090–7129, 2015. ISSN 19447973.

PARK, S.; KIM, B.; KIM, D.-H. 2D GPU-accelerated high resolution numerical scheme for solving diffusive wave equations. *Water (Switzerland)*, MDPI AG, v. 11, n. 7, p. 1–13, 2019.

PEREZ, A. B.; SANTOS, C. I. dos; SÁ, J. H.; ARIENTI, P. F.; CHAFFE, P. L. Connectivity of ephemeral and intermittent streams in a subtropical atlantic forest headwater catchment. *Water (Switzerland)*, v. 12, n. 6, p. 1–15, 2020. ISSN 20734441.

QUARANTA, L.; MADDEGEDARA, L. A novel mpi+mpi hybrid approach combining mpi-3 shared memory windows and c11/c++11 memory model. *Journal of Parallel and Distributed Computing*, v. 157, p. 125–144, 2021. ISSN 0743-7315. Disponível em: <<https://www.sciencedirect.com/science/article/pii/S074373152100143X>>.

RANSOM, O. T.; YOUNIS, B. A. Explicit GPU Based Second-Order Finite-Difference Modeling on a High Resolution Surface, Feather River, California. *Water Resources Management*, Springer Netherlands, v. 30, p. 261–277, 2016.

RODRIGUES, M.; ROSA, A.; CRAVO, A.; JACOB, J.; FORTUNATO, A. B. Effects of climate change and anthropogenic pressures in the water quality of a coastal lagoon (Ria Formosa, Portugal). *Science of the Total Environment*, v. 780, 2021. ISSN 18791026.

RUEDA, F. J.; MACINTYRE, S. Modelling the fate and transport of negatively buoyant storm-river water in small multi-basin lakes. *Environmental Modelling and Software*, v. 25, n. 1, p. 146–157, jan 2010. ISSN 13648152.

RUTAN, D. A.; Louis Smith, G.; WONG, T. Diurnal variations of albedo retrieved from earth radiation budget experiment measurements. *Journal of Applied Meteorology and Climatology*, v. 53, n. 12, p. 2747–2760, 2014. ISSN 15588432.

SÁ, J. H. M.; OLIVEIRA, D. Y. de; ARIENTI, P. F.; PEREZ, A. B. A.; SANTOS, C. I. dos; CHAFFE, P. L. B. VARIAÇÃO DO PROCESSO DE INTERCEPTAÇÃO DURANTE EVENTOS DE PRECIPITAÇÃO EM UMA FLORESTA OMBRÓFILA DENSA. In: *xxiii Simpósio Brasileiro de Recursos Hídricos*. Foz do Iguaçu, Paraná, Brasil: Associação Brasileira de Recursos Hídricos, 2019. p. 1–9. Disponível em: <<http://anais.abrh.org.br/works/6130>>.

SALORANTA, T. M.; ANDERSEN, T. MyLake-A multi-year lake simulation model code suitable for uncertainty and sensitivity analysis simulations. *Ecological Modelling*, v. 207, n. 1, p. 45–60, 2007. ISSN 03043800.

SANTOS, C. I.; CHAFFE, P. L. B.; PEREZ, A. B. A.; ARIENTI, P. F.; SÁ, J. H. M. Precision and accuracy of streamflow measurements in headwater streams during baseflow. *Brazilian Journal of Water Resources*, v. 26, n. 8, p. 1–15, 2021.

SBROGLIA, R. M.; BELTRAME, V. O ZONEAMENTO , CONFLITOS E RECATEGORIZAÇÃO DO PARQUE MUNICIPAL DA LAGOA DO PERI , FLORIANÓPOLIS / SC. p. 5–18, 2012.

SCHNEIDER, T.; LAN, S.; STUART, A.; TEIXEIRA, J. Earth System Modeling 2.0: A Blueprint for Models That Learn From Observations and Targeted High-Resolution Simulations. *Geophysical Research Letters*, v. 44, n. 24, p. 12,396–12,417, 2017. ISSN 19448007.

SDS. *Sistema de Informações Geográficas de Santa Catarina (SIGSC)*. 2016. Disponível em: <<http://sigsc.sds.sc.gov.br/>>.

SELLERS, B. H. A new formula for latent heat of vaporization of water as a function of temperature. *Quarterly Journal of the Royal Meteorological Society*, v. 110, n. 466, p. 1186–1190, 1984. ISSN 1477870X.

SHIN, S.; HER, Y.; SONG, J. H.; KANG, M. S. Integrated sediment transport process modeling by coupling Soil and Water Assessment Tool and Environmental Fluid Dynamics Code. *Environmental Modelling and Software*, Elsevier, v. 116, n. January, p. 26–39, 2019. ISSN 13648152. Disponível em: <<https://doi.org/10.1016/j.envsoft.2019.02.002>>.

SMARI, W. W.; BAKHOUYA, M.; FIORE, S.; ALOISIO, G. New advances in High Performance Computing and simulation: parallel and distributed systems, algorithms, and applications. *Concurrency Computation Practice and Experience*, v. 28, p. 2024–2030, 2016. ISSN 15320626.

SMITH, P. *A Semi-Implicit, Three-Dimensional Model for Estuarine Circulation*. [S.l.], 2006. 176 p.

SOARES, L. M. V.; CALIJURI, M. d. C. Deterministic modelling of freshwater lakes and reservoirs: Current trends and recent progress. *Environmental Modelling and Software*, Elsevier Ltd, v. 144, n. July, p. 105143, 2021. ISSN 13648152. Disponível em: <<https://doi.org/10.1016/j.envsoft.2021.105143>>.

SONG, Y.; JEONG, Y.-H.; SHIN, C.-M.; KWAK, D.-H. Spatial distribution and comparative evaluation of phosphorus release rate in benthic sediments of an estuary dam. *International Journal of Sediment Research*, Elsevier B.V., v. 37, n. 3, p. 355–369, 2021.

TAGUE, C. L.; BAND, L. E. RHESSys: Regional Hydro-Ecologic Simulation System An Object Oriented Approach to Spatially Distributed Modeling of Carbon, Water, and Nutrient Cycling. *Earth Interactions*, v. 8, n. 19, p. 1–42, 2004. ISSN 1087-3562.

Tetra Tech. *The Environmental Fluid Dynamics Code User Manual*. Fairfax, 2007. Disponível em: <<https://www.epa.gov/ceam/environment-fluid-dynamics-code-efdc-download-page>>.

THANG, N. T.; INOUE, K.; TODA, K.; KAWAIKE, K. A model for flood inundation analysis in urban area: verification and application. *Annuals of Disaster Prevention Res. Inst., Kyoto University., No. 47 B*, n. 47, p. 1–13, 2004.

TIAN, P.; WU, H.; YANG, T.; ZHANG, W.; JIANG, F.; ZHANG, Z.; WU, T. Environmental risk assessment of accidental pollution incidents in drinking water source areas: A case study of the Hongfeng Lake Watershed, China. *Sustainability (Switzerland)*, MDPI AG, v. 11, n. 19, 2019. ISSN 20711050.

TRISTRAM, D.; HUGHES, D.; BRADSHAW, K. Accelerating a hydrological uncertainty ensemble model using graphics processing units (GPUs). *Computers and Geosciences*, Elsevier, v. 62, p. 178–186, 2014. ISSN 0098-3004.

UMGIESSER, G.; ZEMLYS, P.; ERTURK, A.; RAZINKOVA-BAZIUKAS, A.; MEZINE, J.; FERRARIN, C. Seasonal renewal time variability in the Curonian Lagoon caused by atmospheric and hydrographical forcing. *Ocean Science*, Copernicus GmbH, v. 12, n. 2, p. 391–402, 2016. ISSN 18120792.

VACONDIO, R.; Dal Palù, A.; FERRARI, A.; MIGNOSA, P.; AURELI, F.; DAZZI, S. A non-uniform efficient grid type for GPU-parallel Shallow Water Equations models. *Environmental Modelling and Software*, Elsevier Ltd, v. 88, p. 119–137, 2017. ISSN 13648152.

VANKA, S. P. 2012 Freeman Scholar Lecture : Computational Fluid Dynamics on Graphics Processing Units. *Journal of Fluids Engineering*, v. 135, n. June, 2013.

VIERO, D. P.; PERUZZO, P.; CARNIELLO, L.; DEFINA, A. Integrated mathematical modeling of hydrological and hydrodynamic response to rainfall events in rural lowland catchments. *Water Resources Research*, n. 50, p. 5941–5957, 2014.

WADE, A. J.; WHITEHEAD, P. G.; BUTTERFIELD, D. The Integrated Catchments model of Phosphorus dynamics (INCA-P), a new approach for multiple source assessment in heterogeneous river systems: Model structure and equations. *Hydrology and Earth System Sciences*, v. 6, n. 3, p. 583–606, 2002. ISSN 10275606.

XIA, X.; LIANG, Q.; MING, X. A full-scale fluvial flood modelling framework based on a high-performance integrated hydrodynamic modelling system (HiPIMS). *Advances in Water Resources*, Elsevier Ltd, v. 132, p. 103392, 2019.

XIE, Z. T.; YANG, F. L.; FU, X. L. Mathematical model for flood routing in Jingjiang River and Dongting Lake network. *Water Science and Engineering*, Editorial Office of Water Science and Engineering, v. 5, n. 3, p. 259–268, 2012. ISSN 16742370.

YU, K.; CHEN, Y.; ZHU, D.; VARIANO, E. A.; LIN, J. Development and performance of a 1D-2D coupled shallow water model for large river and lake networks. *Journal of Hydraulic Research*, Taylor and Francis Ltd., v. 57, n. 6, p. 852–865, nov 2019. ISSN 0022-1686.

ZHANG, J.; HUANG, T.; CHEN, L.; LIU, X.; ZHU, L.; FENG, L.; YANG, Y. Water-exchange response of downstream river-lake system to the flow regulation of the Three Gorges reservoir, China. *Water (Switzerland)*, MDPI AG, v. 11, n. 11, 2019. ISSN 20734441.

ZHANG, L.; LU, J.; CHEN, X.; LIANG, D.; FU, X.; SAUVAGE, S.; PEREZ, J. M. S. Stream flow simulation and verification in ungauged zones by coupling hydrological and hydrodynamic models: A case study of the Poyang Lake ungauged zone. *Hydrology and Earth System Sciences*, Copernicus GmbH, v. 21, n. 11, p. 5847–5861, 2017. ISSN 16077938.

ZHENG, L.; WANG, H.; LIU, C.; ZHANG, S.; DING, A.; XIE, E.; LI, J.; WANG, S. Prediction of harmful algal blooms in large water bodies using the combined EFDC and LSTM models. *Journal of Environmental Management*, Academic Press, v. 295, 2021.

ZIA, A.; BOMBLIES, A.; SCHROTH, A. W.; KOLIBA, C.; ISLES, P. D.; TSAI, Y.; MOHAMMED, I. N.; BUCINI, G.; CLEMINS, P. J.; TURNBULL, S.; RODGERS, M.; HAMED, A.; BECKAGE, B.; WINTER, J.; ADAIR, C.; GALFORD, G. L.; RIZZO, D.; Van Houten, J. Coupled impacts of climate and land use change across a river-lake continuum: Insights from an integrated assessment model of Lake Champlain's Missisquoi Basin, 2000-2040. *Environmental Research Letters*, Institute of Physics Publishing, v. 11, n. 11, 2016. ISSN 17489326.